ALTERED CD38 EXPRESSION IN THIOACETAMIDE-INDUCED RAT MODEL OF LIVER CIRRHOSIS

GAN BONG HWA

NATIONAL UNIVERSITY OF SINGAPORE

2005

ALTERED CD38 EXPRESSION IN THIOACETAMIDE-INDUCED RAT MODEL OF LIVER CIRRHOSIS

GAN BONG HWA

(B. Sc. Biotechnology (Hons.), UPM Malaysia)

A THESIS SUBMITTED

FOR THE DEGREE OF MASTER OF SCIENCE

DEPARTMENT OF BIOCHEMISTRY

NATIONAL UNIVERSITY OF SINGAPORE

2005

ACKNOWLEDGEMENTS

I am most grateful to be given the opportunity to pursue my Master's degree in Professor Chang Chan Fong's lab in National University of Singapore. Although it was not a smooth sailing journey in my research, I was able to overcome the hurdles with Prof. Chang's magnificent supervision, guidance, support, and not to mention patience.

I would like to extend my gratitude and appreciations to Dr. Enoka and all the staffs in Animal Holding Unit for their constant support and advice in the animals handling. Without them, I will not be able to pull me through.

I would like to thank Professor Bay Boon Huat and Mrs. Ng Geok Lan in Department of Anatomy for their help and advice in making my research project a success. I sincerely appreciate the assistance provided by Ms. Yi Er and Mr. Kong Heng in Confocal Microscopy Unit, which simply have been amazing to say the least.

I would also like to express my special appreciation to my fellow talented postgraduate students; Seok Shin, Mann Yin, Li Phing, and Jessie, who doubled as my best buddies. You all have helped me see that I have chosen the right path and have kept me sane while I proceed down it.

A big thank you to everyone in Department of Biochemistry especially the academic staff in my lab, Qian Feng, for their assistance and support.

I extend my heartfelt gratitude to my mum and Lai Peng, especially Dario who is just like my elder sister, for their perpetual love, encouragement, and support in accomplishing my research project. I am so blessed to have them who will stand by me at all times.

Dedicated to my mother, Lai Peng, and friends

for their love and encouragement.

CONTENTS

Chapter 2: Materials and Methods

Awards

- First Prize in poster presentation for Malaysian Science & Technology Congress 2001.

- National University of Singapore Research Scholarship (Jan, 2003 – July, 2005)

SUMMARY

Liver cirrhosis involves progressive fibrosis and severe distortion of the normal lobular architecture of the liver. Because to date, little is still known about the function of CD38 in this deadly disease, so our current study aimed to investigate the possible role of CD38 in thioacetamide-induced rat liver cirrhosis. CD38 is a type II transmembrane glycoprotein, which is widely distributed in many tissues including the liver. CD38 exhibits ADP-ribosyl cyclase and cyclic ADP-ribose (cADPR) hydrolase activities that catalyzes the synthesis and hydrolysis of cADPR, respectively. cADPR is a potent intracellular calcium releaser and is thought to be involved in the regulation of cell division, apoptosis and gene expression. In this study, the gene and protein expressions of CD38 were investigated in a thioacetamide-induced rat model of cirrhosis.

CD38 mRNA content was first characterized using real-time RT-PCR. The CD38 mRNA expression levels of control and TAA-treated rat samples were compared to assess the effect of thioacetamide-induced cirrhosis on CD38 expression. There was enhanced CD38 mRNA expression in liver obtained from TAA-treated rats as compared with the controls and it was an approximate 2.5-fold increase in accordance with the RT-PCR ratiometric analysis.

CD38 protein expression was next characterized in the rat livers using immunohistochemistry and immunoblotting. Similarly, CD38 protein expression was significantly elevated in the cirrhotic liver compared to that in the control and this enzymatically active protein is found localized at the plasma membrane of rat hepatocytes. Western blot analysis of isolated microsomal fraction showed a ~45 kDa

protein band, which is a characteristic of CD38. In this immunoblot analysis, CD38 expression was significantly increased (about 1-fold) in the microsomes of cirrhotic liver compared to the normal liver. The increase in CD38 expression was supported by the detection of higher level of ADP-ribosyl cyclase activity in the cirrhotic liver compared to that in the control, which revealed an approximate 1-fold higher in the CD38 specific activity.

Next the cADPR and NAD^+ contents in the control and TAA-treated rat livers were measured using cycling assay. The fluorescence produced was calibrated using cADPR and NAD^+ standards, respectively. cADPR level was modestly but significantly augmented (22.3%) in cirrhotic liver and in contrast, there was a significant decrease (4-fold lower) in the endogenous NAD^+ in cirrhotic liver compared to that in the control liver. In conclusion, these results raised the possibility that altered CD38 expression and a concomitant elevation of the ADP-ribosyl cyclase activity as well as the cADPR may play an important role in the pathogenesis of liver cirrhosis.

List of Tables

List of Figures

List of Abbreviations

ADP	adenosine diphosphate
ADPR	adenosine diphosphate ribose
AIDS	acquired immunodeficiency syndrome
APS	ammonium persulphate
ATP	adenosine triphosphate
ATRA	all-trans-retinoic acid
BSA	bovine serum albumin
Ca^{2+}	calcium
cADPR	cyclic adenosine diphosphate ribose
cDNA	complementary deoxyribonucleic acid
cGDPR	cyclic guonosine diphosphate ribose
cGMP	cyclic guanosine monophosphate
CICR	calcium-induced-calcium release
C_t	cycle number
Cu^{2+}	copper
Cu^{2+}-IDA	copper-iminodiacetic acid-agarose
DEPC	diethylpyrocarbonate
DNA	deoxyribonucleic acid
dNTP	deoxynucleotide triphosphate
DTT	dithiothreitol
EC	endothelial cells
EDTA	ethylenediaminetetraacetic acid

FITC	fluorescein isothiocyanate
FMN	flavin mononucleotide
HCl	hydrochloride acid
HIV	human immunodeficiency virus
IgG	immunoglobulin G
IgM	immunoglobulin M
IP_3	inositol triphosphate
kDa	kilodalton
kg	kilogram
KSCN	potassium thiocyanate
M	molar
mAbs	monoclonal anibodies
mg	milligram
min	minute(s)
ml	milliliter
mM	millimolar
MOPS	3-(N-Morpholino)propanesulfonic acid
mRNA	messenger ribonucleic acid
NA	nicotinic acid
NAADP	nicotinic acid adenine dinucleotide phosphate
NaCl	sodium chloride
NAD^+	nicotinamide adenine dinucleotide
$NADP^+$	nicotinamide adenine dinucleotide phosphate

NCBI	national center for biotechnology information
NGD^+	nicotinamide guanine dinucleotide
NIDDM	non-insulin-dependent diabetes mellitus
nm	nanometer
nmoles	nanomoles
PARP	poly (ADP-ribose) synthetase/polymerase
PBS	phosphate buffered saline
PCR	polymerase chain reaction
PLP	periodate-lysine-paraformaldehyde
RNA	ribonucleic acid
rRNA	ribosomal ribonucleic acid
RT-PCR	reverse transcriptase – polymerase chain reaction
RyR	ryanodine receptor
SDS	sodium dodecyl sulfate
SDS-PAGE	sodium dodecyl sulfate – polyacrylamide gel electrophoresis
SEM	standard error of the mean
TAA	thioacetamide
µg	microgram
µl	microliter
µm	micrometer
V	volts
XLA	X-linked agammaglobulinemia
Zn^{2+}	zinc

CHAPTER 1

1. INTRODUCTION

1.1 GENERAL FEATURES OF THE LIVER

The liver is the largest visceral organ. The adult liver weighs between 1400 and 1600 g and makes up 2.5 % of the body weight. It is relatively larger in infants and children than in adults. The normal liver extends from the right fifth interspace in the mid-clavicular line down to the right costal margin. There are two main anatomical lobes. The right is separated from the left by a reflected surface of peritoneum, the falciform ligament (Figure 1.1). The right lobe is larger, and the caudate lobe (lying posteriorly along the inferior vena kava in front of the hepatic porta) and quadrate lobe (lying anteriorly between the gallbladder and round ligament) are attached to its posterior-inferior surface. Surgically, the point of division between the right and left hepatic lobes is at the porta hepatis where the hepatic artery and portal vein divide into right and left branches, rather than at the falciform ligament. Together the surgical right and left lobes can be further divided into eight segments that guide the line of surgical resection in typical hepatectomies (Figure 1.2; Bismuth, 1982).

The diaphragmatic surface of the liver, which faces forwards and upwards, lies between the arch of the diaphragm and the anterior abdominal wall. This diaphragmatic surface is differentiated into the pars libera (covered with peritoneum) and the pars affixa. The visceral surface inclines both backwards and downwards. The superior and inferior surfaces form together the sharp liver margin (ventral border). The inferior surface may show impressions caused by adjacent organs (gaster, colon, kidney, duodenum,

gallbladder) and the posterior surface shows a fissure for the ligamentum venosum (Figure 1.1).

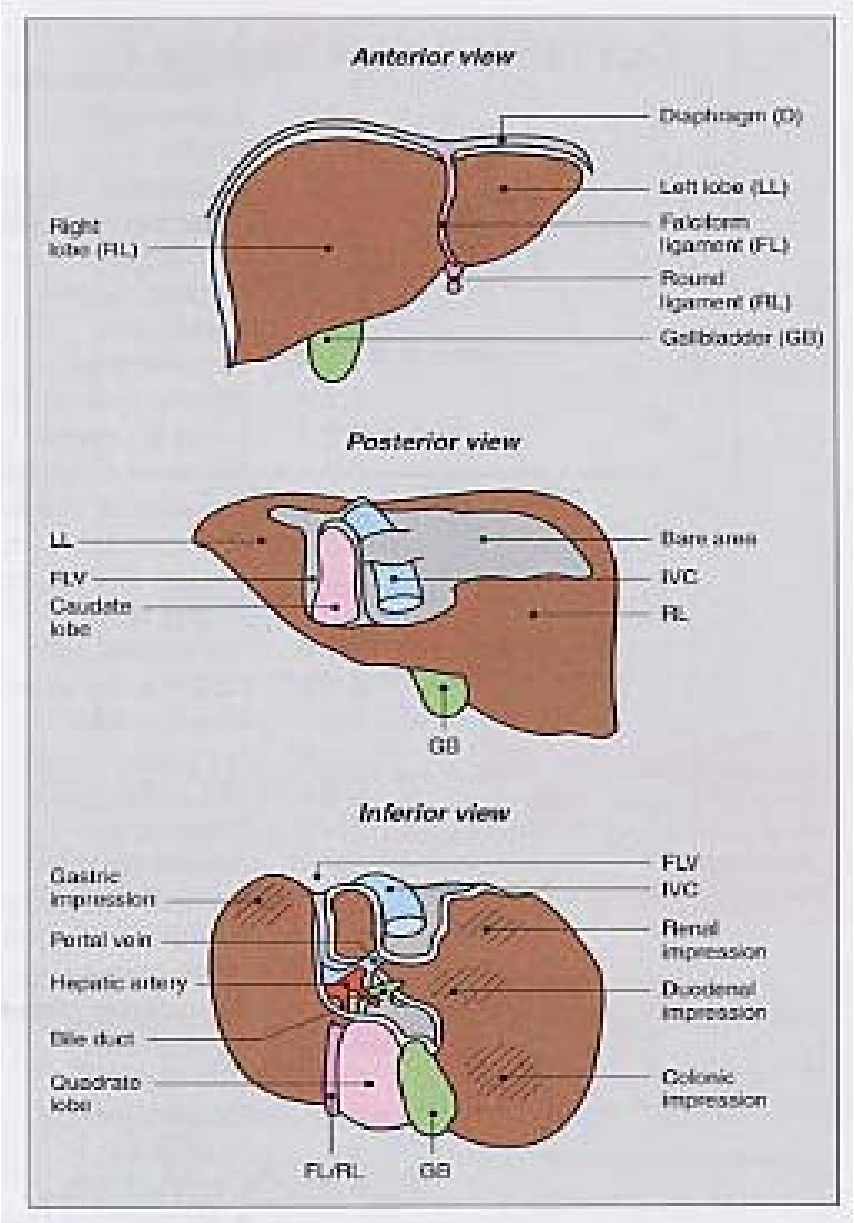

Figure 1.1 Views of the liver: anterior, posterior, inferior.
(LL = left lobe, RL = right lobe, D = diaphragm, GB = gallbladder, FLV = fissure for ligamentum venosum, RL = round ligament (= lig. teres), IVC = inferior vena cava, FL = falciform ligament) (Reproduced from Kuntz, E. and Kuntz, H.D., 2002)

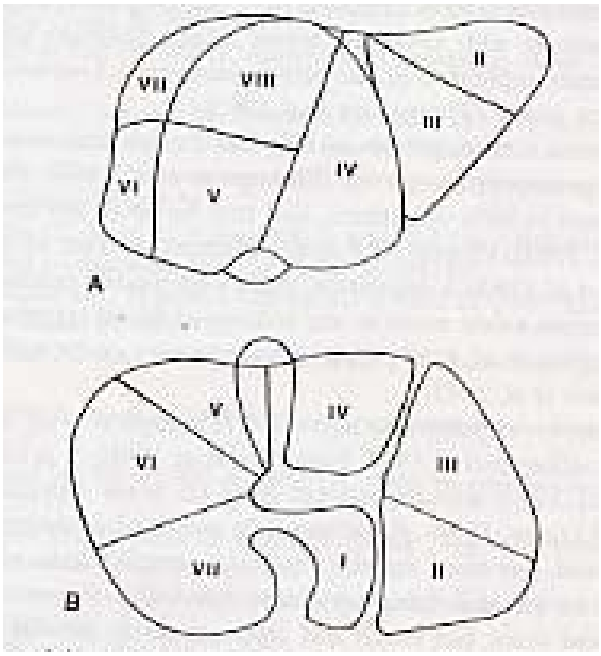

Figure 1.2 The segments of the liver.
A: Superior view; B: Inferior view (Adapted from Bismuth *et al.*, 1982)

The hepatic lobule is the basic histological unit of the liver. It consists of an approximately hexagonal unit around the radicles of the hepatic veins, with cords of hepatocytes and sinusoids radiating outward in a 'bicycle spoke' arrangement. The vein is therefore central (centrilobular). Four to five portal tracts that contain bile canaliculi, portal venules, hepatic arterioles, lymphatics and nerves define the periphery of the lobule. The blood supply to the liver is from the hepatic artery and portal vein (Richardson and Withrington, 1981a; Lautt and Greenway, 1987). These blood vessels enter the liver at the porta hepatis. The hepatic veins drain posteriorly into the inferior vena cava (IVC). The liver is supplied by sympathetic nerve fibres from T7 to T10, that synapse in the celiac plexus along with the right and left vagus nerves and the right phrenic nerve (Bioulac-Sage *et al.*, 1990). Nerve fibres accompany the hepatic artery and bile ducts into the liver parenchyma and innervate Glisson's capsule, the investing membrane of the organ. Lymphatic vessels draining the liver merge at the porta hepatis and most lympatics accompany the IVC into the mediastinum.

The hepatocytes are the main functional units of the liver. Each hepatocyte is polyhedral in shape and has three different surfaces: canculicular, comprising the canalicular wall; lateral, abutting tightly to adjacent hepatocytes; and sinusoidal, facing the sinusoids which are distensible vascular channels that transport blood from branches of the portal vein and hepatic artery between the hepatic cells. Apart from the hepatocytes, the liver parenchyma also comprises other cell types including the endothelial cells, Kupffer cells, stellate cells, Pit cells, and bile duct cells. The composition of subcellular organelles in the liver and the hepatocyte of humans and rats are shown in Table 1.1.

Volumetric Composition of Hepatic Ultrastructure

	Human liver* Percent		Rat Liver† Percent	
	Liver Tissue	Hepatocyte	Liver Tissue	Hepatocyte
Extrahepatocytic space	17.0		20.7	
Hepatocytes	83.0	100.0	79.3	100.0
Nuclei	5.0	6.0	5.6	7.3
Endoplasmic reticulum				12.1
Rough	8.0	9.4	9.6	7.2
Smooth	5.0	5.9	5.6	17.6
Mitochondria	18.0	22.0	14.0	1.8
Lysosomes	0.7	0.8	1.4	1.2
Peroxisomes	1.2	1.4	0.9	50.9
Cytosol	45.0	54.0	41.8	

*Data adapted from Rohr et al. (1976).
†Data adapted from Weibel et al. (1969).

Table 1.1 Volumetric composition of hepatic ultrastructure.
(Adapted from Miyai, 1991)

The liver serves as a guardian located between the digestive tract and the rest of the body. It performs many other functions than making bile. It collects almost all of the blood circulated through the intestines and processes many of the chemicals picked up there (such as alcohol, which the liver detoxifies). Waste products from protein metabolism are processed into the less-toxic form of urea, which will be removed in the kidneys. Old red blood cells are broken down, with important things like the iron recycled; the liver is also a major staging site for white blood cells of the immune system. Temporary storage of sugar occurs in the liver: in response to insulin hormone from the pancreas, sugar in the blood is absorbed and stored as the simple starch glycogen; another pancreas hormone, glucagon, causes conversion of glycogen back to sugar and its release into the blood as needed. That's a partial list of liver functions. Tucked into a recess underneath is the gall bladder, where a secretion called bile, also produced in the liver, is stored. Bile is a salty fluid (if too concentrated, crystals can form - *gallstones)* used in the

small intestine to emulsify fat, physically making tiny, digestible blobs out of big, separated-out globs of fatty material. There are several ducts in the region - a duct connects the liver to the small intestine, with a branch to the gall bladder and a branch to the pancreas. Liver diseases may impair the liver functions as well as affect other organ systems.

1.2 LIVER CIRRHOSIS

Despite the availability of current treatments, liver cirrhosis remains one of the top leading causes of deaths in many countries. Liver cirrhosis is a gradually developing, chronic disease of the liver which always involves the organ as a whole. However, the most concise and probably the best definition of cirrhosis is 'a diffuse process characterized by fibrosis and a conversion of normal architecture into structurally abnormal nodules' (Anthony *et al.*, 1977; Anthony *et al.*, 1978). Cirrhosis is the irreversible consequence and may be caused by chronic alcoholism, infections, drugs and toxins, inherited diseases, and many other causes. The variations of this disease range from symptom-free conditions, non-characteristic complaints and different laboratory findings through to life-threatening complications. Cirrhosis is most satisfactorily classified by its etiology and the etiology conditions are listed in Table 1.2. Apart from impairing the liver functions, cirrhosis also affects the functions of the digestive, hormonal, and circulatory systems. In addition, it has been shown that liver cirrhosis is associated with the development of hepatocellular carcinoma in humans (Kew and Popper, 1984).

Liver cirrhosis is characterized by five criteria: (1) pronounced, insufficiently repaired necroses of the parenchyma (with or without inflammatory processes), (2) diffuse connective tissue proliferation, (3) varying degrees of nodular parenchymal regeneration, (4) loss and transformation of the lobular structure within the liver as a whole, and (5) impaired intrahepatic and intra-acinar vascular supply.

Drugs and toxins	Alcohol Methotrexate Isoniazid Methyldopa Amiodarone
Infections	Hepatitis B Hepatitis C Schistosomiasis
Autoimmune	Chronic active hepatitis Primary biliary cirrhosis
Metabolic	Wilson's disease Haemochromatosis α_1-antitrypsin deficiency Galactosaemia Glycogen storage diseases Tyrosinaemia Urea cycle disorders Abetalipoproteinaemia
Biliary obstruction	Atresia Cystic fibrosis Gallstones Strictures Sclerosing cholangitis
Vascular	Budd–Chiari syndrome Veno-occlusive disease Chronic right heart failure Hereditary haemorrhagic telangiectasia
Miscellaneous	Neonatal hepatitis syndrome Indian childhood cirrhosis Intestinal bypass surgery Sarcoidosis
Cryptogenic	

Table 1.2 Etiology of cirrhosis.
(Adapted from Millward-Sadler, 1994)

It is important to comprehend the pathogenesis of liver cirrhosis to explore alternative treatment for this deadly disease. There are three major pathological mechanisms that involved in the development of cirrhosis. The process is usually initiated by chronic hepatocyte necrosis, leading to the collapse of the delicate reticulin support network in the space of Disse between the sinusoidal endothelial cells and hepatocytes. It is then followed by extensive deposition of collagen types I and III that results in fibrosis. Aberrant collagen deposition also causes the distortion of vascular beds and generates abnormal nodules after parenchymal regeneration. In response to liver damage, stellate cells are also activated and transformed into myofibroblast-like cells that start to synthesize collagen type I under the influences of cytokines like transforming growth factor beta (Figure 1.3).

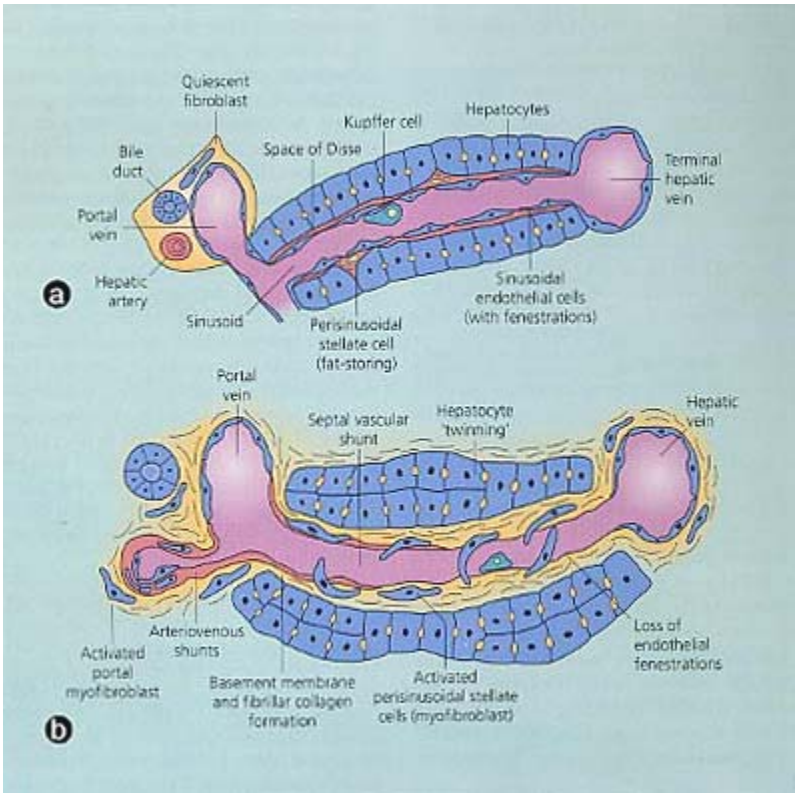

Figure 1.3 Key events in the evolution of cirrhosis.

(a) The normal microanatomy of the liver is depicted, showing especially the channels for flow of portal venous blood through the sinusoids of the parenchyma, and normal sinusoidal architecture.

(b) With evolution to cirrhosis, the following key events occur. Abnormal arteriovenous shunts and vascular shunts from portal to hepatic veins develop. Portal tract fibroblasts proliferate and become myofibroblasts. Perisinusoidal stellate cells lose their fat stores, proliferate and develop a myofibroblast phenotype. Both populations of cells deposit extracellular matrix, expanding portal tracts and the space of Disse, respectively. Hepatocyte regeneration, leading to 'twinning' of hepatocyte plates, also is shown. (Adapted from Crawford, 2002)

As the cirrhotic process continues, blood flow through the liver becomes blocked; portal hypertension may occur (high blood pressure in the veins connecting the liver with the intestines and spleen); glucose and vitamin absorption decrease; the manufacturing of hormones and stomach and bowel function are affected; and noticeable facial veins may appear. Common symptoms of cirrhosis include nausea or indigestion and vomiting, loss of appetite, weight loss, constipation or diarrhea, flatulence, ascites (the accumulation of serous fluids in the peritoneal cavity), edema (fluid retention in the legs), light-colored stools, weakness or chronic dyspepsia, dull abdominal aching, varicosities, nosebleeds, bleeding gums or other internal and external bleeding, easy bruising, extreme skin dryness, intense skin itching, and spider angiomas (a central, raised, red dot about the size of a pin head from which small blood vessels radiate). Excessive bile product deposits cause intense skin itching, often accompanied by jaundice (yellowed skin). Other symptoms are testicular atrophy, gynecomastia (enlargement of the male breast), and loss of chest and armpit hair. Psychotic mental changes such as extreme paranoia can also occur in cases of advanced cirrhosis.

1.3 DRUG-INDUCED CIRRHOSIS

Individuals are exposed to a wide range of lipophilic chemicals including drugs, certain vitamins, carcinogens, pesticides, and other environmental pollutants. In addition, many endogenous substances of physiological importance, such as fatty acids, prostaglandins and sex hormones, are themselves quite hydrophobic. Most drugs and xenobiotics are lipophilic, enabling them to cross the membranes of intestinal cells. Drugs are rendered more hydrophilic by biochemical processes in the hepatocyte, yielding water-soluble

products that are excreted in urine or bile (Weinshilboum, 2003). This hepatic biotransformation involves oxidative pathways, primarily by way of the cytochrome P-450 enzyme system (Guengerich, 2001). After further metabolic steps, which usually include conjugation to a glucuronide or a sulfate or glutathione, the hydrophilic product is exported into plasma or bile by transport proteins located on the hepatocyte membrane, and it is subsequently excreted by the kidney or the gastrointestinal tract. Compounds which produce liver injury can be classified into those that are chemically stable (direct hepatotoxins) and those whose metabolism forms chemically-reactive species (indirect hepatotoxins). Most currently-used agents that can cause drug-induced liver injury are indirect hepatotoxins. Their hepatic metabolism gives rise to electrophilic drug metabolites, free radicals, and reactive oxygen species (ROS).

At least six mechanisms that primarily involve the hepatocyte produce liver injury, and the manner in which various intracellular organelles are affected defines the pattern of disease (Figure 1.4). Injury to liver cells occurs in patterns specific to the intracellular organelles affected. The normal hepatocyte shown in the center of the figure may be affected in at least six ways, labeled A through F. Disruption of intracellular calcium homeostasis leads to the disassembly of actin fibrils at the surface of the hepatocyte, resulting in blebbing of the cell membrane, rupture, and cell lysis (Yun *et al.*, 1993; Beaune *et al.*, 1987). In cholestatic diseases, disruption of actin filaments (B) may occur next to the canaliculus, the specialized portion of the cell responsible for bile excretion (Trauner *et al.*, 1998). Loss of villous processes and the interruption of transport pumps such as multidrug-resistance–associated protein 3 (MRP3) prevent the excretion of bilirubin and other organic compounds. Many hepatocellular reactions involve the heme-

containing cytochrome P-450 system (C), generating high-energy reactions that can lead to the covalent binding of drug to enzyme, thus creating new, nonfunctioning adducts. These enzyme–drug adducts migrate to the cell surface (D) in vesicles to serve as target immunogens for cytolytic attack by T cells, stimulating a multifaceted immune response involving both cytolytic T cells and cytokines (Robin *et al.*, 1997). Activation of apoptotic pathways by tumor necrosis factor α (TNF-α) receptor or Fas may trigger the cascade of intercellular caspases (E), which results in programmed cell death with loss of nuclear chromatin (Reed, 2001). Certain drugs inhibit mitochondrial function by a dual effect on both β-oxidation (affecting energy production by inhibition of the synthesis of nicotinamide adenine dinucleotide and flavin adenine dinucleotide, resulting in decreased ATP production) and the respiratory-chain enzymes (F). Free fatty acids cannot be metabolized, and the lack of aerobic respiration results in the accumulation of lactate and reactive oxygen species. The presence of reactive oxygen species may further disrupt mitochondrial DNA. This pattern of injury is characteristic of a variety of agents, including nucleoside reverse-transcriptase inhibitors, which bind directly to mitochondrial DNA, as well as valproic acid, tetracycline, and aspirin (Pessayre *et al.*, 2001).

Among the various hepatotoxins used to induce liver cirrhosis in laboratory animals, thioacetamide is the most potent because of its rapid elimination and cumulative injury when it is given intermittently (Dashti *et al.*, 1997; Dashti *et al.*, 1987). Further, thioacetamide is very effective in producing liver cirrhosis in laboratory rodents (Fitzhugh and Nielson, 1948; Gupta, 1955; Gupta, 1956b). Various investigators have used different methods of thioacetamide administration in experimental animals for

producing fibrosis and cirrhosis, such as intraperitoneal or subcutaneous administration (Dashti *et al.*, 1987; Gallagher *et al.*, 1956), mixing the toxin with the diet (Gupta, 1956a), or in drinking water (Dashti *et al.*, 1997). Thioacetamide is hepatotoxic owing to effects on DNA, RNA, protein synthesis and gamma-glutamyl transferase (GGT) activity, through which it induces cirrhosis and hepatocarcinoma (Yang *et al.*, 1998). In addition, it is well established that thioacetamide modifies various liver functions including the synthesis of various metal-binding proteins, and some of the plasma and tissue trace element alteration observed in thioacetamide-induced cirrhotic rats may be secondary to the effects of this drug on the liver (Al-Bader *et al.*, 2000). Thioacetamide (TAA), a hepatotoxicant, is taken by liver then is metabolized into TAA-sulfoxide by cytochrome P450 mixed-function oxidase and further transformed into the intermediates and other polar molecules, which irreversibly combine with intrahepatic biomacromolecules to cause hepatic necrosis (Han, 2002).

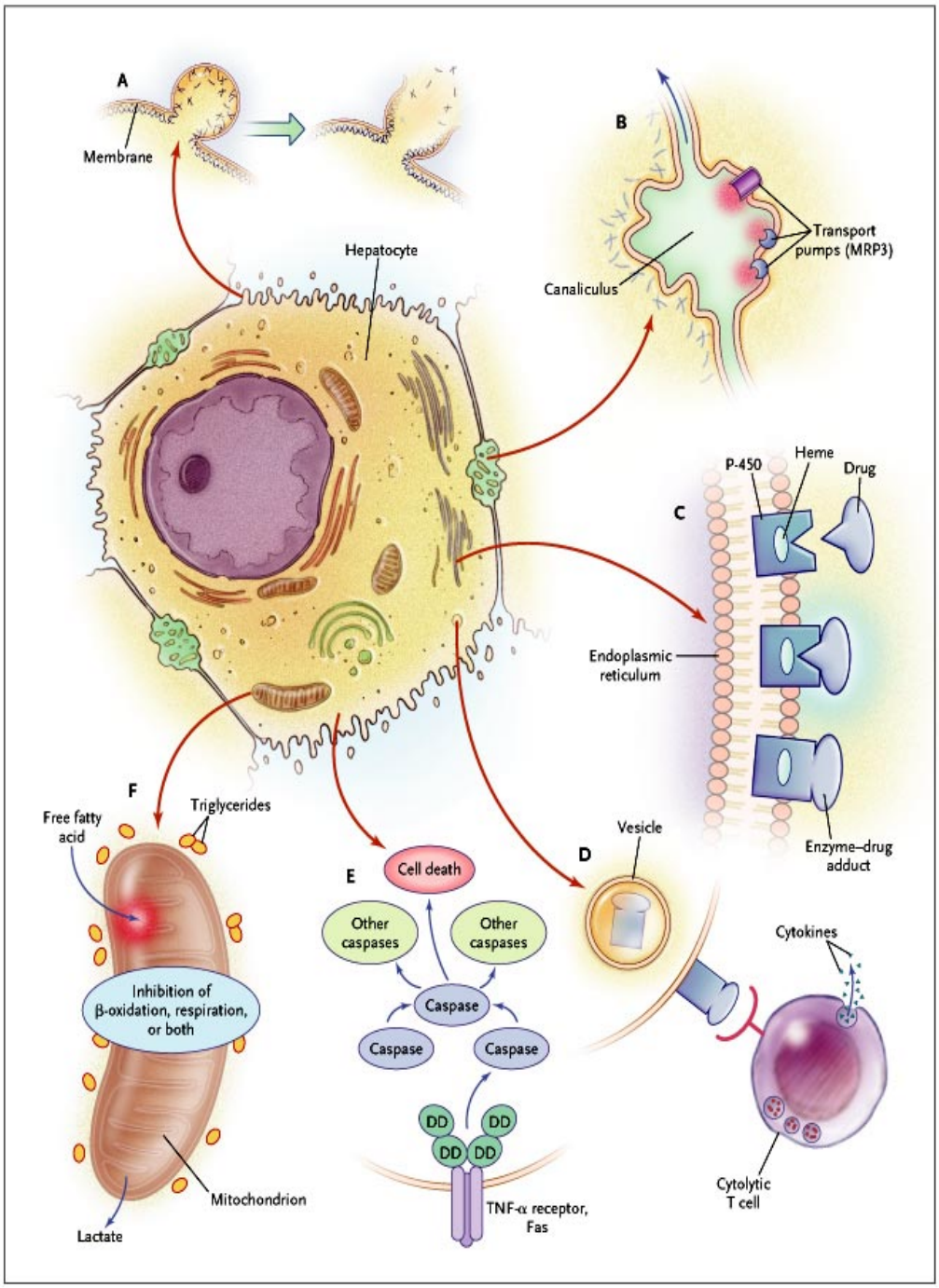

Figure 1.4 Six mechanisms of liver injury.
(Adapted from Lee, 2003)

1.4 GENERAL INTRODUCTION TO CD38

CD38 was originally defined by Reinherz *et al.* (1980) in their pioneering work on thymocyte and T lymphocyte differentiation antigens. The gene encoding the human CD38 antigen has been cloned from T-cell lines and normal lymphocytes (Jackson and Bell, 1990) and is located on chromosome 4 (Katz *et al.*, 1983). Although initial studies concentrated on the immunological aspects of CD38, this molecule subsequently attracted the interest of many scientists from distant areas of research. Since its humble beginnings, the various fields in cellular, molecular, plant and marine biology have subsequently intertwined with that of immunology, biochemistry and crystallography in the paradigmatic quest to solve the riddle of the CD38 story.

The story began when CD38 was discovered to possess a unique distribution pattern, being predominantly expressed by progenitors and early hematopoietic cells, then lost during maturation and only to be expressed again upon cell activation (refer to review by Mehta *et al.*, 1996). Due to the curious nature of its expression, CD38 was initially used primarily as a phenotypic marker of differentiation in normal and leukemic blood cells. Interest in CD38 beyond its use as a marker of cellular differentiation has grown since the discovery that human CD38 has significant amino acid sequence similarity to a 29 kDa cytosolic ADP-ribosyl cyclase enzyme (States *et al.*, 1992) previously isolated from the sea mollusc known as *Aplysia californica* (Hellmich and Strumwasser, 1991; Lee and Aarhus, 1991).

Aplysia cyclase has previously been shown to catalyze the synthesis of cyclic ADP-ribose (cADPR) from NAD^+ and this cyclic nucleotide subsequently proved to have potent calcium mobilizing properties (Lee and Aarhus, 1991; Lee *et al.*, 1994a). As

predicted by its homology with the *Aplysia* cyclase, human CD38 was shown to have the ability to catalyze the conversion of NAD^+ into cADPR as well. CD38 also possesses the ability to hydrolyze the cyclic nucleotide to ADP-ribose (ADPR), an ability that the *Aplysia* cyclase does not have (Howard *et al.*, 1993; Zocchi *et al.*, 1993). Another intriguing observation was that agonistic monoclonal antibodies against CD38 could trigger a myriad of responses including that of cell proliferation (Funaro *et al.*, 1990), apoptosis (Zupo *et al.*, 1994), cytokine release (Ausiello *et al.*, 1995) and tyrosine phosphorylation (Kirkham *et al.*, 1994) in a variety of cell types.

CD38 proteins were detected in humans, mice, and rats (Reinherz *et al.*, 1980; Howard *et al.*, 1993; Koguma *et al.*, 1994). This family also includes the human, murine, and rat bone marrow stromal cell surface molecule BP3/BST-1 (Hirata *et al.*, 1994; Itoh *et al.*, 1994; Furuya *et al.*, 1995); the rat T cell differentiation marker RT6 and its murine and human homologs; Yac-1 and Yac-2 ADP-ribosyl transferases (Okazaki and Moss, 1996); ADP-ribosyl cyclase from sea molluscs (Tohgo *et al.*, 1994); and other ADP-ribosyl transferases.

1.5 FUNCTIONAL STRUCTURE OF CD38

Human CD38 protein is a 45 kDa transmembrane glycoprotein with a short N-terminal cytoplasmic part (21 amino acids) and a long extracellular domain (Jackson and Bell, 1990). The gene encoding human CD38 protein is located on chromosome 4p15 (Nakagawara *et al.*, 1995). CD38 has the hallmarks of a type II integral membrane protein, i.e. amino-terminus in, carboxy-terminus out, with an architecture consisting of three regions: intracellular (20 amino acids), transmembrane (23 amino acids) and

extracellular (257 amino acids) (Jackson and Bell, 1990). The cloning of the murine, rat and human CD38 cDNA sequences has revealed that the rat and murine CD38 cDNA sequences share ~75% homology with human CD38 cDNA sequence (Harada *et al.*, 1993).

An important clue to the three-dimensional structure of the extracellular portion of CD38 came from the determination of the crystal structure of its relative, the *Aplysia californica* cyclase (Prasad *et al.*, 1996). The most interesting feature of the molecule is that, in three different crystal forms, it is crystallized as a dimmer in a head to head fashion as shown in Figure 1.5 (Prasad *et al.*, 1996). Three (α1, α4 and α10) of the ten helices are involved in the formation of the dimer. The dimeric structure is likely to be highly stable since the sequences of the interacting helices suggest the involvement of hydrogen bonding, salt bridges and hydrophobic interaction (Prasad *et al.*, 1996). The central cavity of the dimer has a dimension comparable to a molecule of cADPR. Lys129 (red) is shown by mutagenesis studies to be the binding site for cADPR and ATP (Tohgo *et al.*, 1997). It is thus highly suggestive that the central cavity is the active site of CD38. A molecule of cADPR is superimposed on the model of CD38 and positioned at the central cavity. The central cavity represents the structural feature that may account for the active transport property of CD38 (Franco *et al.*, 1998).

The carboxy-terminal domain has significant structural homology with various nucleotide-binding proteins such as flavodoxin, orotate phosphoribosyltransferase and factor G whereas the amino-terminal domain has a completely unique fold (Prasad *et al.*, 1996). Due to highly conserved sequence homology of the *Aplysia* cyclase to CD38, it is possible to correlate this model to that of CD38 whereby the CD38 molecule can be

imagined to possess two domains connected by a hinge region with a large cleft separating the domains (Figure 1.6). Although there are small gaps in the amino acid alignment of human CD38 and *Aplysia* cyclase, the differences correspond to loop regions in the tertiary structure (Prasad *et al.*, 1996). One relevant difference between the two molecules is that CD38 has six instead of the aplysian five disulphide bonds (Prasad *et al.*, 1996). The residues in question, Cys 119 and Cys 201, may be important for cross-linking to other molecules and their reduction may render the hinge region less flexible (Prasad *et al.*, 1996).

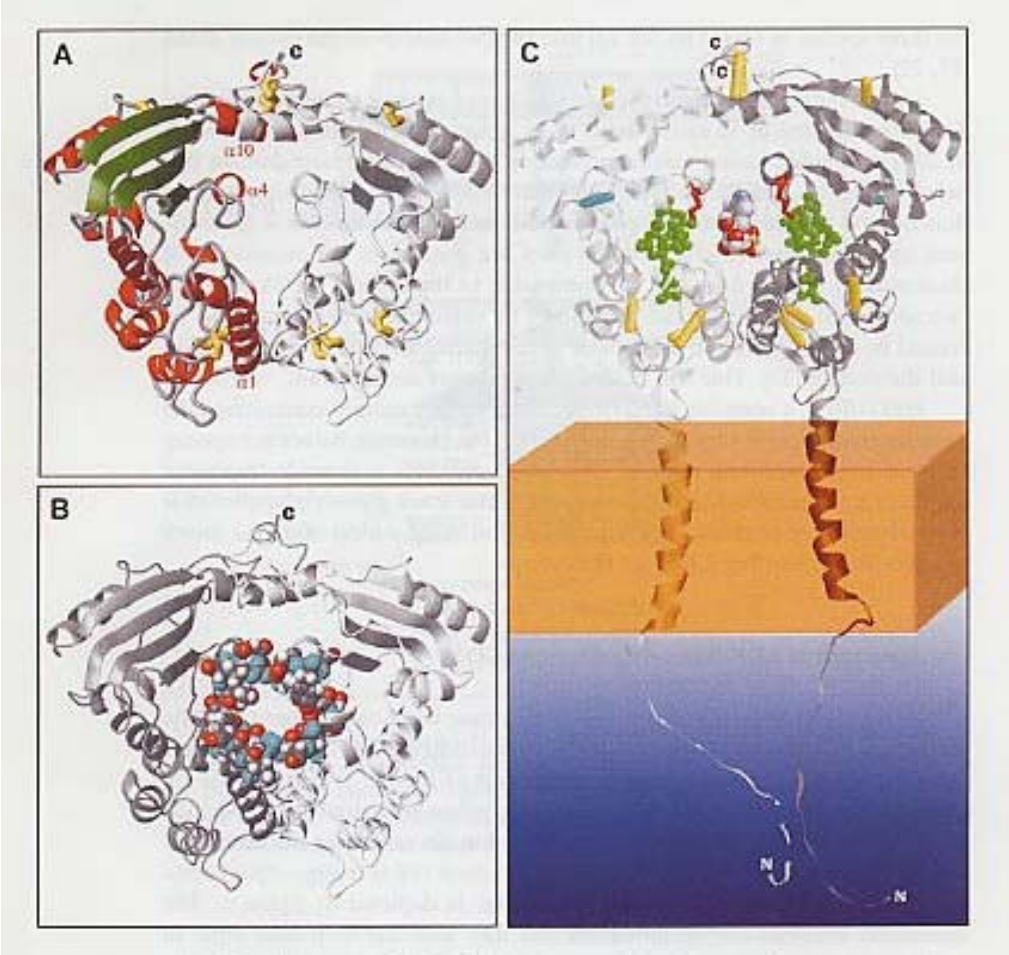

Figure 1.5 Structures of ADP-ribosyl cyclase and CD38.
A: Secondary structures of the cyclase. β-Sheets are shown in green, α-helixes in red and disulphide bonds in yellow. The three helixes involved in forming the dimeric structure are labeled α1, α4 and α10. The carboxy-termini are labeled C. *B*: Structure of the central cavity of the cyclase dimer. The cavity is lined with hydrophilic residues. Nitrogen atoms in basic residues such as arginine, are shown in cyan. Oxygen as present in acidic residues such as glutamate is shown in red and hydrogen in white. *C*: A model of the membrane bound CD38. The membrane is shown in light brown, lysine129 is in red, the conserved sequence in green and disulphide bonds in yellow. The extra pair of disulphides that is in CD38 but not in the cyclase is shown in cyan. A molecule of cADPR is superimposed and positioned in the central cavity. The amino- and carboxy-termini are labeled N and C, respectively. The cyclase structure is displayed by the program MOLMOL (Koradi *et al.*, 1996) and CD38 by RasMol (Sayle, 1996). (Adapted from Lee, 2000)

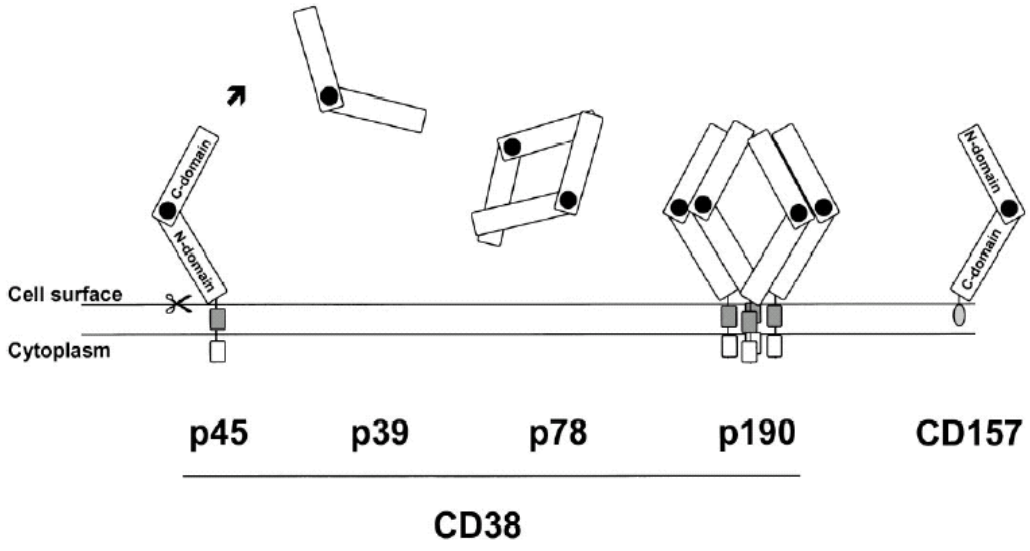

Figure 1.6 Models of CD38 monomers and aggregates.
The two domains of the membrane monomer are indicated. Filled circles represent the hinge region connecting the two domains. The gray shaded boxes represent the transmembrane region and the open boxes represent the cytoplasmic portion of CD38. Cleavage of the membrane form gives rise to p39 (soluble CD38); its dimer is p78 while p190 represents a tetramer of the membrane form. CD157 is shown on the right, the shaded oval represents the GPI anchor. (Adapted from Ferrero and Malavasi, 1999)

The short cytoplasmic domain of CD38 contains no known motifs (Src homology domain 2 or 3 [SH2 or SH3], antigen receptor activation [ARAM], or pleckstrin homology [PH]) that could mediate interactions with other signaling proteins and seems to have no enzymatic activity. It was shown recently that replacement of the cytoplasmic tail and the transmembrane domains of CD38 did not impair CD38 signaling, coreceptor activity, or enzyme activity (Lund *et al.*, 1999). The intracellular part of CD38 contains two conserved serine residues within consensus sites recognized by cyclic guanosine monophosphate (cGMP)-dependent protein kinases (Figure 1.7). cGMP-dependent serine/threonine kinases in sea urchin eggs modulate the activity of ADP-ribosyl cyclase, an enzyme that displays a functional homology to CD38 protein (Lund *et al.*, 1996). The cytoplasmic tail of CD38 might therefore serve as a regulatory subunit of the CD38 ectoenzyme rather than as a tool for transduction of signals into the cell interior. Analysis of the extracellular part of CD38 indicates that it may function in attachment to the extracellular matrix (Nishina *et al.*, 1994). Thus, human CD38 proteins contain three putative hyaluronate-binding motifs (HA motifs). Two of these HA motifs are localized in the extracellular domain of CD38 (amino acid positions 121-129 and 268-276), and one in the cytoplasmic part of the molecule. In addition, four asparagine residues in the extracellular region of CD38 serve as potential N-glycosylation sites.

The human CD38 molecule contains 12 conserved cysteines, 11 of which are located in the extracellular domain. Purified human CD38 undergoes stable homo-oligomerization induced by thiol-reactive agents (Guida *et al.*, 1995). It is tempting to speculate that thiol-dependent interactions underlie the association of the extracellular portion of CD38 with other receptors that may be vital for the signaling function of CD38.

Four cysteines (Cys-119, Cys-160, Cys-173, and Cys-201) play an essential role in the cADP-ribose synthetic and cADP-ribose hydrolytic activity of CD38 (Tohgo *et al.*, 1994). The C-terminal part of CD38, including amino acid sequence 273-285 and particularly Cys-275, also contributes to the NAD glycohydrolytic activity of CD38 (Hoshino *et al.*, 1997). Reducing agents such as dithiothreitol, 2-mercaptoethanol, or reduced glutathione inhibit the enzymatic activity of CD38, suggesting that the disulphide bonds are important for the catalytic activity of the CD38 proteins (Tohgo *et al.*, 1994; Zocchi *et al.*, 1995). The amino acid sequence within the catalytic domain and patterns of secondary structure motifs predicted for different CD38-related NAD hydrolases were similar to those predicted for bacterial mono-ADP-ribosyl transferases (Koch-Nolte *et al.*, 1996). In particular, the conserved pair of amino acids Glu-146-Asp-147 seems to endow ADP-ribosyl transferase activity to the CD38 protein (Grimaldi *et al.*, 1995; Okazaki and Moss, 1996).

A number of leucines within the transmembrane and extracellular regions have the potential to form leucine zipper motifs that can provide association of CD38 with other proteins (Figure 1.7). Two dileucine (LL) motifs are located in the middle of human CD38 proteins. One of these motifs (Leu-149-Leu-150) is conserved for human, murine and rat CD38. Intracellular targeting and internalization of different transmembrane proteins require the LL motif within the C terminus of the cytoplasmic domains (Aiken *et al.*, 1994). The LL motif located within the extracellular region is not accessible to intracellular targeting. However, high-molecular-weight oligomers of CD38 (Figure 1.7) might contain monomeric subunit(s) within the cell interior, rendering the LL motif accessible for intracellular targeting (Umar *et al.*, 1996).

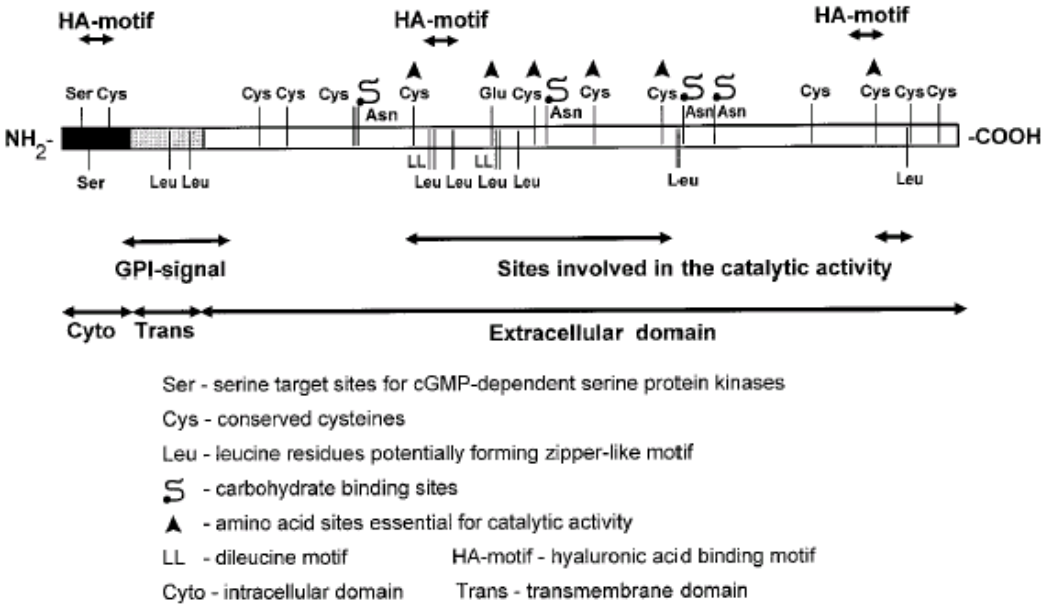

Figure 1.7 Functional structure of the human CD38 molecule.
(Adapted from Shubinsky and Schlesinger, 1997)

1.6 DISTRIBUTION OF CD38

In view of its immunological background, CD38 was studied in great detail in hematopoietic cells where its expression has been most appropriately termed 'discontinuous' (Jackson and Bell, 1990). In fact, CD38 is repeatedly switched on and off as bone marrow precursors develop into mature elements of the various lineages, making it an ideal marker for identifying populations at specific developmental stages. For example, the passage from primitive or uncommitted ($CD34^+/CD38^-$) to committed precursor ($CD34^+/CD38^+$) is marked by surface CD38 expression (Terstappen *et al.*, 1991). CD38 also marks T lymphocyte ontogenesis and it has been shown that more than 80% of medullary thymocytes are $CD38^+$, peripheral blood T cells are mostly $CD38^-$, whereas activated T cells are strongly $CD38^+$ (Malavasi *et al.*, 1992). In B lymphocyte ontogenesis, more than 90% bone marrow B cell progenitors are $CD38^+$ (Kumagal *et al.*, 1995), circulating B cells are $CD38^-$, whereas plasma cells are strong expressors (Malavasi *et al.*, 1992). CD38 is easily detected on erythrocytes, platelets, natural killer cells, as well as in most circulating monocytes whereas neutrophils and endothelial cells are negative for CD38 (Drach *et al.*, 1994; Fernandez *et al.*, 1998; Zocchi *et al.*, 1993; Ramaschi *et al.*, 1996).

In the gut, where a large percentage of cells of the immune system are found, the lamina propria cells are $CD38^+$ while intraepithelial lymphocytes are $CD38^-$ (Fernandez *et al.*, 1998). Increasing evidence points out to the fact that the expression of CD38 outside the hematopoietic system is uncharacteristically widespread for a molecule initially defined as a leukocyte antigen (Koguma *et al.*, 1994). CD38 has been detected on the sarcolemma in skeletal and heart muscle by immunohistochemistry and in the

kidney, proximal convoluted tubules are strongly $CD38^+$, whereas weak expression is detected in distal and collecting tubules (Fernandez *et al.*, 1998). Intra-parenchymatous fibrous septa in the thyroid are also positive for CD38 (Fernandez *et al.*, 1998). The report of CD38 reactivity in neural cells (Mizuguchi *et al.*, 1995) is reinforced by the finding of CD38 mRNA in the brain (Takasawa *et al.*, 1993a). Evidence suggested that CD38 is down-modulated during differentiation into immature human monocyte-derived dendritic cells and expressed again upon maturation (Fedele *et al.*, 2004). Further investigation reported that CD38 is localized to the sinusoidal domain in the plasma membrane and the inner nuclear envelope of the rat hepatocyte (Khoo and Chang, 2000; Khoo *et al.*, 2000). In addition, the cDNA for murine (Harada *et al.*, 1993) and rat (Koguma *et al.*, 1994; Li *et al.*, 1994) CD38 homologues have been isolated, and overall, the mammalian CD38 molecules show high similarity and identity of nucleotide and amino acid sequence.

1.7 ENZYMATIC ACTIVITY OF CD38

CD38 has been shown to be able to catalyze the synthesis of cADPR and NAADP, two structurally distinct calcium-mobilizing molecules (refer to reviews by Lee *et al.*, 1994a; 1997). CD38 is able to cyclize NAD^+ to produce cADPR by linking the N1 of the adenine with the anomeric carbon of the terminal ribose (Lee and Aarhus, 1991; Howard *et al.*, 1993; Lee *et al.*, 1993) as shown clearly in Figure 1.8. Subsequently, it is shown that CD38 cyclizes nicotinamide guanosine dinucleotide (NGD^+), an analog of NAD with guanine substituting for the adenine group, to produce cyclic GDP-ribose (cGDPR), a fluorescent analogue of cADPR and the site of cyclization is N7 of the guanine ring

instead of N1 of the adenine, as in cADPR (Graeff *et al.*, 1994; Graeff *et al.*, 1996). The cyclase can efficiently use NADP as substrate and, in the presence of nicotinic acid, catalyze the exchange of the nicotinamide group of NADP with nicotinic acid, producing NAADP (Aarhus *et al.*, 1995). The exchange reaction predominates at acidic conditions while, at neutral and alkaline pH, the enzyme mainly catalyzes cyclization (Aarhus *et al.*, 1995).

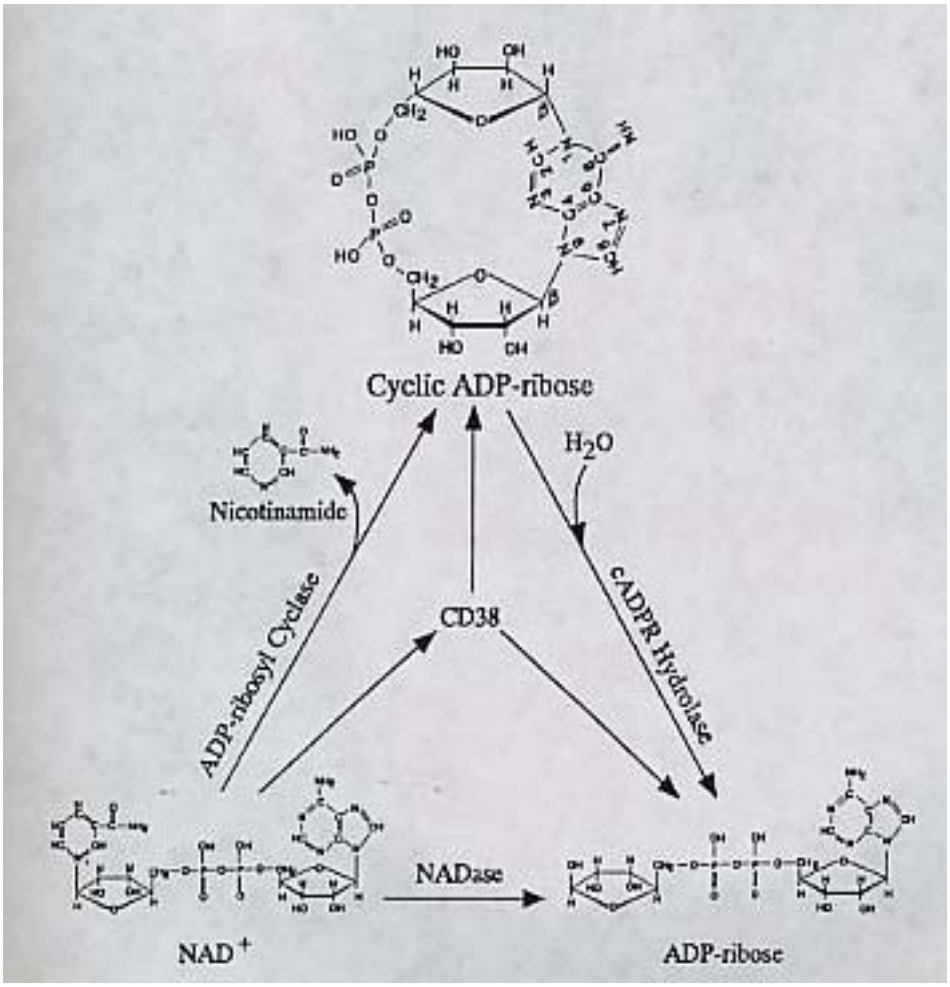

Figure 1.8 Enzymatic pathways involved in the metabolism of cyclic ADP-ribose. CD38 is a lymphocyte antigen that is also a bifunctional enzyme, catalyzing both the synthesis and the hydrolysis of cyclic ADP-ribose. (Adapted from Lee *et al.*, 1994a)

CD38 not only catalyzes the reactions described previously, it can also catalyze the hydrolysis of cADPR to ADP-ribose (ADPR) and NAD to ADPR (reviewed in Lee *et al.*, 1997a). Indeed, the main enzymatic product when CD38 is incubated with NAD is ADPR and not cADPR, the latter of which amounts to only a few percent of the products (Zocchi *et al.*, 1993; Howard *et al.*, 1993; Lee *et al.*, 1993; Takasawa *et al.*, 1993a; Kim *et al.*, 1993a). This property makes it very difficult to distinguish CD38-like enzymes from other unrelated NADases such as the NAD glycohydrolase in *Neurospora*, which neither produces cADPR nor hydrolyzes it (Lee *et al.*, 1995a). However, since neither NGD nor GDP-ribose is fluorescent, the use of NGD provides a continuous assay of cyclization and a simple diagnostic test for distinguishing CD38-like enzymes from the classical NADases as well.

In contrast to the minimal production of cADPR, CD38 catalyzes a highly efficient hydrolysis of cADPR to ADPR. CD38 is thus more appropriately considered as a specific hydrolytic rather than synthetic enzyme for cADPR. In fact, CD38 is the only known enzyme that specifically hydrolyzes the glycosidic linkage between the N1 of the adenine ring and the anomeric carbon of the terminal ribose of cADPR to produce ADPR. Many other common hydrolytic enzymes, including alkaline phosphatase, NADase and phosphodiesterase, cannot degrade cADPR (Takahashi *et al.*, 1995; Graeff *et al.*, 1997). Figure 1.9 lists a series of reactions catalyzed by the cyclase.

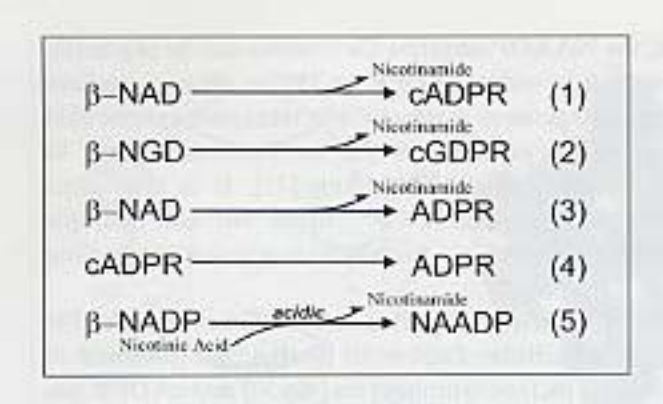

Figure 1.9 Enzymatic reactions catalyzed by the cyclase family.
(Reproduced from Lee, 2000)

1.8 REGULATION OF CD38

Zocchi *et al.* (1993) reported that the cyclase activity was found to be markedly stimulated by Cu^{2+} and Zn^{2+}, which subsequently led to the use of immobilized Cu^{2+} in a column chromatography step as an efficient method for the purification of CD38. Later, it was reported that Zn^{2+} could stimulate the ADP-ribosyl activity of recombinant human CD38 fused with a maltose binding protein (MBP-CD38) and also of the native membrane-bound CD38 of HL-60 cells induced by the addition of retinoic acid (Kukimoto *et al.*, 1996). However, such stimulation of the cyclase is in contrast to the inhibition of the apparent NAD^+-glycohydrolase activity of both MBP-CD38 and native CD38 by Zn^{2+}. This was interpreted as a negative regulation of Zn^{2+} on the accessibility of a water molecule to the ADP-ribosyl-enzyme complex (Kukimoto *et al.*, 1996), and thus was accordingly ascribed to the inhibition of the hydrolase activity rather than to the stimulation of its ADP-ribosyl cyclase activity.

Another example of the selective regulation of the enzymatic activities is from the reported inhibition of the cADPR hydrolase activity by ATP (Takasawa *et al.*, 1993a). This finding is especially interesting when one considers the fact that ATP is a candidate for correlating glucose as a stimulus for insulin secretion in islet cells and that cADPR in turn, is generated by pancreatic islets as a result of glucose stimulation (Takasawa *et al.*, 1993b). Furthermore, it has been shown that Lys-129 of CD38 participates in cADPR binding and that ATP competes with cADPR for the binding site, resulting in the inhibition of the cADPR hydrolase activity of CD38 (Tohgo *et al.*, 1997).

The study by Genazzani *et al.* (1996) gives further credence to the fact that the cADPR hydrolase activity is a selective target for inhibitory mechanisms, which will result in the increase of cADPR concentrations. In that study, it was shown that ADPR was able to decrease cADPR degradation in sea urchin eggs and to potentiate the synthesis of cADPR from NAD^+. This finding is closely reminiscent of the report by Meszaros *et al.* (1995) whereby they found that in heart muscle homogenates, the accumulation of cADPR was preceded by the generation of ADPR from NAD^+.

1.9 CD38 AND ITS INVOLVEMENT IN CA^{2+}-SIGNALING

Release of calcium from intracellular stores, endoplasmic/sarcoplasmic reticulum (ER/SR), is one of the key signal transduction mechanisms that play a pivotal role in the regulation of numerous cellular functions (Berridge, 1997). There are two major systems for Ca^{2+} release from intracellular stores (Mackrill, 1999).

1) Calcium mobilization mediated through inositol triphosphate (IP_3). The binding of certain external ligands to surface receptors can activate phospholipase C, which

will then in turn, cleave the head group of phosphatidylinositol biphosphate and produce IP_3. IP_3 in turn, will mobilize Ca^{2+} from intracellular stores upon binding to its specific receptor.

2) Calcium mobilization mediated through Ca^{2+}-induced-Ca^{2+} release (CICR). This kind of mechanism has been well characterized in cardiac myocytes whereby the influx of Ca^{2+} can itself activate further Ca^{2+} release from intracellular stores and is believed to be mediated through the ryanodine receptor.

Recently two different pyridine dinucleotides have been shown to be effective activators of intracellular Ca^{2+} stores (Clapper *et al.*, 1987). Cyclic ADP-ribose (cADPR) is a cyclic nucleotide derived from NAD^+ (Lee *et al.*, 1989) and evidence suggests that it is an endogenous modulator of the CICR mechanism in cells (Galione *et al.*, 1991; Lee, 1993). cADPR requires calmodulin (Tanaka and Tashjian, 1995) to activate calcium mobilization and calcium itself can act as a co-agonist (Lee, 1993; Lee *et al.*, 1995b). Nicotinic acid adenine dinucleotide phosphate (NAADP), a metabolite of $NADP^+$, is also a potent calcium-mobilizing agent of intracellular Ca^{2+}-stores (Clapper *et al.*, 1987; Lee and Aarhus, 1995). The Ca^{2+}-release mechanism activated by NAADP is pharmacologically different from that activated by either cADPR or IP_3 (Clapper *et al.*, 1987; Lee and Aarhus, 1995; Chini and Dousa, 1996) and the Ca^{2+}-stores NAADP acts on are separable by gradient fractionation from those sensitive to cADPR and IP_3 (Clapper *et al.*, 1987; Lee and Aarhus, 1995), indicating a hitherto unknown Ca^{2+}-signaling mechanism.

As mentioned previously, CD38 is able to catalyze the production of cADPR from NAD^+ as well as catalyzing the exchange of the nicotinamide group of $NADP^+$ with

nicotinic acid to produce NAADP (Lee and Aarhus, 1991; Howard *et al.*, 1993; Aarhus *et al.*, 1995). The fact that a single enzyme can produce two signaling molecules is reminiscent of phospholipase C, which is able to catalyze the synthesis of both IP_3 and diacylglycerol. The chemical structures of cADPR and NAADP are shown in Figure 1.10.

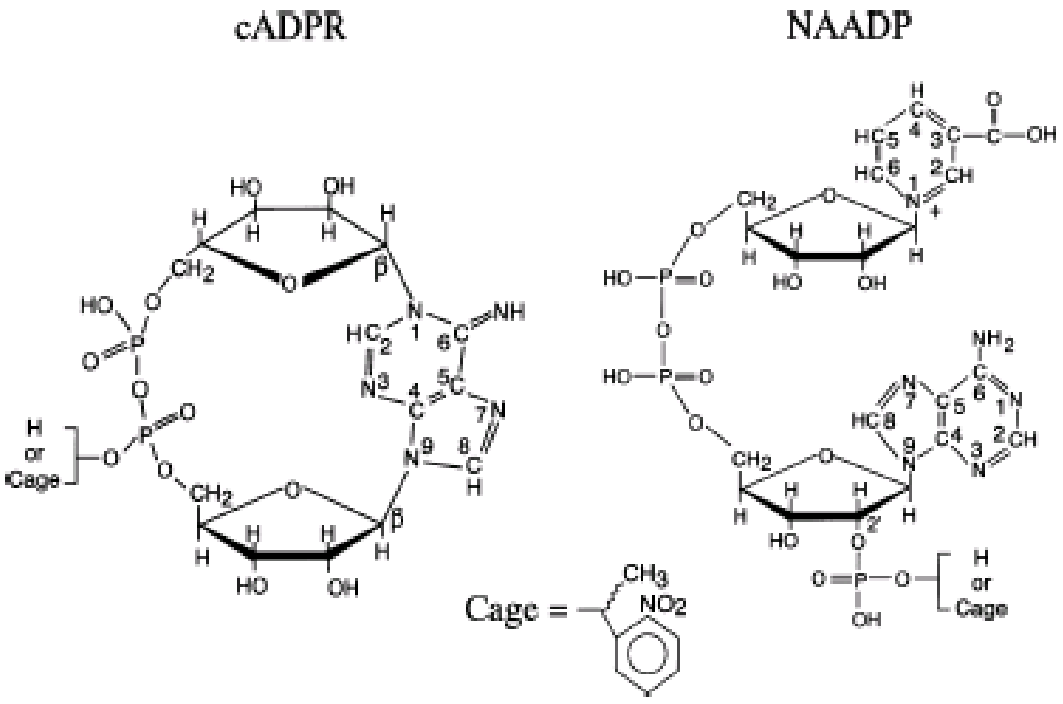

Figure 1.10 Structure of cADPR, NAADP and their caged analogs.
The structure of cADPR is based on X-ray crystallography (Lee *et al.*, 1994b). The caging group is attached to either of the phosphates. The structure of NAADP was based on measurements published previously (Lee and Aarhus, 1995) and the caging group is attached to the 2'-phosphate. (Adapted from Lee *et al.*, 1999)

The cyclic structure of cADPR is formed as a result of linking the adenine ring of NAD^+ to the terminal ribose and displacing the nicotinamide group (Lee *et al.*, 1989). X-ray crystallography results have confirmed the cyclic nature of the molecule and showed that the site of cyclization is at N1 of the adenine ring (Lee *et al.*, 1994b). Both of the ribosyl linkages to the adenine are in the β-configuration and C6 is double bonded to N6. This cyclic linkage can be hydrolyzed chemically by heat (Lee and Aarhus, 1993) as well as through the CD38 enzymatic action (Howard *et al.*, 1993; Lee *et al.*, 1993) to produce ADPR.

The other Ca^{2+}-mobilizing metabolite synthesized by CD38 is NAADP, which is a derivative of $NADP^+$ in which the nicotinamide group is replaced by nicotinic acid (Lee and Aarhus, 1995). It can be formed from $NADP^+$ chemically by an alkaline treatment (Lee and Aarhus, 1995) or enzymatically through CD38 via a base exchange reaction with NA (Aarhus *et al.*, 1995). NAADP can be readily degraded by either alkaline phosphatase, which cleaves the 2'-phosphate, or through the nucleotide pyrophosphatase enzyme, which cleaves the pyrophosphate linkage (Lee *et al*., 1997b). It can be seen then that natural synthesis and degradation pathways exist for both metabolites, which further enhance the evidence that both are signaling molecules.

1.10 CD38 AND THE IMMUNE SYSTEM

CD38 and CD31

A correlation between CD38 expression and migratory behavior was found in T cell subpopulations, consisting in a greater tendency of resting/naïve T cells ($CD4^+/CD45RA^+/CD38^+$) to emigrate from blood to lymph nodes than activated/memory

T cells ($CD4^+/CD45RO^+/CD38^-$) (Dianzani *et al.*, 1994). These findings led to a large collaborative effort investigating the possible role of CD38 in adhesion. Anti-CD38 mAbs were found to inhibit T and B lymphocyte binding to endothelial cells (EC) using an assay optimized to reveal non-integrin-mediated cell adhesion (Deaglio *et al.*, 1998). This inhibition was operative on the lymphocyte side because vascular and lymphatic EC do not express CD38 (Fernandez *et al.*, 1998). Using the same assay with a panel of anti-EC mAbs, a counter-receptor on EC cells was identified to be CD31 (PECAM-1), a member of the immunoglobulin superfamily (Deaglio *et al.*, 1998). Biochemical support for the CD38/CD31 interaction came from the finding that purified soluble CD38 bound to a 130-kDa protein from U937 cells and that binding could be inhibited by several anti-CD31 mAbs (Horenstein *et al.*, 1998). This interaction also plays a role in cytotoxicity, an independent observation that emerged while studying the effects of the tumoricidal potential of the T-ALL 104 human cell line (Cesano *et al.*, 1998).

A clue to assessing the physiological relevance of the CD38/CD31 interaction has come from a disease model. It is suggested that the engagement of CD38 by CD31 plays a role in the retinoic acid syndrome (RAS), a life-threatening complication of ATRA therapy in acute myeloid leukemia. A significant proportion of patients given ATRA for acute promyelocytic or myeloblastic leukemia develop acute respiratory distress caused by massive pulmonary infiltration with newly differentiated granulocytes (Mehta *et al.*, 1996). Normal granulocytes or dimethyl sulfoxide-treated leukemic cells are $CD38^-$ but a single dose of ATRA induces strong CD38 expression in the leukemic cells (Drach *et al.*, 1994), leading to the speculation that their interaction with CD31 on lung endothelium represents an important pathogenetic factor.

Transmembrane signaling in T-cells

The first hint that CD38 might be playing an important role in signaling came from the observation that ligation of CD38 on peripheral blood mononuclear cells and T-cell lines with certain anti-CD38 monoclonal antibodies induced activation and proliferation signals (Funaro *et al.*, 1990). Subsequent experiments revealed that this ligation is also able to induce the transcription of various cytokines including that of interleukin-1 (IL-1), tumor necrosis factor-alpha and granulocyte-macrophage colony-stimulating factor at levels similar to that obtained after triggering the T cell receptor CD3. However, the cytokines triggered in response to CD38 are qualitatively distinct from those induced via CD3 (Ausiello *et al.*, 1995).

CD38-mediated cytokine induction did not require either T-cell proliferation or the addition of antigen-presenting cells. Furthermore, it was also observed that signaling via CD38 in a T-cell acute lymphoblastic leukemia (Jurkat) cell line led to calcium mobilization kinetics that were distinct from those induced via the T-cell receptor CD3 (Deaglio *et al.*, 1996). This raises the possibility that certain signaling pathways mediated by CD38 are distinct from that activated by CD3. Incubation of peripheral blood T-cells or Jurkat cells with the agonistic anti-CD38 mAb, IB4, has been shown to be able to trigger signaling pathways that lead to activation and proliferation (Funaro *et al.*, 1990), increase intracellular calcium levels, down-modulation of the TCR/CD3 complex, up-regulation of CD5, CD28, CD69 and CD95 as well as cell death by apoptosis (Morra *et al.*, 1998). CD38 ligation is also able to induce tyrosine phosphorylation of a variety of cellular substrates including that of phospholipase C-γ1, c-cbl, ζ-associated protein (ZAP)-70, Shc, extracellular signal-regulated protein-kinase-2 (Erk-2), and CD3-ζ. In

comparison, the phosphorylation induced by anti–CD3 was both qualitatively and quantitatively different (Zubiaur *et al.*, 1997).

Transmembrane signaling in B-cells

The B-cell receptor (BCR) is also necessary for CD38-mediated signaling in B lymphocytes, at least in mouse (Lund *et al.*, 1996) although the same mechanism has yet to be proven conclusively in human cells. Proliferation has been shown to be activated in splenic B-cells in response to IB4 mAb (Funaro *et al.*, 1997). Addition of anti-CD38 mAbs (either IB4 or T16) to normal bone marrow B cells (>90% $CD38^+$) co-cultured on stromal layers (mostly $CD38^-$ but $CD157^+$) drastically reduces the number of cells recovered after a 7-day culture period (Kumagal *et al.*, 1995). However, this effect does not occur with circulating or tonsillar B cells (Kumagal *et al.*, 1995).

The interesting thing is that the result of CD38 ligation in mature B-cells is markedly different. It has been shown that tonsillar germinal center B-cells ($CD38^+$/$sIgG^+$) incubated with IB4 mAb have prolonged cell survival rates due to the inhibition of apoptosis and up-regulation of bcl-2 has also been observed (Zupo *et al.*, 1994). The pathway activated via CD38 in these cells is neither addictive nor synergistic with the CD40-CD40L pathway (Zupo *et al.*, 1994). The signal transduction events triggered by T16 mAb in immature B-cells include phosphorylation of c-cbl, PLC-γ1, phosphatidylinositol 3-kinase (PI3-K) p85 subunit, and protein kinase *syk* (Silvennoinen *et al.*, 1996). A further effect of CD38 ligation is phosphorylation of CD19 and induction of its association with *lyn* and PI3-K (Kitanaka *et al.*, 1997). Indeed, both CD38- and CD19-mediated signaling pathways would seem to overlap as they induce similar

patterns of protein tyrosine phosphorylation. CD38 engagement leads to down-regulation of CD19 (Kitanaka *et al.*, 1997).

Transmembrane signaling in myeloid and natural killer cells

CD38 ligation on retinoic acid-induced differentiated HL-60 cells resulted in an increase of superoxide generation by G protein-coupled receptors (Tsujimoto *et al.*, 1997) as well as causing the tyrosine phosphorylation of c-cbl, *syk*, HS1 and FcγRII (Inoue *et al.*, 1997). Another process which CD38 might be involved is the proliferation of T lymphocytes in response to super-antigen whereby the engagement of CD38 on monocytes inhibits the T cell proliferation induced by *Staphylococcus* enterotoxin A or toxic shock syndrome toxin-1 (refer to review by Ferrero and Malavasi, 1999). The cytotoxic activity of peripheral blood natural killer cells mediated by granule exocytosis can be triggered by anti-CD38 upon activation with IL-2 (refer to review by Ferrero and Malavasi, 1999).

1.11 CD38 AND THE DISEASE MODEL

In view of the fact that CD38 seems to be involved in a myriad of immune-regulatory functions in a multitude of hematopoietic cell populations, it is no surprise to know that there was a spate of recent discoveries regarding the association of CD38 with certain human diseases. More than a decade ago, it was observed that in AIDS patients, $CD8^+$ T-cells have an increased expression of CD38 (Salazar-Gonzales *et al.*, 1985). It was subsequently shown that the expansion of these cells preceded the decline in $CD4^+$ T-cells and the development of AIDS (Bofill *et al.*, 1996). This observation was further expanded by some researchers who used CD38 as a useful and reliable prognostic marker

for the pathological development of AIDS (Liu *et al.*, 1998). However, CD38 may also be more directly involved in AIDS pathogenesis as there is a report postulating an inhibitory role of CD38 in HIV binding to CD4 (Savarino *et al.*, 1996).

Zupo *et al.* (1996) reported that B-chronic lymphocytic leukemia (B-CLL) patients can be subdivided into two different groups depending on the presence or absence of CD38 on the malignant cells. *In vitro* exposure of these malignant cells with high CD38 expression to anti-μ antibodies (antibodies raised against the *mu* heavy chains of IgM) resulted in calcium mobilization followed by apoptosis, while neither of these phenomena was observed in the CD38-negative cells. These data suggest that CD38 expression can be utilized as a marker for B-cells that have a propensity for apoptosis. The fact that normal germinal center B-cells (Zupo *et al.*, 1994) and the malignant cells of Burkitt's lymphomas (Cutrona *et al.*, 1995), both of which express abundant CD38, are prone to apoptosis.

Bruton's disease or X-linked agammaglobulinemia (XLA) is characterized by a reduced concentration of serum Ig secondary to a dramatic decrease of circulating B-cells (refer to review by Conley, 1992). The gene responsible for XLA is Bruton's tyrosine kinase (Btk), which encodes a protein sharing similar features with the *src* tyrosine kinase family. The precise function of Btk is currently unknown but is thought to be involved in mediating signal transduction after cell activation (refer to review by Bolen, 1993). Results derived from X chromosome-linked immunodeficient mice (Xid, the homologue of human XLA) indicate a close relationship between Btk and CD38. Purified splenic B-cells from Xid mice were totally unresponsive to stimulation via CD38 in the presence of accessory stimuli, even though the expression and catalytic functions of CD38 on these

cells were comparable to wild-type B-cells (Santos-Argumedo *et al.*, 1995). It was also reported that B-cells from Xid mice did not respond to signaling via CD38, which was coupled in turn, to the complete absence of tyrosine phosphorylation of Btk (Kikuchi *et al.*, 1995). It is thus believed that CD38 plays an important role in the life of B-cells, although a direct physical association between Btk and CD38 has not been observed (Santos-Argumedo *et al.*, 1995).

CD38 has been shown to play an important regulatory role in the murine model with regards to insulin secretion via calcium mobilization of cADPR-sensitive stores (Kato *et al.*, 1995). The studies on the causal relationship between CD38 and insulin release has been extrapolated to man where it was shown that autoantibodies to CD38 might be playing a key role in impaired glucose-induced insulin secretion (Ikehata *et al.*, 1998). Then, it was shown that the Arg140Trp mutation on CD38 might be responsible for the development of Type II diabetes mellitus via the impairment of glucose-induced insulin secretion (Yagui *et al.*, 1998). Recently, experiments using CD38 knockout mice corroborated the growing evidence that CD38 is essential in intracellular Ca^{2+}-mobilization via cADPR for the secretion of insulin (Kato *et al.*, 1999).

The considerably poor prognosis of myeloma has prompted the use of radical treatments involving immunotoxins and hormonotoxins. However, the use of antibodies or hormones conjugated with modified toxins, which targets surface molecules on myeloma cells is hampered by the inherent lack of specificity. An interesting alternative method used the increased expression of CD38 in these myeloma cells as a target for the *in vivo* and *in vitro* depletion of tumor cells (Ellis *et al.*, 1995). It is shown that recombinant anti-CD38 mAb with a murine anti-CD38 variable region mounted on a

human IgG Fc sequence cross-linked to a modified ricin molecule (Stevenson *et al.*, 1991). Another approach entailed the use of bispecific antibodies for the delivery of other toxins in human acute T-cell lymphoblastic leukemia via CD7 and CD38 as target molecules (Flavell *et al.*, 1992). CD22 and CD38 as target molecules for bispecific antibodies in the immuno-treatment of lymphoma have also been used (French *et al.*, 1995). A similar approach was tested for the treatment of B-cell lymphoma using anti-CD19 and anti-CD38-saponin immunotoxins (Flavell *et al.*, 1995).

The results obtained from these studies suggest that anti-CD38-toxin immunoconjugates might prove to be useful therapeutic tools in the treatment of myeloma, leukemia and lymphoma. In each and every case, it has been proven that the toxic potential on tumor cells with higher expression of CD38 was significant, whereas effects on normal peripheral blood cells or hematopoietic progenitor cells were negligible (refer to review by Mehta *et al.*, 1996).

1.12 OBJECTIVES OF THE STUDY

To date, the function of CD38 in liver cirrhosis is still unknown. Therefore, the objective of this study is to characterize the role of CD38 in liver cirrhosis. To investigate this, thioacetamide-induced rat model of liver cirrhosis was generated. Control and cirrhotic rat livers were isolated for the determination of CD38 transcript (mRNA) and protein level. This was done by using a variety of methods:

1) Real time reverse transcriptase – polymerase chain reaction (RT-PCR)
2) Immunohistochemistry method in conjuction with confocal microscopy technique

3) Biochemical and immunological characterization via the use of enzymatic assays and immunoblotting

We went on further to investigate the cADPR and NAD^+ levels by using cycling assay. The data gathered, in conjunction with previous studies on CD38, are expected to provide special insight into the physiological, cellular and functional role of CD38 in liver cirrhosis and hopefully shed more light into the currently unresolved questions facing researchers in the CD38 field.

CHAPTER 2

MATERIALS AND METHOD

2.1 Materials

2.1.1 Chemicals and Reagents

Standard analytical grade laboratory chemicals for the preparation of general reagents were obtained from BDH, Poole, England; Merck, Darmstadt, Germany; Sigma Chemicals Co., St. Louis, MO, USA and J.T. Baker, Phillipsburg, NJ, USA. Special reagents were obtained from:

Bio-Rad, Hercules, CA, USA.
Bio-Rad Protein Assay Kit
Nitrocellulose membrane (0.2 μm)
Polyacrylamide gel reagents
Bio-Safe Coomassie Blue G250
Precision Plus Protein™ Standards All Blue (protein marker) for SDS-PAGE

Sigma, St. Louis, MO, USA.
Thioacetamide
Leupeptin
Phenylmethylsulfonyl fluoride
Soybean trypsin inhibitor
BSA
DEPC
NADase
cADPR
ADP-ribosyl cyclase
NAD^+
NGD^+
Nicotinamide
Alcohol dehydrogenase
Resazurin
Diaphorase
FMN
β-mercaptoethanol

Amersham Biosciences, Buckinghamshire, England.
Blue Sepharose CL-6B
Concanavalin (Con) A-Sepharose
ECL™ Western blotting detection reagents

Applied Biosystems, Cheshire, UK.
SYBR Green PCR master mix
Real-time PCR supplied materials

Invitrogen, Carlsbad, CA, USA.
TRIzol
Superscript II RNase H^- Reverse Transcriptase

Roche, Penzberg, Germany.
RNase-free DNase 1

Promega, Madison, WI, USA.
PCR reagents
100 bp DNA marker

Spectrum Chemical, Gardena, CA, USA.
Perchloric acid

2.1.2 Commercial Antibodies

Santa Cruz Biotechnology Inc., Santa Cruz, CA, USA.
Goat polyclonal anti-rat CD38 (M-19)

Sigma, St. Louis, MO, USA.
Horseradish peroxidase-conjugated rabbit anti-goat IgG
FITC-conjugated rabbit anti-goat polyclonal

2.1.3 Instruments and General Apparatus

1. **Beckman Avanti™ J-20 XP Centrifuge** (Beckman Instruments Inc., Palo Alto, CA, USA)
2. **Beckman DU® 640B Spectrophotometer** (Beckman Instruments Inc., Palo Alto, CA, USA)
3. **Beckman Ultracentrifuge XL-100** (Beckman Instruments Inc., Palo Alto, CA, USA)
4. **BellyDancer®/Hybridization Water Bath** (Stovall Life Sciences Inc., Greensboro, NC, USA)
5. **Biometra Thermocycler** (Biometra, Goettingen, Germany)
6. **Mini-Sub® Cell GT Cell** (Bio-Rad, Hercules, CA, USA)
7. **ABI Prism 7000 Sequence Detection System (Real-Time PCR Machine)** (Applied Biosystems, Cheshire, UK)
8. **Eppendorf Centrifuge 5415 R** (Eppendorf-Netheler-Hinz GmbH, Hamburg, Germany)
9. **Constant Voltage Power Supply Model 200/2.0** (Bio-Rad, Hercules, CA, USA)
10. **Mini-PROTEAN® II Cell** (Bio-Rad, Hercules, CA, USA)
11. **Mini Trans-Blot® Cell** (Bio-Rad, Hercules, CA, USA)
12. **FluoView 300 Laser Scanning Microscope** (Olympus, Melville, NY, USA)
13. **Histostat Microtome** (American Opticals, USA)
14. **SpectraMax Gemini Fluorescence Reader** (Molecular Devices, Sunnyvale, CA, USA)
15. **Centricon-3 Filters** (Millipore, Bedford, MA, USA)

16. **Centriprep 30** (Millipore, Bedford, MA, USA)
17. **Ultra-Turrax T25 Tissue Homogenizer** (Janke and Kunkel, Staufen, Germany)
18. **PRO 200 Homogenizer** (PRO Scientific, Oxford, CT, USA)
19. **LS 50B Luminescence Spectrophotometer** (Perkin Elmer, Foster, USA)

2.2 Animals

Male Wistar rats weighing 250-280 g were obtained and kept in the animal holding facilities. All animals were housed under controlled conditions of temperature, humidity, light cycle (12-h cycle), and fed with standard laboratory chow and water *ad libitum*. The animals used in the present study were divided into 2 groups: control (20 rats) and thioacetamide (TAA)-treated (25 rats). The treated group was injected intraperitoneally (i.p.) with thioacetamide freshly dissolved in sterile water at a dose of 300 mg/kg body weight, twice a week for 10 weeks. Control group received the similar volume of sterile water. Thioacetamide was prepared at the concentration of 0.1 g/ml and was stored in a bottle wrapped with aluminium foil due to light sensitivity. The animals were allowed to rest for one week before being sacrificed for the subsequent experiments. Animals were treated following the standard procedures indicated in the "Responsible Care and Use of Laboratory Animals" published by National University of Singapore.

2.3 Perfusion of Rats

The rats were perfused with a periodate-lysine-paraformaldehyde (PLP) fixative according to the method of McLean and Nakane (1974). Briefly, the fixative was made by initially mixing 10.96 g of L-lysine to 300 ml of distilled water. This was followed by

the addition of 0.1 M di-sodium hydrogen orthophosphate 2-hydrate ($Na_2HPO_4 . 2H_2O$) until the pH of the solution reached 7.4 (approximately 100 ml was added). Subsequently, 200 ml of phosphate buffer (pH 7.4) was added to the solution. Finally, paraformaldehyde (2% final concentration) and 1.712 g of sodium-m-periodate were added to make up a final 800 ml of fixative solution.

For the perfusion of an adult rat, the animal was sacrificed after anesthesia with 7% sodium chloral hydrate. The animal was laid on its back and the thorax opened carefully to avoid excessive bleeding. The rib cage was cut through carefully and the diaphragm was removed for easy access to the heart. A phosphate-buffered saline (PBS)-filled syringe with an attached 23-G needle was carefully inserted into the left ventricle and at the same time, the right ventricle was cut for drainage allowing the PBS to be slowly but constantly perfused into the heart (Figure 2.1). After most of the blood has been flushed out, the syringe was removed and the syringe filled with the fixative was inserted into the same puncture of the left ventricle. The animal was then slowly perfused with the fixative. Following perfusion, the liver was dissected out and transferred into labeled glass vials filled with the same fixative and further post-fixed for one hour before infiltrated with 15% sucrose in PBS pH 7.4 overnight at 4°C. The rat liver tissues were then frozen at -45°C using isopentane cooled by liquid nitrogen and embedded in Tissue Tek (Miles, Elkhart, IN). Cryostat sections of 10 μm were cut from the frozen tissues using a Histostat Microtome (American Opticals, USA) and placed on gelatin-coated slides. The sections were dried in the air and kept frozen at -80°C until all slides were ready for processing.

2.4 Liver Histopathology

Histopathology of the livers from both control and TAA-treated rats was investigated according to a previously described procedure (section 2.3). Briefly, pieces of hepatic tissues from control and TAA-treated rats were fixed in 2% paraformaldehyde in phosphate-buffered saline and were processed for cryostat sectioning. Sections of about 10-μm thickness were stained with haematoxylin and eosin (H & E) to study the general structure of the liver.

2.4.1 Haematoxylin and Eosin (H & E) staining

The fixed slides were immersed in 10% formalin for overnight. Following day, the slides were left in each solution for approximately 10 seconds (with agitation) using the following order; deionised water (2 changes), 50% alcohol, 70% alcohol, 90% alcohol, absolute alcohol II, absolute alcohol I, equal parts of xylene and absolute alcohol, xylene II and xylene I. Next, the slides were left in Haematoxylin stain which had been filtered, for 15 minutes. The slides were washed in deionised water and differentiated in differentiating fluid (70% alcohol with a few drops of HCl) for a few to 30 seconds, depending on the tissue. The slides were rinsed in deionised water and differentiation was checked under the microscope. The slides were immersed in the differentiating fluid again if under differentiated or washed thoroughly in water, then re-stain if over differentiated. Then, sections were blued in tap water for 15 minutes and rinsed with deionised water. It was followed by Eosin staining (1-3% Eosin dissolved in water) for 10 minutes. The slides were dehydrated quickly in 90% alcohol, 3 changes of absolute alcohol, equal parts of absolute alcohol and xylene, and 3 changes of xylene. The sides of the slides were wiped and were mounted with an addition of a drop of Permount and a

coverslip was placed over the section. The slides were then viewed under a light microscope at low magnification to compare the liver structure of control with that of TAA-treated rats.

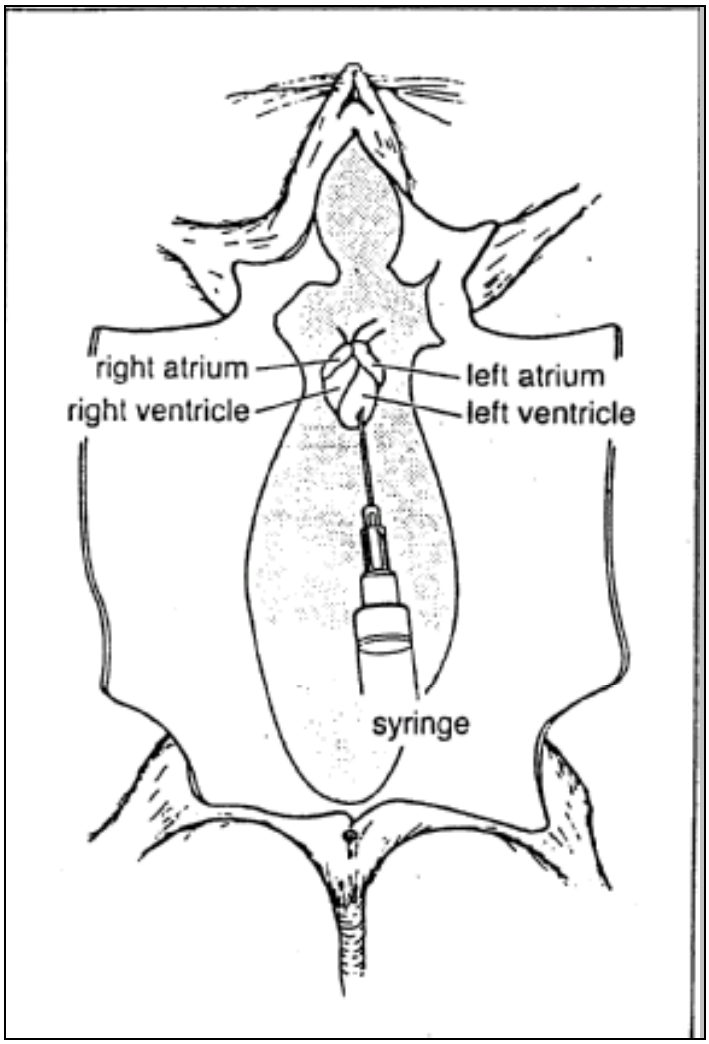

Figure 2.1 Perfusion of a rat.
This diagram illustrates the chambers of the heart and the correct positioning of the syringe in the left ventricle for perfusion. (Adapted from Khoo, 1999)

2.5 Detection of CD38 mRNA Expression

CD38 expression at transcript level of both control and TAA-treated rats was investigated using a conventional two-step RT-PCR and the changes in CD38 expression between the control and TAA-treated rats were then confirmed in real-time quantitative RT-PCR. Ribosomal RNA (rRNA) was used as endogenous/internal control due to its relatively invariant during the course of the experimental manipulation.

2.5.1 Total RNA extraction from rat liver

Liver tissues from control and TAA-treated rats were frozen in liquid nitrogen and weighed prior to total RNA extraction using TRIzol (Invitrogen, Carlsbad, CA, USA) as per manufacturer's protocol. Briefly, 1 ml of TRIzol reagent was used for extraction of every 50 mg of liver tissues. The tissues were homogenised on ice using an Ultra-Turrax T25 homogenizer (Janke and Kunkel, Germany). The homogenate was incubated at room temperature for 5 minutes to permit the complete dissociation of nucleoprotein complexes, following which 200 μl of chloroform was added per ml TRIzol reagent used for the extraction. The mixture was then shaken vigorously for 15 seconds and incubated for another 3 minutes at room temperature before being subjected to centrifugation at no more than 12,000 X g for 15 minutes at 4°C. The solution was separated into a lower red, phenol-chloroform phase (organic phase), an interphase, and a colorless upper aqueous phase, in which RNA resides. This aqueous layer was carefully transferred into a clean eppendorf tube and incubated at 37°C for 15-20 minutes with 3 μl RNase-free DNase 1 (Roche, Penzberg, Germany) and 30 μl of 1 M magnesium chloride. Following removal of contaminating DNA, 500 μl of isopropyl alcohol (isopropanol) per ml TRIzol reagent used for the initial homogenization was added to precipitate RNA and also to remove

DNase 1. The mixture was then incubated at room temperature for 10 minutes and subsequently subjected to centrifugation at no more than 12,000 X g for 10 minutes at 4°C. The supernatant was later discarded and 1 ml of ice-cold 75% ethanol was added to wash the pellet by vortexing and followed by centrifuging at no more than 7,500 X g for 5 minutes at 4°C. Upon removal of the ethanol, the RNA pellet was air-dried for 10 minutes prior to dissolving in 50 µl of DEPC-treated water (RNase-free water). Each RNA sample was stored at –80°C in small aliquots in DEPC-treated water. To prepare RNase-free water (DEPC-treated water), MilliQ water was drawn into RNase-free glass bottle. 0.1% diethylpyrocarbonate (DEPC) was added to the water which will inactivate any ribonucleases (RNases) that are present by covalent modification. Then, it was allowed to stand overnight and was autoclaved on the following day to inactivate the DEPC.

2.5.2 RNA quantitation

5 µl of RNA extract was diluted with 495 µl (1:100) DEPC-treated water and the absorbance was measured at 260 nm using a DU640B Spectrophotometer (Beckman, USA). Given, 1 OD_{260nm} = 40 µg RNA/ml. The RNA concentration was calculated as follows; [RNA] = OD_{260nm} x 100 (dilution factor) x 40 µg RNA/ml. The ratio of OD_{260nm}/OD_{280nm} was also analysed to assess the purity of the RNA extract. Typically, a ratio of 1.8 - 2.0 is deemed pure.

2.5.3 RNA gel electrophoresis

The RNA integrity and purity were analyzed by RNA gel electrophoresis. 0.5 g agarose was boiled in 43.5 ml DEPC-treated water and subsequently allowed to cool down to about 60°C prior to the addition of 5 ml of 10X MOPS buffer (0.4 M MOPS, pH 7; 0.1 M

sodium acetate, 0.01 M EDTA), 0.8 ml of 37% formaldehyde, and 1 μl of 10mg/ml ethidium bromide. Sample preparation was carried out by mixing 5 μg of RNA samples with 3 μl of 10X MOPS buffer, 3 μl of 37% formaldehyde, 10 μl of deionised formamide and RNA loading buffer (Sigma, St. Louis, MO, USA), used in a ratio of 1:2 with respect to the volume of RNA sample added. The mixture was heated at 65°C for 10 minutes before loaded into the wells. The samples were allowed to separate on the gel that was run at 80 volts using 1X MOPS as running buffer (1 – 2 hours).

2.5.4 Two-step reverse transcriptase – polymerase chain reaction (RT-PCR)

Residual genomic DNA was removed by incubating the RNA samples with RNase-free DNase I (Roche, Penzberg, Germany) prior to RNA precipitation by isopropanol according to the method described in section 2.5.1. Isolated total RNA was quantified using Beckman DU® 640B Spectrophotometer (Beckman Instruments Inc., Palo Alto, CA, USA) and equal amounts (5 μg) from control and TAA-treated animals were used for RT-PCR.

Total RNA was reverse transcribed using random hexamers and oligo (dT) primers to synthesize first strand cDNA from the mRNA using Superscript II RNase H^- Reverse Transcriptase (Invitrogen) following the manufacturer's directions. Briefly, a 20-μl reaction volume was prepared by mixing total RNA with oligo (dT)/random hexamers, dNTP mix, 5 X first-strand buffer, DTT, Superscript II and nuclease-free water. Reverse transcription reaction was carried out at 42°C for 50 minutes and the first-strand cDNA synthesized was subjected to PCR. The PCR primers were as follows:

CD38 forward primer, 5' CTCAGTGAGCCATTTTAC 3';

CD38 reverse primer, 5' TCACACATTAAGTCTACATG 3';

28S rRNA forward primer, 5’ GGCCAAGCGTTCATAGCGAC 3’;

28S rRNA reverse primer, 5’ GAGGCGTTCAGTCATAATCC 3’.

PCR was performed in a final volume of 50 µl in a Biometra thermocycler (Goettingen, Germany) under the following conditions: 94°C for 5 minutes denaturing, 30 cycles of 94°C for 30 seconds, 53°C for 30 seconds (CD38 primers) or 62°C for 30 seconds (28S rRNA primers), 72°C for 30 seconds, and a final extension at 72°C for 2 minutes. Samples without reverse transcriptase were used as negative controls and rat 28S rRNA was used as internal control. The amplification products were separated on ethidium bromide stained 1% agarose gels at 100V for 45 minutes. The product size was then determined by concurrently separating a 100-bp DNA ladder on the gel and visualized under UV transillumination. The intensity of the bands was quantified by densitometry using Analytical Imaging Station (Ontario, Canada) and the results were expressed as the ratio of intensity of PCR products of CD38 to that of 28S rRNA in samples from control and TAA-treated rats.

2.5.5 Real-Time Quantitative PCR

Real-time Polymerase Chain Reaction (PCR) offers researchers a powerful tool for the quantitation of target nucleic acids and has the ability to monitor the progress of the PCR as it occurs (i.e., in real time). Data is therefore collected throughout the PCR process, rather than at the end of the PCR. This completely revolutionizes the way one approaches PCR-based quantitation of DNA and RNA. In real-time PCR, reactions are characterized by the point in time during cycling when amplification of a target is first detected rather than the amount of target accumulated after a fixed number of cycles. The higher the starting copy number of the nucleic acid target, the sooner a significant increase in

fluorescence is observed. In contrast, an endpoint assay (also called a "plate read assay") measures the amount of accumulated PCR product at the end of the PCR cycle.

In the present study, quantitative real-time PCR was performed using SYBR Green PCR master mix (Applied Biosystems, Cheshire, UK), which uses SYBR Green I dye, a highly specific double-stranded DNA binding dye, to detect PCR product as it accumulates during PCR cycles. Total RNA from control and TAA-treated rat livers was converted to first strand cDNA by reverse transcription. PCR was then carried out in a total volume of 25 µl consisting of SYBR Green mix, first strand cDNA, forward and reverse primers, and sterile water. The CD38 and 18S rRNA (internal control) primers were used:

CD38 forward primer, 5' GAAAGGGAAGCCTACCACGAA 3';

CD38 reverse primer, 5' GCCGGAGGATTTGAGTATAGATCA 3';

18S rRNA forward primer, 5' ATGGCCGTTCTTAGTTGGTGGAGTG 3';

18S rRNA reverse primer 5' GTGTGTACAAAGGGCAGGGACGTA 3'.

The primers were designed based on the sequence data obtained from the NCBI database (http://www.ncbi.nlm.nih.gov/), using Primer Express® Software v2.0 (Applied Biosystems). All the samples were run using ABI Prism 7000 (Applied Biosystems) in triplicates under the following conditions: 50°C for 2 minutes, 95°C for 10 minutes, 40 cycles of 95°C for 15 seconds, 60°C for 1 minute, and a final extension at 60°C for 2 minutes. The readings were normalized on the basis of its 18S rRNA content and the relative quantitation was performed using a calculation method known as comparative C_t method. Results of the real-time PCR were expressed as $2^{-\Delta\Delta Ct}$, and the expression level of CD38 was indicated by the number of cycles required to achieve the threshold level of

amplification. The $2^{-\Delta\Delta Ct}$ value from control rats was compared with that of TAA-treated rats.

2.6 Immunohistochemistry

Immunohistochemical localization of cellular molecules is based on the ability of antibodies to bind specific antigens (usually proteins) with high affinity. The techniques may be used to localize antigens to subcellular compartments or individual cells within tissues, which is indeed our aim with regards to CD38 in this study.

2.6.1 Immunohistochemical localization of CD38 in rat liver

For immunofluorescence studies involving control and TAA-treated rats, liver tissues were fixed in PLP and processed for cryostat sectioning as described previously. The frozen slides were immediately thawed in phosphate buffered solution (PBS) and washed with PBS for three times. The sections were then incubated with PBS buffer containing 10% bovine serum albumin (BSA) for 2 hours at room temperature as a blocking agent to minimize non-specific binding. Next, the sections were incubated overnight at 4°C with goat polyclonal antibodies against rat CD38 at a dilution of 1:100 in 10% BSA, rinsed four times with PBS buffer and incubated for 2 hours with the corresponding secondary FITC-conjugated anti-goat polyclonal antibody diluted at 1:100 in 10% BSA. After final wash with PBS buffer for four times, the slides were mounted with Vectashield Mounting Medium (Vector Lab, Burlingame, USA) and viewed under confocal microscope.

The optimal incubation time and dilution of antibodies, defined as the highest dilution producing maximal staining and minimal background were determined for all batches of antibodies and conjugates. All experiments were repeated at least twice and slides were

made in duplicate. Negative controls with the omission of primary antibody were carried out.

2.7 Confocal Microscopy

Confocal microscopy was performed using a FluoView 300 laser scanning microscope (Olympus, Melville, NY) at low (20 x Fluar objective) and high (60 x Fluar objective, oil immersion) magnifications. Excitation of the FITC fluorescent dye was performed at 488 nm and the emission signal was collected with BP 510-550 emission filter. The quantification of fluorescent dye for both control and TAA-treated rat liver tissues was done using Image-Pro Plus Version 4.5 (Media Cybernetics, North Reading, MA).

2.8 Isolation of Microsomal Fraction

Microsomal fractions were isolated (at 0-4°C) from control and TAA-treated rat liver tissues according to a modified method described by Kim *et al.* (1993). Rat livers were minced with scissors and homogenized using Ultra-turrax T25 tissue homogenizer (Janke and Kunkel, Staufen, Germany) in 4 volumes of homogenization buffer containing 20 mM Hepes (pH 7.2), 1 mM MgCl, 0.1 mM phenylmethylsulfonyl fluoride, leupeptin (10 μg/ml), aprotinin (10 μg/ml), and soybean trypsin inhibitor (50 μg/ml). The homogenate was centrifuged at 8000 X g for 15 minutes at 4°C. The supernatant was saved and the pellet was resuspended in 2 volumes of homogenization buffer. The resulting suspension was then centrifuged as above. The first and second supernatants were pooled and further centrifuged at 100,000 X g for 45 minutes at 4°C. The pellet containing the microsomal fraction was resuspended in 2 volumes of homogenization buffer by 15 passes of Dounce

glass homogenizer with a loose-fitting pestle followed by another 15 passes of tight-fitting pestle. The suspension was solubilized by adding 2 volumes of homogenization buffer containing 4% Triton X-100 and allowed to stand for 1 hour (with occasional agitation). After centrifuging the suspension at 100,000 X g for 45 minutes, the supernatant was collected and the protein content was determined in duplicates using the Bio-Rad protein assay kit (Bio-Rad, Hercules, CA, USA), with bovine serum albumin (BSA) as the standard. In another set of experiment, the solubilized microsomal fraction was subjected to purification (section 2.9) via affinity chromatography to obtain positive control for subsequent experiments.

2.9 Purification of CD38

The purification and analysis of proteins are integral to designing oligonucleotide probes for gene cloning, confirming DNA sequence data and synthesizing peptides for eliciting anti-peptide antibodies. The principle methods that were used in this study have its basis in bioproperties or affinity of the protein in question. This powerful method for separating the protein of interest from others depends on the uniqueness of particular or specific biological properties of the protein to be studied. Most desired proteins have a specific ligand and immobilization of the ligand to which the protein binds or of an antibody to the protein enable selective adsorption of the desired protein to the technique known as affinity chromatography.

CD38 was purified for the preparation of positive control from microsomes of rat liver tissues that were isolated according to the method described in section 2.8. The resulted supernatant, which consists of the solubilized microsomal fraction, was subjected

to a series of column chromatography, in the order of Blue Sepharose CL 6B, copper-iminodiacetic acid-agarose (Cu^{2+}-IDA), and concanavalin (Con) A-sepharose. These various affinity columns have previously been shown to be highly selective for the purification of CD38 (Kim *et al.*, 1993a; Zocchi *et al.*, 1993).

Blue Sepharose CL-6B is Cibacron Blue 3G-A covalently attached to Sepharose CL-6B by the triazine coupling method. The structure of the blue dye in Blue Sepharose mimics that of NAD^+ and thus it binds to enzymes that require adenyl-containing cofactors including CD38, which uses NAD^+ as a substrate for both its ADP-ribosyl cyclase and NADase enzymatic activities.

The discovery of the cyclase activity of CD38 being stimulated by Cu^{2+} has led to the use of Cu^{2+} immobilized in a column for the purification of CD38 (Zocchi *et al.*, 1993).

Concanavalin A (Con A) is a lectin which binds reversibly to molecules which contain α-D-mannopyranosyl, α-D-glucopyranosyl and sterically related residues. Therefore, it is useful for separation and purification of glycoproteins, polysaccharides and glycolipids. Con A has also been used in the purification of enzyme-antibody conjugates, purification of IgM, isolation of cell surface glycoproteins from detergent-solubilized membranes, separation of membrane vesicles, and the study of changes in composition of carbohydrate-containing substances.

2.9.1 Purification of CD38 from the rat liver

The solubilized microsomal fraction was applied to 60 ml of blue Sepharose CL-6B that has been equilibrated with 3 volumes of equilibration buffer [20 mM HEPES (pH 7.2), 0.1% Triton X-100 and 0.2 M NaCl]. The column was then washed with 3 volumes of

washing buffer [20 mM HEPES (pH 7.2), 0.1% Triton X-100 and 0.5 M NaCl] and eluted with 3 volumes of elution buffer [20 mM HEPES (pH 7.2), 0.1% Triton X-100 and 0.5 M KSCN].

The eluate was subjected to 15 ml of Cu^{2+}-IDA column after equilibrating with 3 volumes of equilibration buffer [50 mM sodium phosphate (pH 7.2), 0.1% Triton X-100 and 0.5 M NaCl]. The column was washed with 3 volumes of washing buffer [50 mM sodium phosphate (pH 7.2), 0.1% Triton X-100 and 0.5 M NaCl] and bound proteins were then eluted with elution buffer [50 mM sodium phosphate (pH 7.2), 0.1% Triton X-100 and 0.5 M NaCl and 0.2 M imidazole]. The eluate was dialyzed overnight in 20 mM Tris-HCl (pH 7.2) containing 0.1% Triton X-100 and 0.9% NaCl.

The dialyzed eluate was loaded into the 50 ml Falcon tube containing 2 ml of Con A-Sepharose equilibrated with 3 volumes of equilibration buffer [20 mM HEPES (pH 7.2), 0.1% Triton X-100 and 0.1 M NaCl] and rotated for 2 hours. After centrifuging at 200 X g using Beckman JA-20 rotor (Palo Alto, CA) for 5 minutes, the breakthrough containing the unbound proteins was collected. The remaining content was sequentially washed with 3 volumes of washing buffer A [20 mM HEPES (pH 7.2), 0.1% Triton X-100 and 0.1 M NaCl] and 3 volumes of washing buffer B [20 mM HEPES (pH 7.2), 0.1% Triton X-100, 0.1 M NaCl and 0.2 M glucose]. Then 3 volumes of elution buffer [20 mM HEPES (pH 7.2), 0.1% Triton X-100, 0.1 M NaCl and 0.5 M methyl α-D-glucopyranoside] was added to the tube and rotated overnight. The content in the tube was centrifuged at 200 X g for 5 minutes (Beckman JA-20 rotor, Palo Alto, CA) and the eluate was collected and kept. Next, 1 volume of the elution buffer was loaded to the tube

and rotated for 1 hour. The eluate was collected, pooled and concentrated using Centriprep 30 (Millipore, Bedford, MA, USA).

2.10 Protein Concentration Assay

Protein estimation is of paramount importance in every investigation in biochemistry. For example, laboratory practice in protein purification often requires a rapid and sensitive method for the quantitation of protein. Presently, a variety of methods are available for the determination of protein content of a given sample. The methods employ different principles, and may be sensitive to interferences by certain salts, buffer components, and some solvents. Each method therefore has certain unique and useful characteristics as well as certain limitations. In the biochemical laboratory, the most widely used methods often employ photometric and/or colorimetric analyses as these methods are simple, rapid and have the required sensitivities.

2.10.1 Bio-Rad protein assay

The Bio-Rad Protein Assay Kit (Bio-Rad, Hercules, CA, USA), based on the method of Bradford (1976), is a simple and accurate procedure for determining concentration of solubilized protein. It basically involves the addition of an acidic dye to a protein solution and the subsequent measurement at 595 nm with a spectrophotometer. The comparison to a standard curve, which uses bovine serum albumin (Sigma, St. Louis, MO, USA) as a standard, provides a relative measurement of protein concentration.

Five different dilutions of bovine serum albumin (BSA) between the range of 1.2 to 10.0 µg/ml using water as diluent were prepared. 800 µl of each standard and unknown sample solution were pipetted into clean, dry tubes. For the blank, 800 µl of water was

pipetted into the tube instead. 200 µl of dye reagent was added and vortexed. The respective mixtures were then incubated at room temperature for 5 minutes and absorbance at 595 nm was measured. Protein solutions were measured in duplicates. A standard calibration curve of absorbance against BSA was then plotted.

2.11 Fluorometric Detection of ADP-ribosyl Cyclase Activity

2.11.1 Fluorometric detection of cyclic GDP-ribose

The enzymatic activity of ADP-ribosyl cyclase was determined as described (Graeff *et al.*, 1994). This assay is based on the fluorescent properties of cyclic GDP-ribose (cGDPR), which is produced from the non-fluorescent substrate, NGD^+. Unlike cADPR, cyclic GDP-ribose is a poor substrate for the hydrolase activity of CD38 and furthermore, the end product GDP-ribose is not fluorescent, thus making the fluorometric detection of cGDPR production from NGD^+ a suitable assay for the determination of cyclase activity.

Briefly, microsomal fractions from both control and TAA-treated rats (50 µg protein) were incubated at 37°C for 15 minutes with 100 µM NGD^+ in 20mM Tris-HCL (pH 7.2) containing 0.1% Triton X-100. The product cGDPR was measured as an increase in fluorescence intensity at an excitation and emission wavelength of 300 and 410 nm, respectively, using LS 50B luminescence spectrophotometer (Perkin-Elmer, Foster, USA). The enzymatic activity was calculated from the initial linear slope; change in fluorescence (Δ) was calibrated from standard curves construed with known concentrations of cGDPR.

2.12 Sodium Dodecyl Sulphate-Polyacrylamide Gel Electrophoresis

In sodium dodecyl sulphate-polyacrylamide gel electrophoresis (SDS-PAGE) separations, the migration of proteins is not determined by the intrinsic electrical charge of the proteins in question but rather by the molecular mass (Shapiro *et al.*, 1967). There are two SDS systems currently in use today. The Weber and Osborn system (1969) is a continuous SDS system while the Laemmli system (1970) is a discontinuous SDS system. The discontinuous system of Laemmli (1970) provides for excellent resolution of proteins and is probably the most widely used electrophoretic system today. In our present study, the Laemmli system was the method of choice.

2.12.1 Solutions for SDS-PAGE

Buffer C: stack buffer

1 M Tris-HCl	121.14 g
H_2O to 1 liter, pH with HCl to 6.8	

Buffer D: resolving buffer

1.5 M Tris-HCl	181.71 g
H_2O to 1 liter, pH with HCl to 8.8	

SDS

10% SDS	100 g
H_2O to 1 liter	

Ammonium persulphate (APS)

10% APS
Fresh on the day of use

H6X

60 mM Tris-HCl	6 ml 1 M pH 6.8
SDS	12 g
Sucrose	45 g
H_2O to 100 ml	
Warm to dissolve SDS	

Reducing sample buffer

H6X	400 µl
β-mercaptoethanol	25 µl
2% bromophenol blue (0.2 g / 10 ml ethanol)	5 µl

2.12.2 Preparation of SDS-polyacrylamide gel

10% resolving gel	**10 ml**
Resolving buffer (buffer D)	2.5 ml
H_2O	4 ml
30% Acrylamide/Bis	3.3 ml
10% SDS	0.1 ml
10% APS	0.1 ml
TEMED (N,N,N',N'-tetramethyl-ethylenediamine	4 µl

4% stacking gel	**3 ml**
Stacking buffer (buffer C)	0.38 ml
H_2O	2.3 ml
30% Acrylamide/Bis	0.4 ml
10% SDS	30 µl
10% APS	30 µl
TEMED (N,N,N',N'-tetramethyl-ethylenediamine	3 µl

For the preparation of 10% SDS-PAGE gel (1.5 mm thick) in the mini-PROTEAN® II electrophoresis system (Bio-Rad), 10 ml of the resolving gel solution and 3 ml of the stacking gel solution were prepared. After setting the resolving gel, the stacking gel was layered on top of the resolving gel and the appropriate gel comb was inserted.

2.12.3 Addition of sample buffer to protein samples

Four parts of the respective protein samples were mixed with one part of the sample buffer (reducing buffer). The mixtures were put in a boiling water bath for 5 minutes and then on ice until ready to be used.

2.12.4 Loading the samples and running the gel

The comb was slowly removed from the stacking gel. The upper and lower buffer chambers were filled with tank buffer containing 0.025 M Tris-HCl (pH 8.3), 0.192 M glycine and 0.1% SDS. Boiled samples, microsomal proteins (300 μg) from control and TAA-treated rats, were loaded into each well. Model 200/2.0 Power Supply from Bio-Rad was turned on, and adjusted to 100 V. After the samples entered the separating gel, the voltage was increased to 150 V. When the dye reached the bottom of the gel, the power supply was turned off. For the determination of molecular mass, pre-stained SDS-PAGE standard protein marker, Precision Plus Protein^{TM} Standards, (Bio-Rad, Hercules, CA, USA) was used.

2.13 Western Blotting

Microsomal proteins (200 μg) and purified CD38 (20 μg), which serves as a positive control, were subjected to 10% (w/v) SDS-PAGE according to Laemmli (1970). Immunoblotting was performed following the method of Towbin *et al.* (1979). Briefly, the proteins resolved in the gel were electrophoretically transferred to a 0.2-μm nitrocellulose membrane (Bio-Rad) using tank transfer system Mini Trans-Blot® Cell (Bio-Rad) at 100 V for 1 hour. The transfer buffer contained 25.6 mM Tris-base, 192 mM glycine and 20% methanol. The 20% methanol decreased the rate of elution from the gel but increased the efficiency of protein binding to the nitrocellulose. The transferred membrane was then blocked in TBS (20 mM Tris-HCl, 137 mM NaCl, pH 7.5) containing 5% (w/v) skim milk and 0.1% Tween 20 for 1 hour. The membrane was then incubated overnight at 4°C with polyclonal goat anti-rat CD38 antibody (1:100). This

was followed by washing (3 times) and incubation for 2 hours at room temperature with a horseradish peroxidase-conjugated rabbit anti-goat IgG (1:2500). In a separate set of experiment, the primary anti-CD38 antibody was incubated with 10X excess amount of the CD38 blocking peptide (Santa Cruz) for 1 hour at room temperature before subsequent addition of the mixture to the membrane. After washing for 3 times with washing buffer (TBS-T), the membrane was subjected to the same secondary antibody staining as described previously. The membrane was then developed using the ECL™ system (Amersham Biosciences, Buckinghamshire, England).

The ECL™ Western blotting assay system was used according to the manufacturer's instruction. Briefly, an equal volume of ECL™ detection solution 1 was mixed with detection solution 2 (both solutions are provided in the ECL™ Western blotting kit). This mixture was directly added to the blot, which was subsequently incubated for 1 minute at room temperature and immediately wrapped in Saran Wrap. The signals on the blot were visualized by exposing to CL-X Posure™ film (PIERCE, Rockford, IL, USA) for 1 minute (subjective). A standard protein marker (Bio-Rad) was electrophoresed simultaneously for comparing the molecular weights of the visualized proteins in the membrane. Same blot was subjected to Coomassie Blue (Bio-Rad) staining according to the method described below, section 2.12.1, to detect total protein in the samples and was used for loading control. The X-ray films were scanned and the intensity of the bands was quantified by densitometry (Analytical Imaging Station, Ontario, Canada).

2.13.1 Coomassie Blue staining of membrane

The membrane that was used in Western Blot was then stained with Bio-Safe Coomassie Blue G250 (Bio-Rad) according to the manufacturer's protocol to detect total protein in the samples and was used for loading control. Briefly, the membrane was washed 3 times for 5 minutes each in 200 ml of ddH_2O per membrane. Water was removed from the staining container and then 50 ml (or enough to completely cover the membrane) of Bio-Safe Coomassie Stain (Bio-Rad) was added. The membrane was gently shaken for 1 hour and protein bands were visible within 20 minutes. Next, the membrane was rinsed in 200 ml of ddH_2O for at least 30 minutes (change water during washing) and stored in water. Rinsing the membrane extensively in water after staining will remove background and allow proper visualization of the protein bands.

2.14 Extraction of cADPR From Rat Liver Tissues

Control and TAA-treated rat livers were frozen in liquid nitrogen and endogenous cADPR was extracted as described by da Silva *et al.* (1998), with some modifications. Briefly, the tissues were weighed and 1 ml of perchloric acid was used for extraction for every 100 - 200 mg of tissue prior to extraction. Rat tissues were homogenized using PRO 200 Homogenizer (PRO Scientific, Oxford, CT, USA) in 0.9 ml of MilliQ water (Millipore, Bedford, MA) and homogenization was performed for 3 times, each for 30 seconds at the maximum speed, with a 30 seconds pause in between. An aliquot (10 µl) was removed for protein determination and the remaining sample was de-proteinized by addition of 0.1 ml of 6 M perchloric acid, $HClO_4$. The $HClO_4$ extract was immediately vortex-mixed and kept at -20°C for 20 minutes. Then, precipitated protein was removed

by centrifugation at 15,000 X g for 10 minutes (4°C). The supernatant was collected and titrated to pH 7-8 by addition of 1 M KOH to remove the perchloric acid. After standing for 30 minutes on ice, the samples were again centrifuged at 15,000 X g for 10 minutes (4°C) to remove the $KClO_4$ precipitate. A mixture containing 0.0625 unit/ml *Neurospora crassa* NADase, 2.5 mM $MgCl_2$ and 20 mM sodium phosphate (pH 8.0) was added to the samples for removal of contaminating nucleotides (NAD^+) except cADPR, which is resistant to NADase. The incubation proceeded overnight at 37°C. Enzyme was removed by filtration with Centricon-3 filters (Millipore) and samples were recovered in the filtrate after centrifugation at 4°C and 3000 X g for 30 minutes using a Beckman JA-20 rotor (Palo Alto, CA).

2.15 Cycling Assay for cADPR

The cycling assay was first described by Graeff and Lee (2002) and provides an efficient one-step method of quantifying cellular cADPR and NAD^+, with an exceptionally high sensitivity within the nanomolar range. It captures the unique ability of ADP-ribosyl cyclase to catalyse the reverse of cADPR synthesis from NAD^+. In the presence of high concentrations of nicotinamide, NAD^+ can be produced from cADPR stoichiometrically. The NAD^+ formed can then be coupled to a cycling assay involving alcohol dehydrogenase and diaphorase. Each time NAD^+ cycles through these coupled reactions, a molecule of highly fluorescent resorufin is generated. (Scheme 2.1)

In this study, cADPR was measured by the cycling enzymatic assay according to the method described by Graeff and Lee (2002), the sensitivity of which is in the nanomolar range. Briefly, reactions were conducted in black opaque 96-well plates. 50 µl

of the tissue samples that contain extracted cADPR from control and TAA-treated rat livers (section 2.14), was added to each well and topped up to a final volume of 0.1 ml with 20 mM sodium phosphate, pH 8. To 0.1 ml of cADPR samples, 50 µl of reagent was added containing 1 µg/ml ADP-ribosyl cyclase (Sigma), 30 mM nicotinamide (Sigma) and 100 mM sodium phosphate, pH 8. This initiated the conversion of cADPR in the samples to NAD^+. The conversion was allowed to proceed for 15 minutes at room temperature (≈ 25°C). The cycling reagent (0.1 ml) was then added, which contained 2% ethanol, 100 µg/ml alcohol dehydrogenase, 20 µM resazurin, 10 µg/ml diaphorase, 10 µM FMN, 10 mM nicotinamide, 0.1 mg/ml BSA and 100 mM sodium phosphate, pH 8. The cycling reaction was allowed to proceed for 4 hours and the increase in the resorufin fluorescence (with excitation at 544 nm and emission at 590 nm) was measured periodically (30-minute intervals) using SpectraMax Gemini Fluorescence Reader (Molecular Devices, Sunnyvale, CA, USA). The cycling assay was performed in the presence and absence of ADP-ribosyl cyclase to allow quantification of the background contribution by residual NAD^+ and other interfering nucleotides. The difference in the resorufin signal in the presence and absence of the cyclase was calibrated using cADPR standards. Standard solutions of cADPR (ranging from 0-10 nM) were prepared in 20 mM sodium phosphate, pH 8, and taken through the same steps as the samples. The assay was done in triplicates.

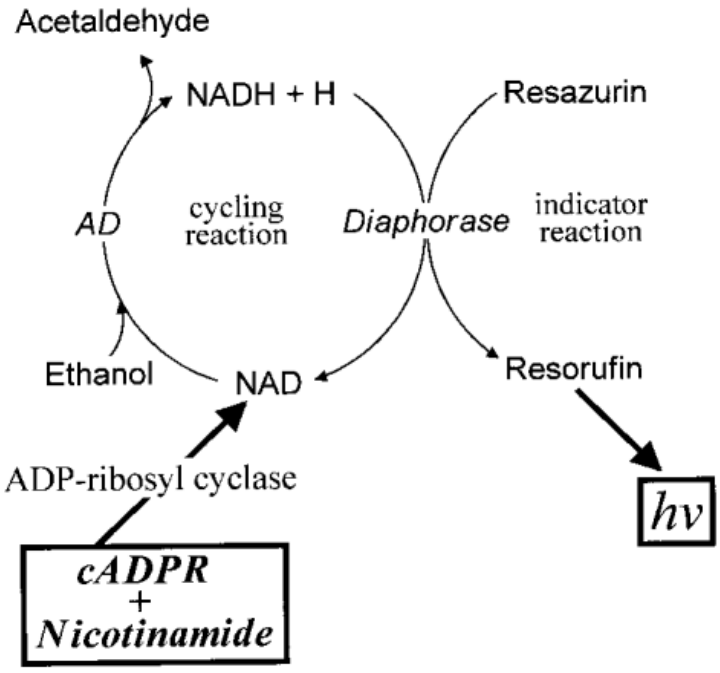

Scheme 2.1 The cycling assay for cADPR.
AD, alcohol dehydrogenase; *hv*, fluorescence light. (Adapted from Graeff and Lee, 2002)

2.16 Extraction and Cycling Assay of NAD^+ From Rat Liver Tissues

Endogenous NAD^+ in perchloric acid extracts of rat liver tissues can also be measured. The extraction method was performed as described previously in section 2.14, for cADPR extraction without the addition of the NADase enzyme. The acid extract was diluted 400-fold in 100 mM sodium phosphate buffer (pH 8), adjusted to pH 8, and assayed by the complete cycling assay as described for cADPR without the conversion of cADPR to NAD^+ step (section 2.15). Briefly, 1 µl and 10 µl of diluted aqueous tissue samples from control and TAA-treated rat livers, respectively, were added to each well and topped up to a final volume of 0.1 ml with deionised water. To each well, 0.1 ml of cycling reagent was added, which contained 2% ethanol, 100 µg/ml alcohol dehydrogenase, 20 µM resazurin, 10 µg/ml diaphorase, 10 µM FMN, 10 mM

nicotinamide, 0.1 mg/ml BSA and 100 mM sodium phosphate, pH 8, and deionised water. The reaction was allowed to proceed for 2 hours during which, the increase in resorufin fluorescence (with excitation at 544 nm and emission at 590 nm) was measured periodically at 15-minute intervals using a fluorescence microplate reader (SpectraMax GeminiXS, Molecular Devices, USA).

As can be seen in the scheme of the cycling assay (Scheme 2.1), endogenous NAD^+ levels can be measured by conversion into NADH. Tissue extracts were incubated with and without alcohol dehydrogenase, and the difference in NADH fluorescence produced was calibrated with NAD^+ standards. Standard solutions of NAD^+ (ranging from 0-10 nM) were prepared using deionised water. The assay was carried out in triplicates.

2.17 Statistical Analysis

Data were assessed with a Student *t*-test for unpaired samples, and significance was set at $P < 0.05$. Values are presented as mean ± SEM, and n refers to the number of determinations.

CHAPTER 3

RESULTS

4.1 Development of Liver Cirrhosis in Thioacetamide-Administered Rats

Liver cirrhosis was successfully induced in male Wistar rats through intraperitoneal injection of the hepatotoxin (thioacetamide) at a dosage of 300 mg/kg, twice a week for 10 weeks. Control group received the similar volume of sterile water. In the control group, animals showed a normal gain in body weight. In the TAA-treated groups, the body weight decreased and is in accordance with previous observation (Al-Bader *et al.*, 2000). The development of liver cirrhosis in the TAA-treated rats was further judged by the gross examination of the liver (Figure 3.1). Numerous macronodular nodules can be seen on the surface of the cirrhotic liver.

Histopathological analysis using H & E-stained cryostat sections as described previously in section 2.4.1, Chapter 2, showed that the livers of the control animals revealed a normal histology. However, all animals on thioacetamide treatment developed liver cirrhosis by the end of the experimental period. Figure 3.2 shows histopathological changes typical of liver cirrhosis, including focal necrotizing cholangitis, coarse fibrous septa, bile duct proliferation and hepatocyte nodules with diffuse steatosis.

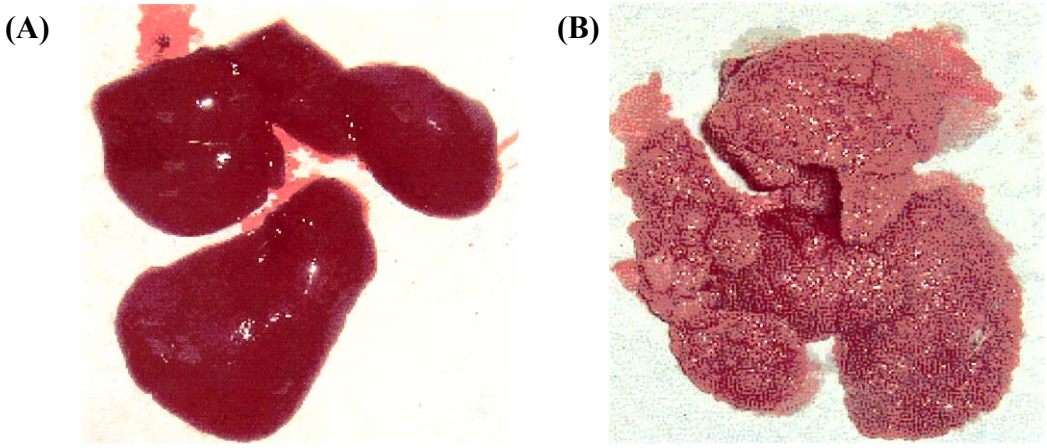

Figure 3.1 Macroscopic view of the livers.
(A) Control rat. **(B)** TAA-treated rat. Numerous macronodular nodules can be seen on the surface of the cirrhotic rat liver.

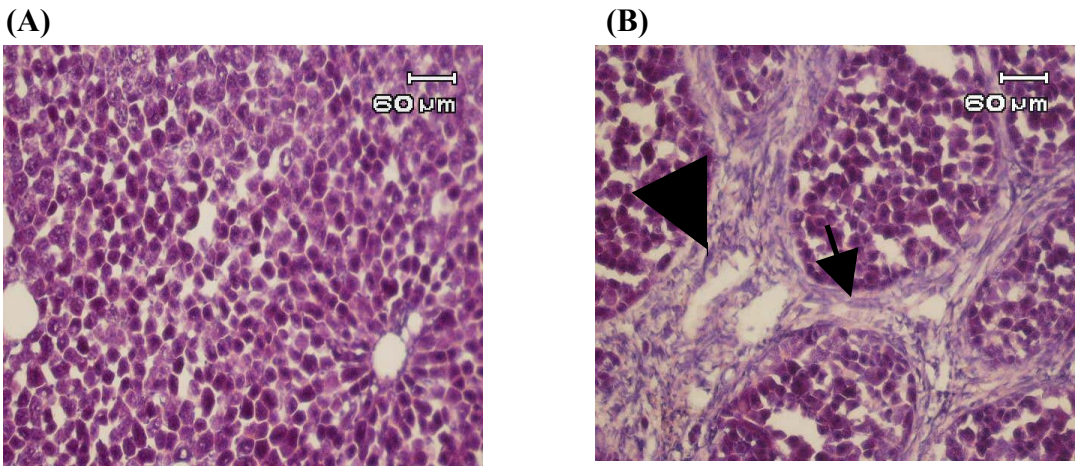

Figure 3.2 Haematoxylin and eosin stained hepatic section of control (A) and cirrhotic rats (B).
Liver sections from cirrhotic rats show fibrous bridges (arrow) and other factors typical of established cirrhosis such as bile duct proliferation (arrowhead). Scale bar, 60 µm.

3.2 Analysis of CD38 Expression by RT-PCR and Real-Time Quantitative PCR

Total RNA isolated from rat livers was reverse transcribed to cDNA and further amplified by PCR using primers specific for rat CD38 as described in section 2.5.1 and 2.5.4, respectively. The intensity of the bands (267 bp) in control and TAA-treated rat samples was compared to assess the effect of thioacetamide-induced cirrhosis on CD38 expression. As can be seen from Figure 3.3, there was enhanced CD38 mRNA expression in livers obtained from TAA-treated rats as compared with the controls. Ratiometric analysis of the intensity of the bands using Analytical Imaging Station (Ontario, Canada) showed an approximately 2.5-fold ($P < 0.05$) increase in CD38 transcript level in liver samples from TAA-treated rats. The differences in the density of the individual bands demonstrate the variability of response of the rats to TAA treatment. 28S rRNA PCR products (~270 bp) show a uniform expression (Figure 3.3) indicating that the endogenous control expression level is similar in all samples in the study. The endogenous control (28S rRNA) was used in the ratiometric analysis to normalize differences in the amount of cDNA that was loaded into PCR reaction wells. Therefore, it is critical to determine if the study treatment or intervention is affecting the expression level of the candidate endogenous control gene.

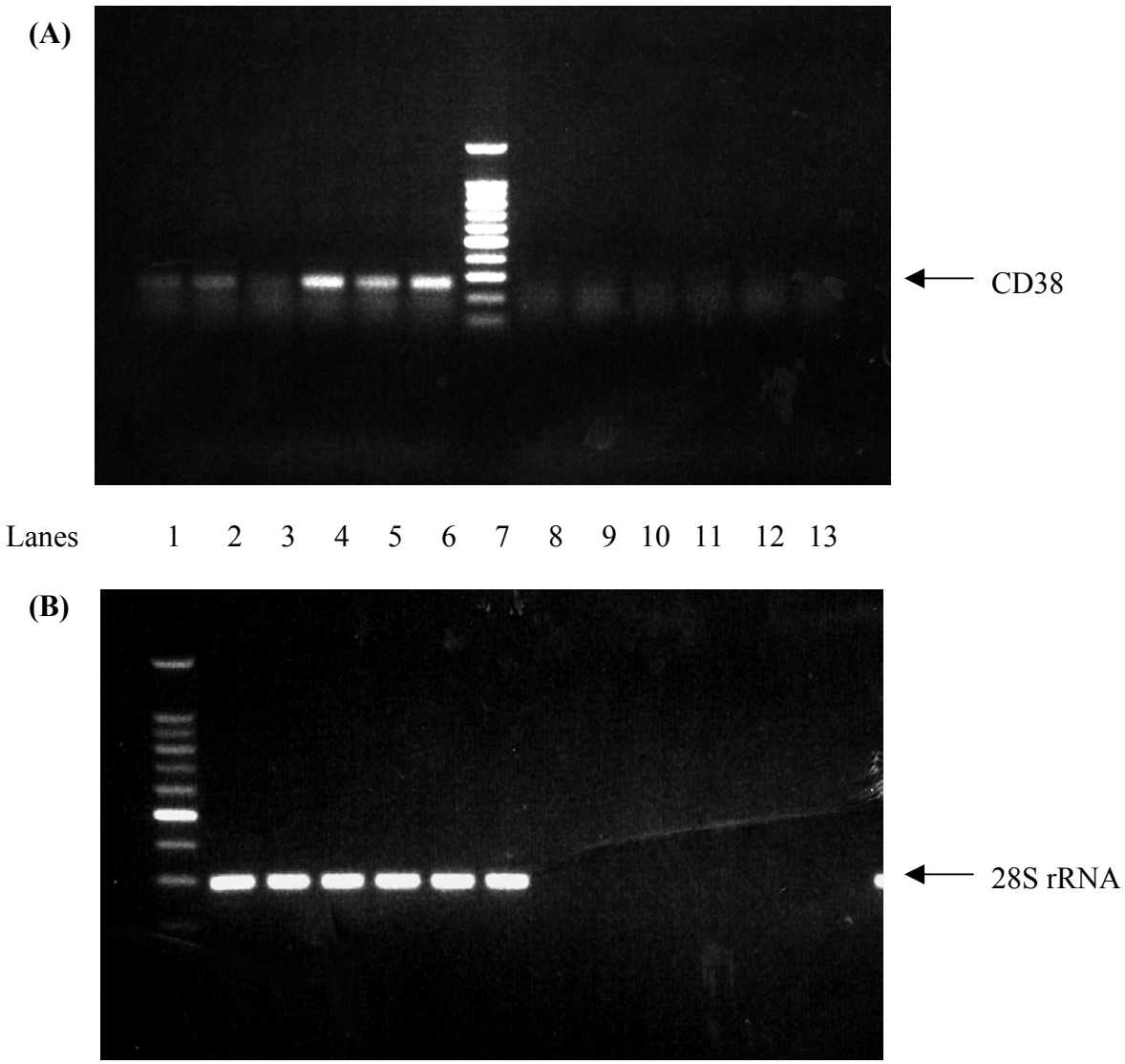

Figure 3.3 RT-PCR of CD38 mRNA and 28S rRNA in rat liver.
(A) Lanes 1 to 3 and lanes 4 to 6 represent PCR products using rat CD38 primers from control and TAA-treated rats, respectively. Lane 7 represents 100-bp DNA ladder.
(B) Lane 1 represents 100-bp DNA ladder. Lanes 2 to 4 and lanes 5 to 7 represent PCR products using rat 28SrRNA primers (~270 bp) from control and TAA-treated rats, respectively. Lanes 8 to 10 and lanes 11 to 13 represent negative controls (without reverse transcriptase) from control and TAA-treated rats, respectively. Data represent 3 independent experiments.

Real-time RT-PCR of RNA extracted from livers of control and TAA-treated rats was performed according to the method described in section 2.5.5, Chapter 2, using the ABI PRISM 7000 sequence detection system (Applied Biosystems) with the DNA binding SYBR Green 1 dye for the detection of PCR products. Results confirmed that there was an increased expression of CD38 in TAA-treated rat liver. Emitted fluorescence for each reaction was measured during the annealing-extension phase, and amplification plots were analyzed by using the ABI PRISM 7000 sequence detection system (Figure 3.4). Product specificity was determined by melting curve analysis with the ABI PRISM dissociation curve software (Figure 3.5). A relative quantitation assay ($\Delta\Delta C_t$ method) was used to analyze changes in CD38 expression in the livers of TAA-treated rats relative to the control rats by measuring the C_t (threshold cycle) values. The C_t is defined as the cycle number at which the fluorescence generated within a reaction crosses the threshold line. To take into account the variability in the initial concentration and quality of the total RNA introduced into the reaction, transcripts of 18S rRNA were quantified as an endogenous RNA control, and each sample was normalized to 18S rRNA.

The mean C_t values for control and TAA-treated samples were 26.27 and 25.16, respectively, and these values were used to calculate the fold-differences in CD38 between the control and TAA-treated samples ($2^{-\Delta\Delta Ct}$). The ΔC_t value was calculated by subtracting of the average 18S rRNA C_t value from the average CD38 C_t value of the control/TAA-treated samples. Then, $\Delta\Delta C_t$ was obtained by subtracting the ΔC_t of the control/TAA-treated samples from the ΔC_t of the control (calibrator sample). A calibrator sample is a sample used as the basis for comparative expression results. From the calculations, there was an approximate 2.5-fold increase of CD38 in the livers of TAA-

treated rats relative to that of the control rats (Figure 3.6) and this is in accordance with the RT-PCR ratiometric analysis.

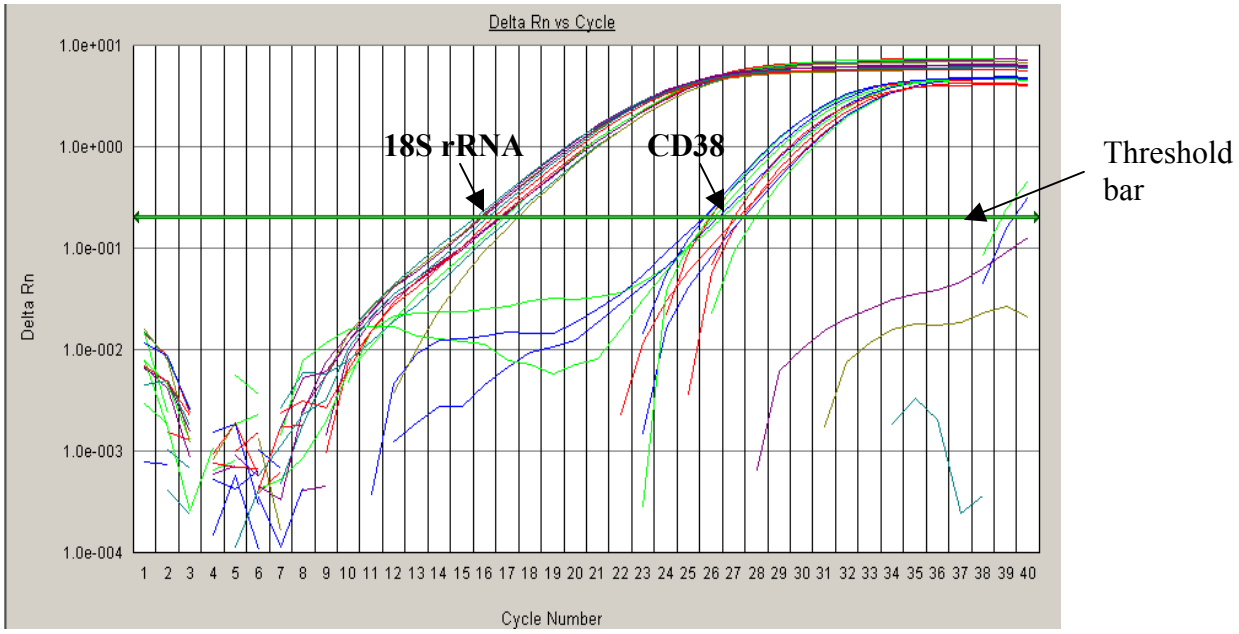

Figure 3.4 Representative amplification plot (fluorescence generated versus cycle number) for both amplified CD38 and 18S rRNA PCR products.
The C_t value of CD38 replicates is higher than the C_t value of 18S rRNA replicates. (n = 6)

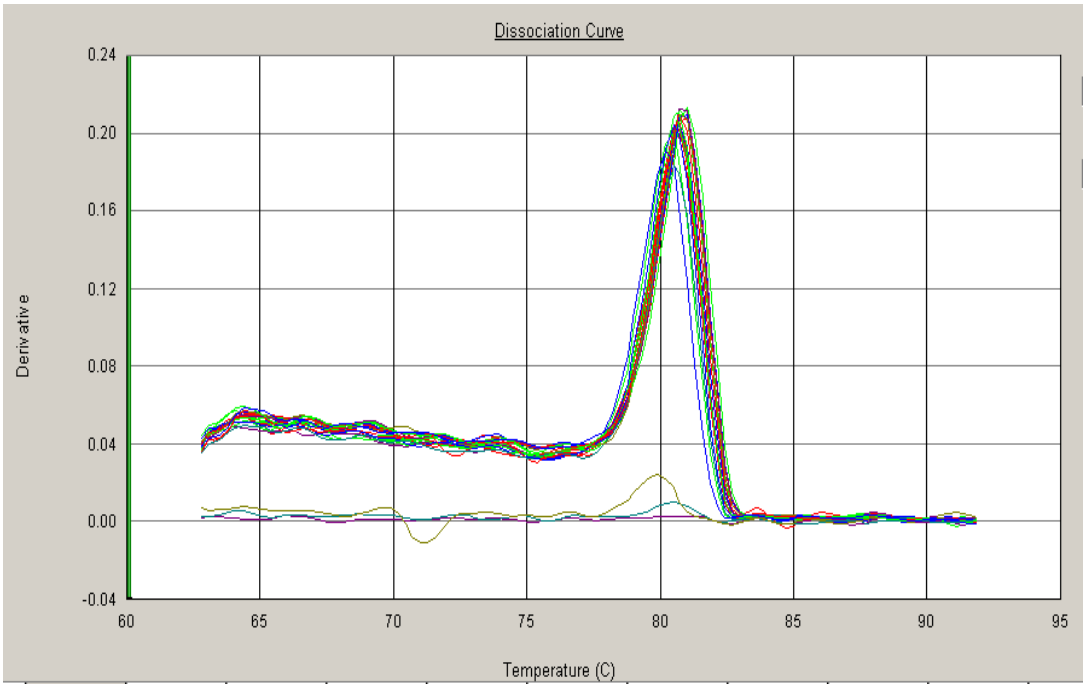

Figure 3.5 Representative dissociation curves that display dissociation data from the amplicons of quantitative PCR runs.
Change in fluorescence (due to SYBR Green 1 dye interacting with double stranded DNA) was plotted against temperature. The dissociation curves above show specific amplification without primer-dimer formation. The specific product is shown with a melting temperature (Tm) of 81°C. (n = 6)

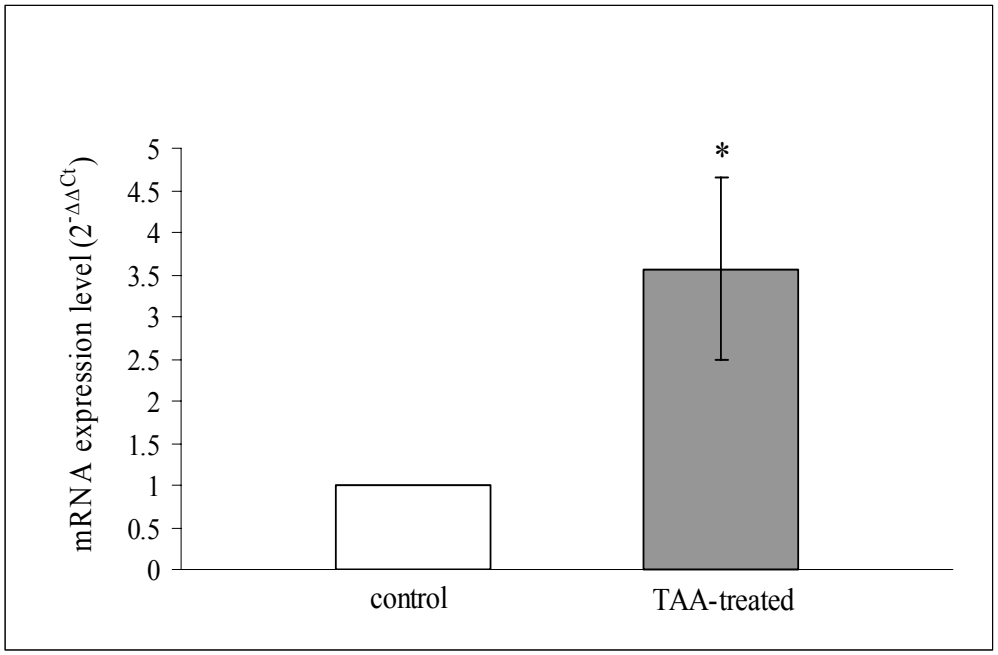

Figure 3.6 CD38 mRNA expression level ($2^{-\Delta\Delta Ct}$) in control and TAA-treated determined by quantitative real-time RT-PCR.

Values are mean ± SEM of 6 independent experiments performed in triplicate (n = 6). *Significantly different from control ($P< 0.05$).

4.3 Immunohistochemical detection of CD38

Immunohistochemical methods in conjunction with confocal microscopy techniques were performed to localize the distribution of CD38 in the control and cirrhotic rat liver tissues. The periodate-lysine-paraformaldehyde (PLP) fixative was used according to the method of McLean and Nakane (1974) to fix the liver tissues in order to obtain an optimal balance between ideal morphology and yet not too harsh a fixative to prevent drastic modification of the CD38 antigen. The fixed cryostat liver sections were immunolabeled with anti-CD38 antibodies and observed at low (20 x Fluar objective) and high (60 x Fluar objective with oil immersion) magnifications using confocal microscopy as described in sections 2.6.1 and 2.7, respectively. There was no fluorescent signal for negative controls (data not shown). The level of CD38 protein expression in control rats was relatively low and in contrast, CD38 was significantly increased in TAA-treated rats (Figure 3.7, low magnification). As can be seen from Figure 3.8 (high magnification), the staining was observed almost exclusively to the hepatocyte plasma membrane domain and again, it was observed that there was an increased CD38 expression in TAA-treated liver tissue section. The quantification of fluorescent dye using Image-Pro Plus Version 4.5 (Media Cybernetics, North Reading, MA) revealed an approximate 1-fold ($P < 0.05$) increase in CD38 expression in liver tissues of TAA-treated rats compared with that of control rats.

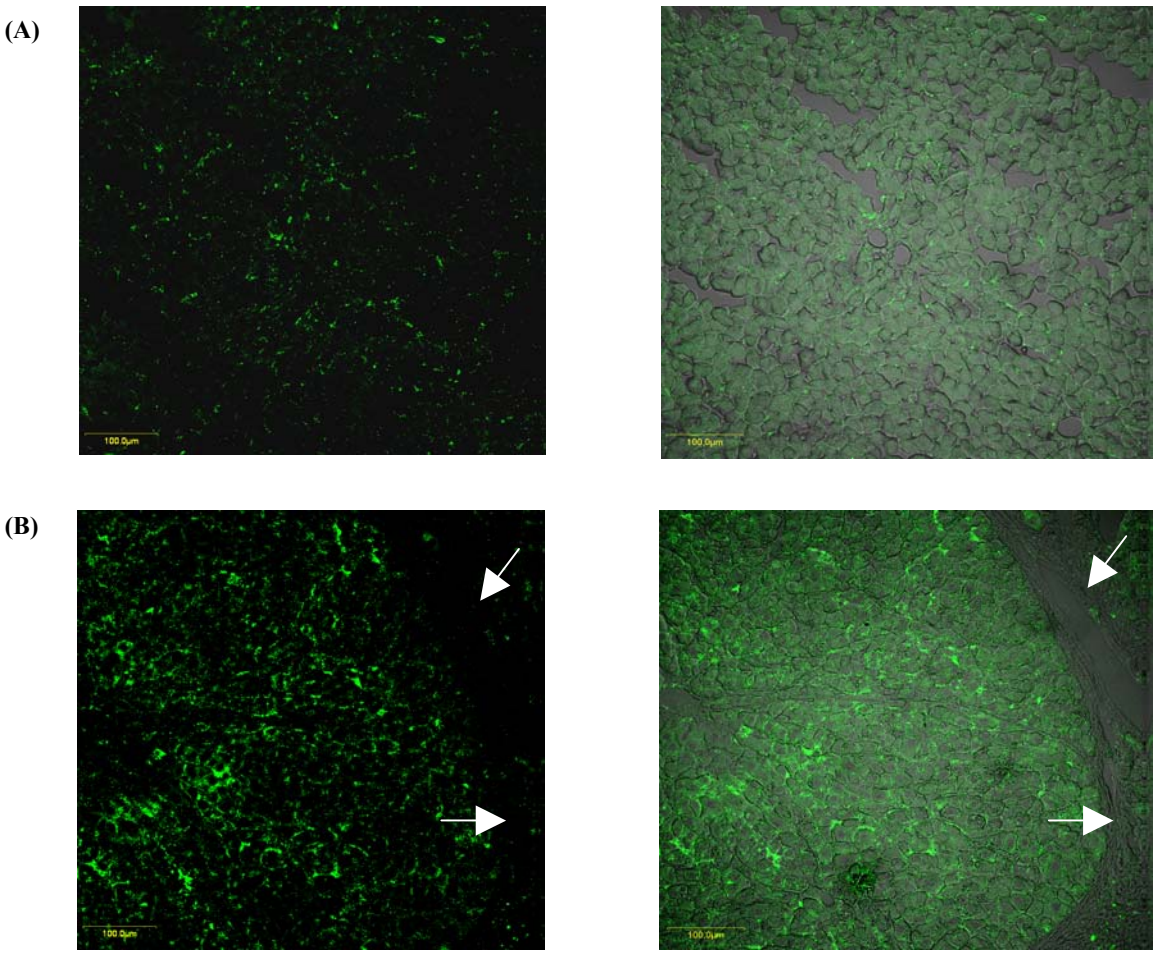

Figure 3.7 Localization of CD38 in rat hepatocytes (low magnification, 20x). Fixed liver sections were immunostained with anti-CD38 antibodies (green signal). **(A)** Control rat liver section and **(B)** TAA-treated rat liver section, with fluorescent (left) and combined fluorescent and transmitted light (right) images in a single photomicrograph. A higher level of CD38 immunoreactivity was detectable in TAA-treated rats by immunohistochemistry. Arrows indicate the fibrous septa (fibrosis). Results are representative of 3 experiments performed in duplicate. Scale bar, 100 μm.

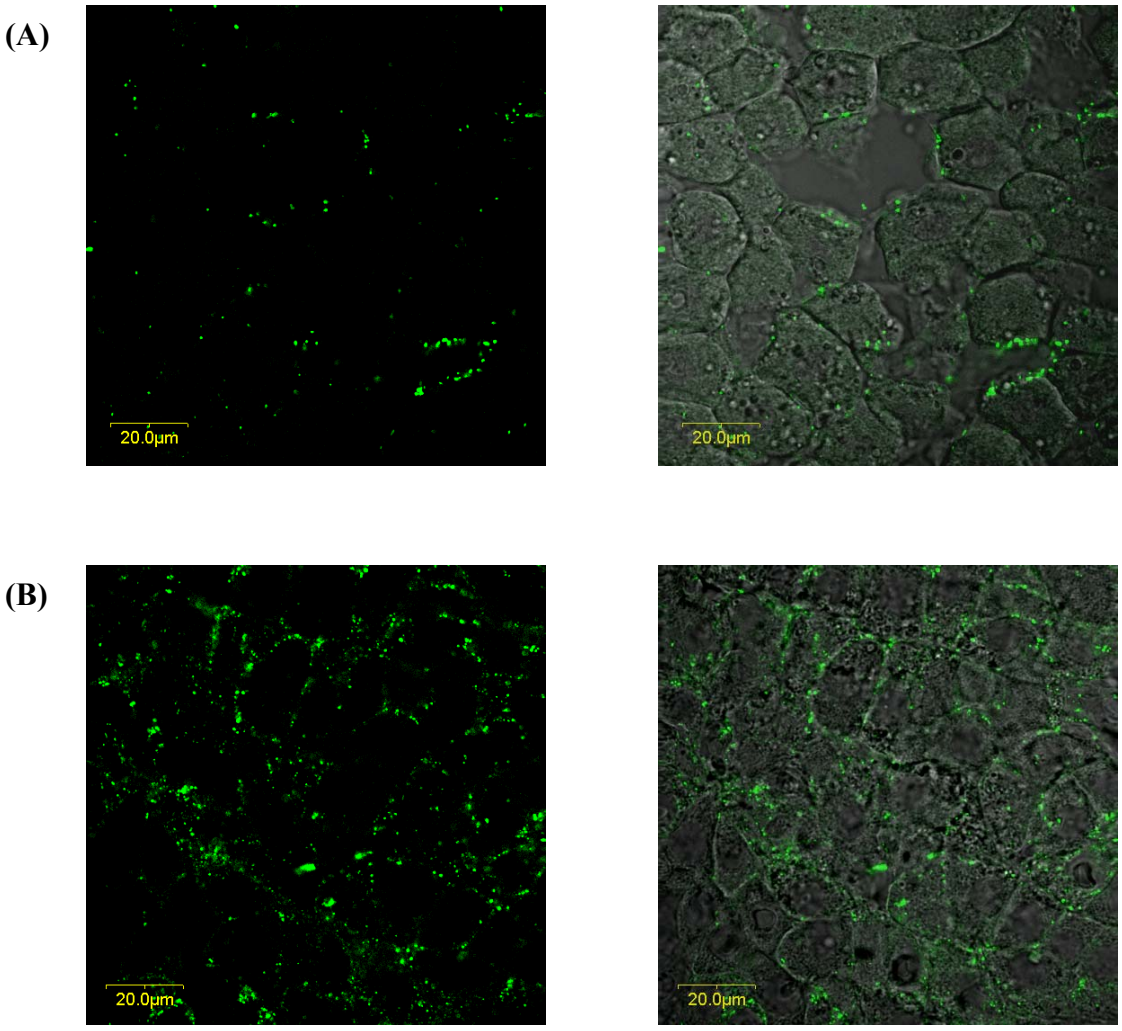

Figure 3.8 Localization of CD38 in rat hepatocytes (high magnification, 60x with oil immersion).

Fixed liver sections were immunostained with anti-CD38 antibodies (green signal). **(A)** Control rat liver section and **(B)** TAA-treated rat liver section, with fluorescent (left) and combined fluorescent and transmitted light (right) images in a single photomicrograph. A higher level of CD38 immunoreactivity was detectable in TAA-treated rats by immunohistochemistry. Results are representative of 3 experiments performed in duplicate. Scale bar, 20 µm.

3.4 ADP-Ribosyl Cyclase in Rat Liver Microsomes

The microsomal fractions were isolated from the homogenized livers of control and TAA-treated rats according to the method described in section 2.8. After solubilization with 4% Triton X-100, the supernatants were collected and assayed for GDP-ribosyl cyclase activity (section 2.11.1). Incubation of solubilized microsomal extracts from the livers of control and TAA-treated rats with NGD^+ resulted in time-dependent conversion to cGDPR. It was observed that all samples possessed GDP-ribosyl cyclase activity. The enzymatic activity was calculated from the initial linear slope; change in fluorescence (Δ) was calibrated from standard curves construed with known concentrations of cGDPR. Microsomes obtained from TAA-treated rats exhibited increased rates of conversion of NGD^+ to cGDPR (Figure 3.9A) and significantly higher specific activity (Figure 3.9B; 133.52 ± 12.95 and 234.73 ± 29.88 nmoles mg^{-1} min^{-1} in control and TAA-treated groups, respectively; $P < 0.05$).

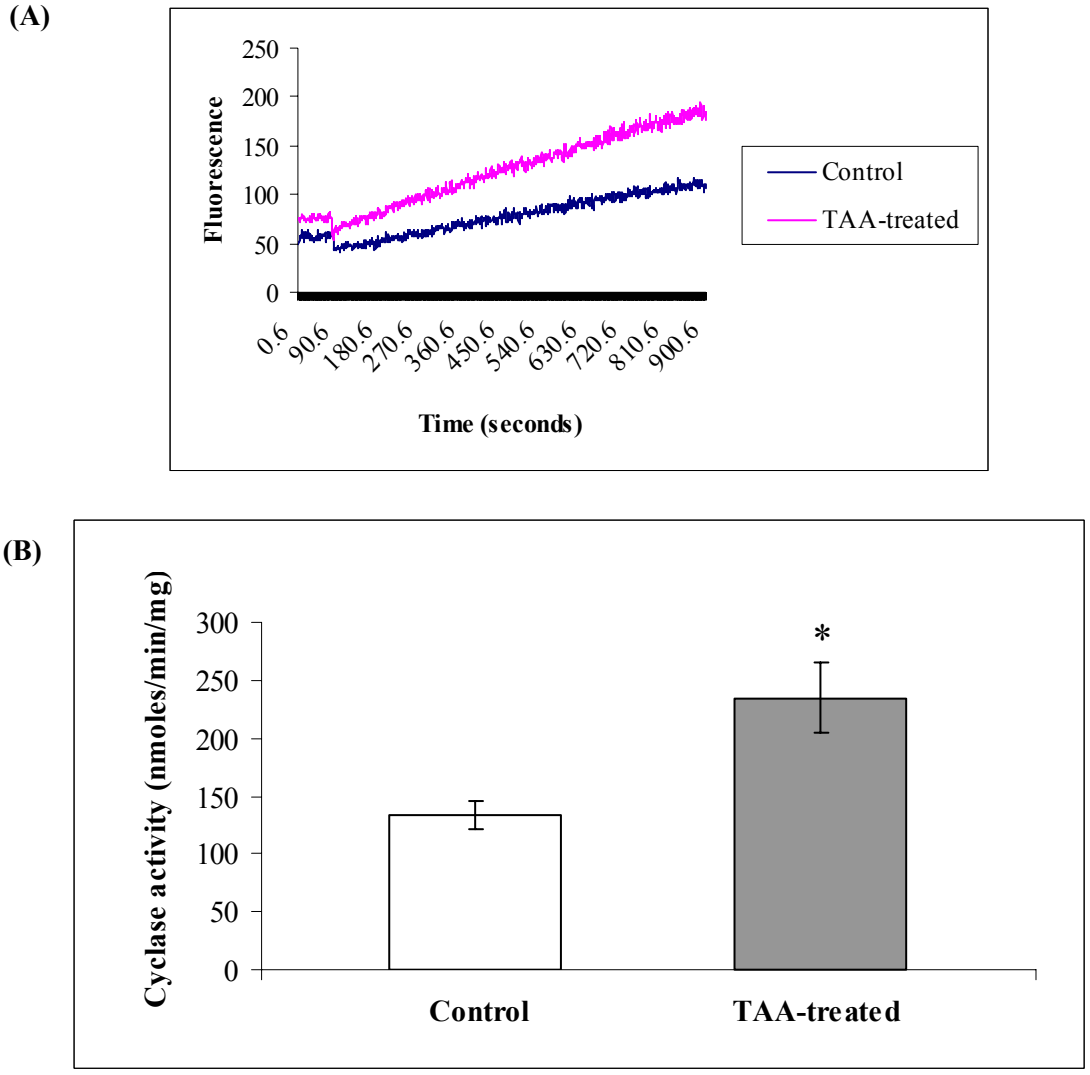

Figure 3.9 ADP-ribosyl cyclase activity in solubilized microsomal extracts obtained from control and TAA-treated rats.
(A) Representative tracing of ADP-ribosyl cyclase activity (expressed in fluorescence intensity in arbitrary units) versus time (in seconds) in the presence of 100 μM NGD^+ and 50 μg of microsomal proteins. **(B)** Specific activity of ADP-ribosyl cyclase (nmoles min^{-1} mg^{-1}) in liver microsomes obtained from control and TAA-treated rats (n = 6). Values are mean ± SEM. *Significantly different from control ($P < 0.05$).

3.5 Western Blot Detection of CD38 in Microsomes

Microsomal proteins were fractionated by SDS-PAGE and the separated proteins were transferred to a nitrocellulose membrane according to section 2.13, Chapter 2. From Figure 3.10, it can be seen that there was a consistent detection of CD38 in the microsomal fraction with a polyclonal goat anti-rat CD38 antibody under reducing condition. We also observed that CD38 expression was significantly greater in microsomes from TAA-treated rats than those from controls (Figure 3.10). Densitometric analysis of the bands in the Western blots using Analytical Imaging Station (Ontario, Canada) revealed an approximately 1-fold ($P < 0.05$) increase in CD38 expression in microsomes from TAA-treated rats as compared with those from the controls. This result correlates well with the elevation of GDP-ribosyl cyclase activity and the increased immunofluorescence (immunohistochemistry) in the livers of TAA-treated rats. However, the protein band of CD38 (45 kDa) disappeared in the experiment when blocking peptide was added together with the polyclonal goat anti-rat CD38 antibody (primary antibody) prior to application on the membrane for the Western blot studies (Figure 3.11). This demonstrates that the polyclonal goat anti-rat CD38 antibody is specific for rat CD38 which is at the molecular weight of 45 kDa. There are also other non-specific bands (other than 45 kDa) detected on the Western blot that cannot be removed by the blocking peptide. This non-specificity is due to the polyclonal antibody's properties which could recognize other epitopes from other antigens.

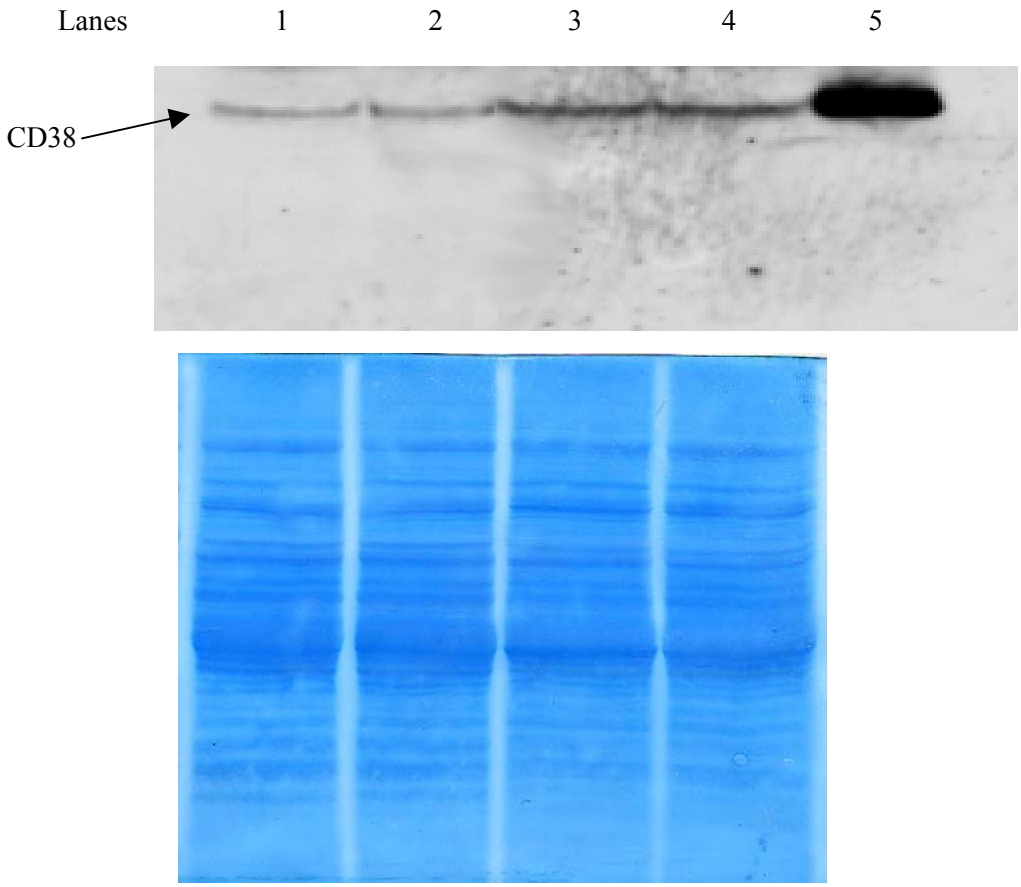

Figure 3.10 Representative Western blot showing increased CD38 expression in liver microsomes from TAA-treated rats compared with controls.
Lanes 1 and 2 are liver microsomes from 2 different control rats, and lanes 3 and 4 are liver microsomes from 2 different TAA-treated rats. Lane 5 is purified CD38 that serves as positive control. Arrow indicates the CD38 band at a molecular weight of ~45 kDa. Lower panel shows the total protein detection (same blot used for CD38 detection) which was stained with Bio-Safe Coomassie Blue (Bio-Rad) that was used as loading control. Data represent 6 separate determinations.

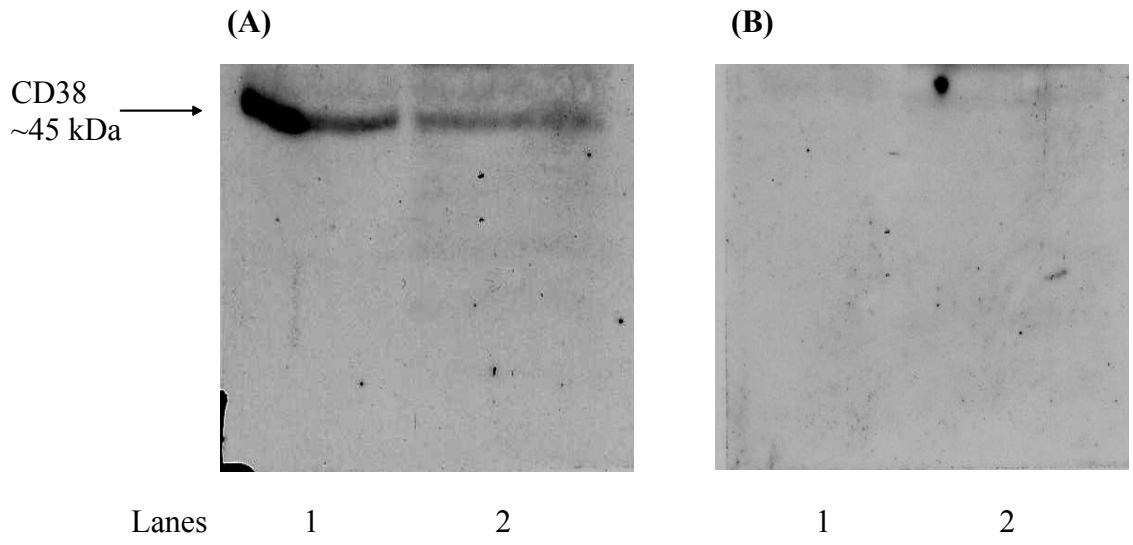

Figure 3.11 Detection of CD38 with Western blotting.
Lane 1 represents purified CD38 (positive control) and lane 2 represents microsomal fraction from rat liver. Both were probed with anti-CD38 polyclonal antibody without the addition of Santa Cruz blocking peptide **(A)**. Both of these bands disappeared when the anti-CD38 polyclonal antibody was incubated with the Santa Cruz blocking peptide for 1 hour prior to probing and visualized using the ECL™ system **(B)**. Arrow indicates the position of the molecular weight of CD38. Total protein loaded for lane 1 was 20 µg and lane 2 was 200µg. Certain minor protein bands were due to nonspecific immunoreactivity.

3.6 cADPR Levels in Rat Liver Tissues

ADP-ribosyl cyclase normally catalyses the synthesis of cADPR from NAD^+, but the reaction can be reversed in the presence of high concentrations of nicotinamide, producing NAD^+ from cADPR stoichiometrically. The resultant NAD^+ was then coupled to cycling assay involving alcohol dehydrogenase and diaphorase. Each time NAD^+ cycles through these coupled reactions, a molecule of highly fluorescent resorufin is generated. As expected from the design of the assay, resorufin produced from cADPR absolutely required the presence of the cyclase, which is in contrast to NAD^+.

cADPR was extracted from rat liver tissues of both control and TAA-treated rats according to the method described by da Silva *et al.* (1998) with some modifications. Rat tissue extracts were first treated with *Neurospora crassa* NADase to remove endogenous NAD^+. The cycling assay was then performed in triplicates and repeated twice, in the presence and absence of *Aplysia* ADP-ribosyl cyclase. The latter condition provided a convenient means to distinguish between contributions of authentic signals from that of the background, such as contaminating NAD^+. The difference in the resorufin signal in the presence and absence of the cyclase was calibrated using cADPR standards. Figure 3.12A shows that both the amounts of resorufin fluorescence and the linearity of the assay were very similar to those seen with NAD^+ standards, indicating that the conversion of cADPR into NAD^+ was stoichiometric. The cycling assay exhibited a linear relationship between the rate of resorufin fluorescence increase and starting cADPR concentrations (Figure 3.12B). The linear relation held for all concentrations of cADPR standard tested (0 – 10 nM).

Figure 3.13A shows the linear relationship between the resorufin fluorescence and time. The rates of fluorescence were obtained from the linear regressions of both control and TAA-treated rats. Figure 3.13B illustrates the cellular cADPR level in control and TAA-treated rat liver tissues. Interestingly, cADPR content was only slightly augmented (22.3% higher) in TAA-treated rats compared to that in the control group. The average of cADPR levels in both control and TAA-treated were 1.04 ± 0.15 and 1.28 ± 0.03 pmoles/mg protein ($P < 0.05$), respectively.

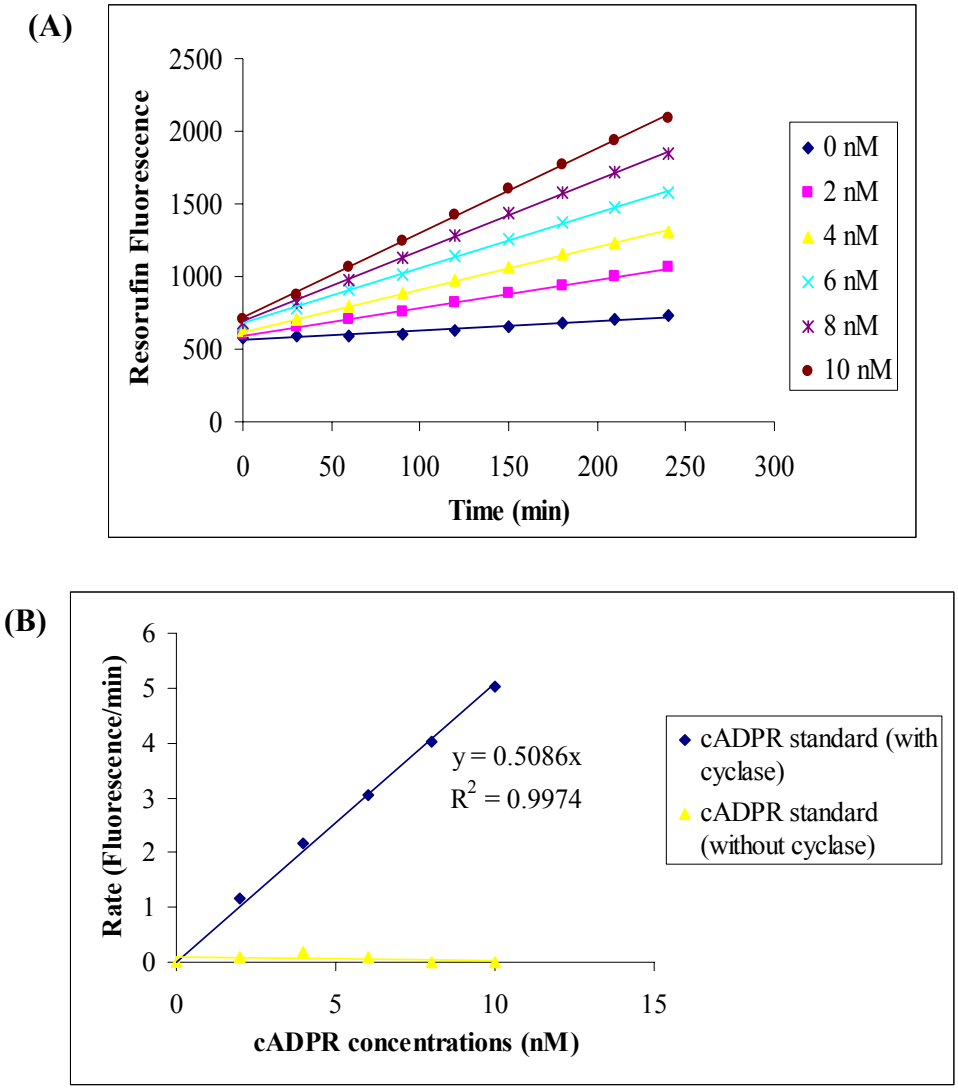

Figure 3.12 The cycling assay for cADPR standard.
(A) Various concentrations of cADPR standard were incubated in triplicates with the complete mixture of the cycling assay, including the ADP-ribosyl cyclase (+ cyclase), as described in the section 2.15. The resultant continuous increase in resorufin fluorescence was measured periodically using a multiwell plate reader. **(B)** The rates of resorufin fluorescence increase were obtained by linear regression analyses of fluorescence time courses and plotted against cADPR standard concentrations. In the absence of the cyclase, no increase in resorufin fluorescence was observed. The inset contrasts the cycling assay for cADPR and NAD^+. For cADPR, the assay was completely dependent on the presence of the cyclase, whereas, in the case of NAD^+, it was totally independent of the cyclase.

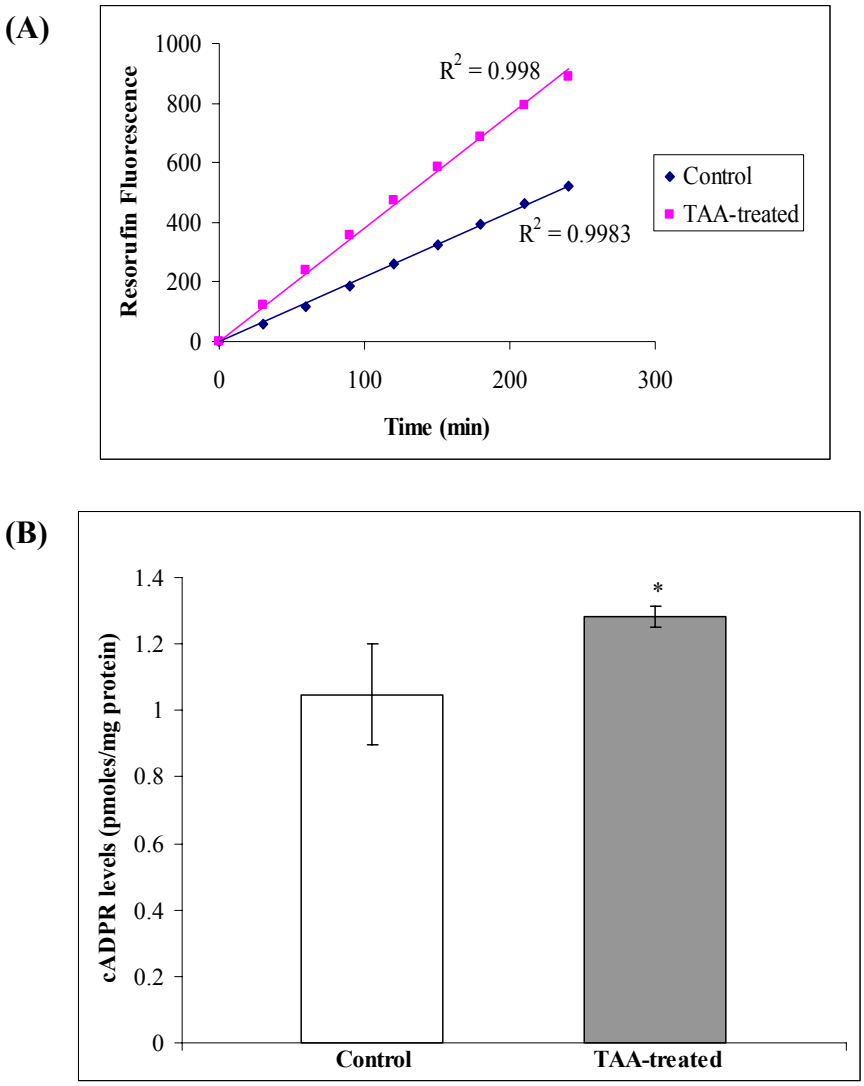

Figure 3.13 cADPR levels in control and TAA-treated rats.
(A) Representative results show that the rates of resorufin fluorescence increase were obtained from the slopes of the linear regression lines, and they were perfectly linear (R^2 > 0.99) with respect to cADPR concentrations. The rate of fluorescence produced in TAA-treated rats was higher than that in the control rats. **(B)** cADPR levels in livers of control and TAA-treated rats. cADPR levels in the livers of the TAA-treated rats were significantly higher than in the group of control rats. The values are expressed in pmoles/mg protein and are mean ± SEM (n = 6). *Significantly different from control (P < 0.05).

3.7 NAD^+ Levels in Rat Liver Tissues

According to Scheme 2.1, cellular NAD^+ levels may also be determined via the cycling assay by bypassing the ADP-ribosyl cyclase step. NAD^+ was fed into the coupled-enzyme cycling reaction, consisting of alcohol dehydrogenase and diaphorase. The former reduced NAD^+ to NADH, while the latter cycled NADH back to NAD^+ with the production of a highly fluorescent resorufin molecule from the non-fluorescent substrate, resazurin.

We first verified the cycling reactions with nanomolar concentrations of NAD^+. Figure 3.14A shows the amplification of NAD^+ resulted in a linear increase in resorufin fluorescence for up to 2 hours. The linear relation held for all concentrations of NAD^+ tested (0 – 10 nM). The rates of increase of resorufin fluorescence were obtained from the slopes of the linear regression lines, and they were extremely linear ($R^2 = 0.9855$) with respect to NAD^+ concentration (Figure 3.14B). Similar results were reproduced upon repetition of this experimental setup. The linearity of the assay was quite remarkable considering that two different enzyme reactions were coupled. The assay is thus clearly sensitive enough to detect as low as 1 – 2 nM NAD^+. This cycling reaction can be monitored conveniently in a fluorescence multiwell plate reader, which can be set to measure the increase in resorufin fluorescence periodically. It is therefore a one-step assay, not requiring any further separation or manipulation of the samples, making it highly convenient and reproducible.

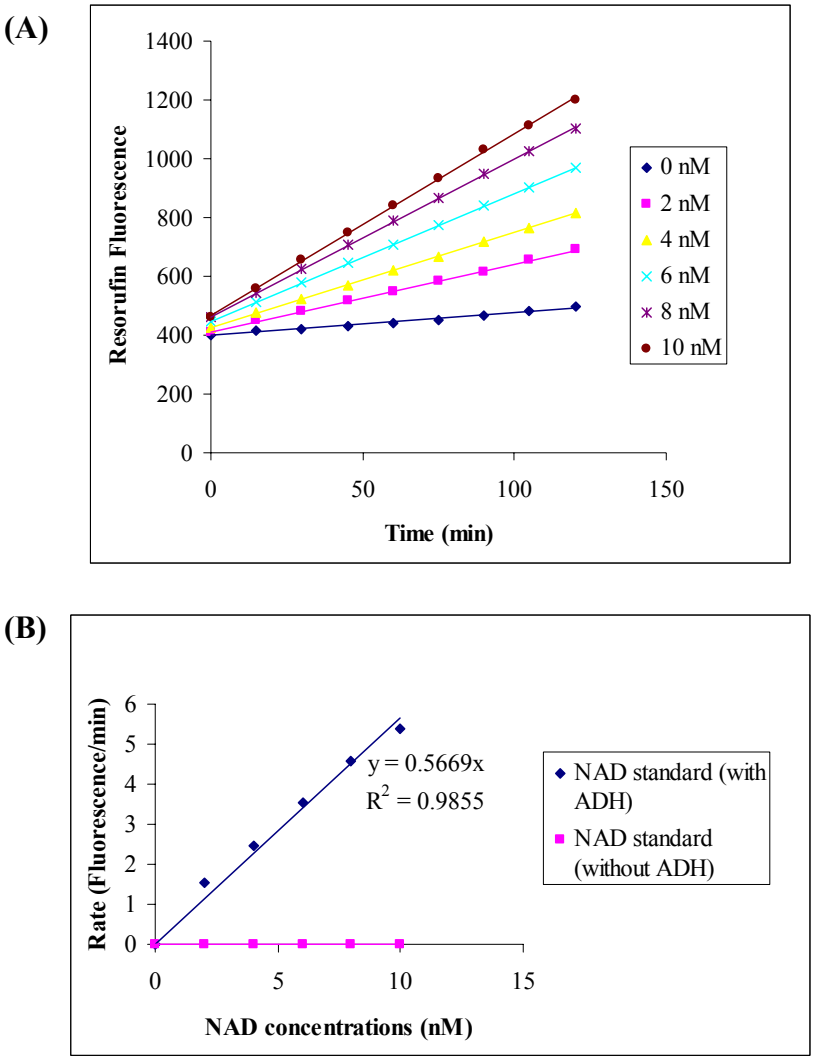

Figure 3.14 The cycling assay for NAD^+ (standard assay).
(A) Various concentrations of NAD^+ were incubated in triplicates with the cycling assay reagent mix, including alcohol dehydrogenase (AD), as described in the section 2.16, Chapter 2. Resorufin fluorescence was observed to increase linearly with time and this linearity held for all concentrations of NAD^+ tested (0 – 10 nM). **(B)** The rates of resorufin fluorescence increase were obtained by linear regression analyses of fluorescence time courses and plotted against NAD^+ standard concentrations. In the absence of the alcohol dehydrogenase (ADH), no increase in resorufin fluorescence was observed.

Figure 3.15 illustrates the endogenous NAD^+ levels in control and TAA-treated rat liver tissues. We observed that the NAD^+ levels were drastically decreased in TAA-treated rats compared to that in the control group. The average of NAD^+ levels in both control and TAA-treated rats were 5.68 ± 0.75 and 1.44 ± 0.51 nmoles/mg protein ($P < 0.05$), respectively.

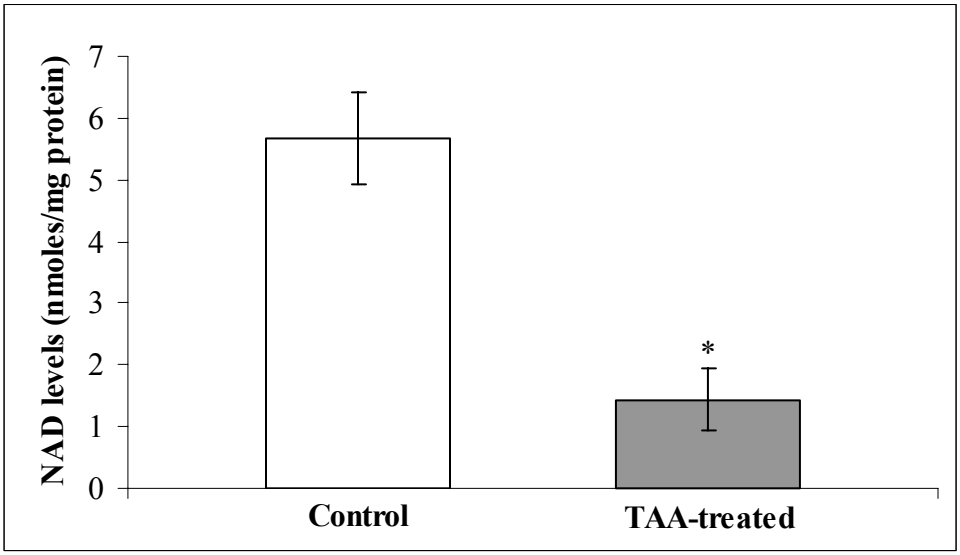

Figure 3.15 NAD^+ levels in livers of control and TAA-treated rats.
NAD^+ levels in the livers of the TAA-treated rats were significantly lower than in the group of control rats. The values are expressed in nmoles/mg protein and are mean ± SEM (n = 6). *Significantly different from control ($P < 0.05$).

CHAPTER 4

DISCUSSION

CD38 is a 42-45 kDa type II transmembrane glycoprotein (Jackson and Bell, 1990) and was first defined by monoclonal antibody typing more than 20 years ago as a lymphocyte surface antigen (Reinherz *et al.*, 1980). It is now known that CD38 is expressed not only in many other hematopoietic cells (Zocchi *et al.*, 1993; Ramaschi *et al.*, 1996), but is also widely distributed among nonhematopoietic tissues (Koguma *et al.*, 1994). The question of what function of CD38 is in the liver cirrhosis has yet to be answered conclusively. A large body of evidence supported the view that Ca^{2+} homeostasis is altered in liver cirrhosis. It has been reported that hepatic intracellular Ca^{2+} was elevated while the endoplasmic reticulum sequestered Ca^{2+} was decreased in thioacetamide-administered rats (Diez-Fernandez *et al.*, 1996). Further, there was differential regulation and expression of three isoforms of IP_3 receptors in liver cirrhosis (Dufour *et al.*, 1999). The expressions of types 1 and 3 isoforms were increased while the expression of type 2 isoform was decreased in bile duct-ligated rats. The localizations of type 2 isoform to the apical domain of hepatocytes and type 3 isoform to the intrahepatic bile duct epithelial cells suggest that Ca^{2+} homeostasis is altered in these cells.

Together, these data raise a question of whether CD38 could be involved in altering the Ca^{2+} homeostasis through cADPR formation that activates ryanodine receptors and then lead to CICR. In this study, a possible answer(s) to this matter was provided by performing a study to investigate the biochemical and immunohistochemical characteristics of CD38 as well as the cADPR and NAD^+ levels in thioacetamide-induced

rat liver cirrhosis. The reason why thioacetamide-induced rats was used was that it is a reliable model as thioacetamide (TAA) induces prominent regenerative nodules and liver fibrosis, and the histology of the TAA-induced model is more similar to human cirrhosis (Zimmermann *et al.*, 1987). It was demonstrated here that there was a significant increase in CD38 mRNA level in the cirrhotic liver. Similarly, CD38 protein expression was elevated in the cirrhotic liver compared to the control liver and it was found to be localized at the plasma membrane of rat hepatocytes in immunohistochemistry. The increased enzymatically active CD38 expression is reflected by significantly enhanced ADP-ribosyl cyclase activity in liver microsomes. In addition, analysis of cADPR levels in liver from TAA-treated rats revealed a 22.3% increase ($P < 0.05$) compared to that from control rats.

Calcium (Ca^{2+}) is an important second messenger and the mobilization of Ca^{2+} from intracellular stores is a fundamental mechanism of signaling that not only mediates muscle contraction but also triggers and regulates many cellular processes, including the progression through G_1/S and mitosis (Berridge, 1990; Lu and Means, 1993). Sustained elevations of intracellular calcium activate cytotoxic mechanisms, contributing to cell injury and death induced by hepatotoxic agents (DiMonte *et al.*, 1984; Moore *et al.*, 1985). The alteration of Ca^{2+} homeostasis in liver cirrhosis may be involved in cell necrosis and in the acute mitogen response during the abnormal regeneration of the nodules. Diez-Fernandez *et al.* (1996) reported that hepatic intracellular Ca^{2+} was elevated while the endoplasmic reticulum sequestered Ca^{2+} was decreased which indicated that the effect of thioacetamide on calcium mobilization from its intracellular stores, was followed by a chronological sequence of events which could be related to cell

death and regeneration. The increased CD38 expression at both transcript and protein levels as well as cADPR in TAA-treated rats in this study suggests that CD38 might be involved in altering Ca^{2+} homeostasis through ADP-ribosyl cyclase-catalyzed formation of cADPR that plays a role in the activation of ryanodine receptors via Ca^{2+}-induced Ca^{2+} release.

cADPR has been most extensively studied and shown to function as a calcium-mobilizing second messenger in a number of cell types isolated from a variety of organisms (Lee, 2001). CD38 as an ectoenzyme on the plasma membrane, possesses ADP-ribosyl cyclase activity which is able to catalyze the synthesis cADPR and nicotinamide from β-NAD^+, and cADPR hydrolase activity, which degrades cADPR to ADPR (Zocchi *et al.*, 1993; Inageda *et al.*, 1995). Later, Cakir-Keifer *et al.* (2000) reported that under normal physiologic pH conditions (pH 7), CD38 first catalyzes the release of nicotinamide from NAD^+ and then mediates the formation of an oxocarbenium intermediate. This intermediate is either cyclized to form cADPR (cyclase reaction) or is hydrolyzed to form ADPR (glycohydrolase reaction).

Since the active site of CD38 is extracellular, the substrate for CD38 is likely to be found outside the cell. NAD^+, the substrate for CD38, is normally localized inside the cells and is not found in high concentrations in the extracellular milieu of serum or exudate (Kim *et al.*, 1993b). Despite the ectoenzyme nature of CD38 and the intracellular localized NAD^+, a significant increase of intracellular cADPR levels has been observed in TAA-treated rat liver in the present study. It is hypothesized that high local concentrations of extracellular NAD^+ would be present at sites of cell necrosis and tissue damage (Adriouch *et al.*, 2001; Liu *et al.*, 2001). Therefore, it is now thought that under

normal homeostatic conditions, minimal substrate is available for ecto-CD38, thus limiting its enzyme activity. However, near sites of inflammation or cell necrosis as a consequence of cirrhosis, extracelllular NAD^+ is likely to be present in concentrations sufficient to be utilized efficiently by CD38. cADPR thus formed may then be transported back via oligomeric CD38 to act intracellularly on ryanodine receptors (Franco *et al.*, 1998) and led to the increase of cADPR level in cirrhotic rat liver. It has been shown that cADPR could enter the cells through a channel generated by two or four CD38 monomers as suggested by the presence of catalytic active monomers, homodimers and homotetramers in CD38-transfected HeLa cells (Bruzzone *et al.*, 1998).

Previously, Zocchi *et al.* (1996) has shown that there was a corresponding increase in cADPR levels in CD38 internalized cells. Based on this observation, they concluded that intravesicular localization of internalized CD38 did not cause the unavailability of cytosolic NAD^+ to the catalytically active site (Lund *et al.*, 1995), possibly because of permeation of NAD^+ across the endocytotic CD38-containing vesicles. It has also been postulated that internalization might represent an alternative mechanism of intracellular signaling which is unrelated to its enzymatic properties and the calcium-releasing properties of cADPR. Indeed, this postulation has been given credence through the studies performed by Funaro *et al.* (1998) whereby they have shown that the internalization step could be a negative feedback control mechanism which interrupts signal transduction processes mediated by the surface membrane CD38. Despite the various models that were proposed thus far for the mechanism of CD38 mediated cADPR-calcium mobilizing activities in the cell, the ecto-location of CD38 and the means to transport its product, cADPR, into the intracellular environment where it

can exert its calcium release activity (De Flora *et al.*, 1997) remains an unresolved issue with researchers in the CD38 field.

CD38, unlike the *Aplysia* enzyme, is a very inefficient cyclase, with cADPR representing only 1-3% of the final product and ADPR accounting for the rest (Howard *et al.*, 1993). Although the present study revealed a marginal increase (22.3%) of cADPR content in TAA-treated rat liver (section 3.6), it has been shown that this relative paucity of cADPR produced by CD38 is biologically relevant (Howard *et al.*, 1993). The production of cADPR by CD38 is of particular interest to biologists, as cADPR has been shown to induce intracellular calcium release from ryanodine receptor (RyR)-gated stores in a number of different mammalian cell types including smooth muscle and neuronal cells (Guse *et al.*, 1999). Interestingly, the cADPR-triggered, RyR-gated intracellular calcium stores in these cell types are spatially, functionally and pharmacologically distinct from the calcium stores controlled by inositol trisphosphate (IP_3), indicating that cADPR mobilizes intracellular calcium in an IP_3-independent fashion (Lee, 2001). Recently, more experiments have begun to focus on identifying the signal transduction cascades that utilize cADPR. Experiments using competitive antagonists of cADPR have demonstrated that signaling through a number of receptors such as muscarinic acid receptor and acetylcholine receptor expressed by a variety of mammalian cell types is dependent on cADPR-induced calcium release (Guse, 1999). All of these data suggest that CD38 could potentially regulate calcium signaling through production of cADPR.

Further, present study also showed that the endogenous NAD^+ levels (section 3.7) in the liver of TAA-treated rats were about 4-fold lower than that in the control rats ($P < 0.05$). In addition to that, other studies have also shown that there was a decreased hepatic

NAD^+ levels in stressed liver (Cuomo *et al.*, 1994; 1995). It is believed that free radicals play a major role in the development of liver cirrhosis and was suggested that the mechanisms by which various toxic chemicals induced their effect in the body involved the release of free radicals (Di Luzio, 1963). Okamoto and Takasawa (2002) reported that the accumulation of these free radicals would result DNA strand breaks (DNA damage) and activation of poly (ADP-ribose) synthetase/polymerase (PARP). This PARP then acts to repair the DNA breaks, consuming NAD^+ as a substrate. Consequently, there would be a sharp drop in the intracellular levels of NAD^+ (Okamoto and Takasawa, 2002), which was what observed in the present study. Paradoxically, despite its beneficial effect, PARP can induce necrotic cell death through NAD^+ depletion (Takasawa and Okamoto, 2002; Germain *et al.*, 2000). Based on their work, Okamoto and his colleagues found that the cellular NAD^+ reduction would severely impair such cellular functions as insulin synthesis and secretion and cause lethal injury to the β-cells. According to the Okamoto model, the decreases in the NAD^+ level cause decreases in cADPR in β-cells. Thus, they proposed that insulin secretion by glucose occurs via cADPR-mediated Ca^{2+} mobilization of an intracellular Ca^{2+} pool, the endoplasmic reticulum. In this model, ATP inhibits the cADPR hydrolase activity of CD38, which results in the accumulation of cADPR. This metabolite then acts as a second messenger for Ca^{2+}-mobilization from intracellular stores resulting in insulin secretion (Takasawa *et al.*, 1993a; Takasawa *et al.*, 1993b; Okamoto *et al.*, 1995; Kato *et al.*, 1995). Collectively, these data strongly suggest that the possibility of utilization of extracellular NAD^+ by CD38, which is localized to the plasma membrane, and transportation of cADPR produced into the cell which subsequently induces intracellular calcium release via the ryanodine receptor as well as cell signaling.

The presence of a ryanodine-sensitive Ca^{2+}-induced Ca^{2+} release pool in the hepatocyte cells has been shown in the study by Osada *et al.* (1994). Later, Martinez-Merlos *et al.* (1997) reported that the rat livers contain the highest level of ryanodine receptor when compared to other rodent species. These data provide evidence for a possible model where the increase in cyclase activity in cirrhotic liver causes the increase in cADPR levels that would mobilize Ca^{2+} from internal stores, contributing to the elevation of intracellular Ca^{2+}. However, there have been conflicting reports on the nature of the ryanodine receptors in the liver. Giannini *et al.* (1995) showed that the messenger RNAs encoding the three known RyR forms are absent in liver extracts. The first corollary to account for such observation is that RyR could exist as a novel isoform in the liver. This novel isoform might be identified by Lee *et al.* (2002) as a modified RyR1 that is localized in the liver. The second corollary is that cADPR may mobilize internal calcium stores in a novel mechanism. Another possibility that could explain the observation above is that the low densities of RyR in non-excitable mammalian cells that suggest that the levels of RyR could be below the limits of current detection method (Bennett *et al.*, 1996).

Apart from Ca^{2+} signaling, CD38 might also participate in liver cirrhosis in other manners. A role for CD38 in cell activation and proliferation pathways has been suggested by the agonistic features of selected anti-CD38 monoclonal antibodies (mAbs). Funaro *et al.* (1990) have demonstrated that the CD38 mAbs A10 and IB4 elicit activation and proliferation of human T cells, thymocytes, and NK cells, suggesting that CD38 transduces activation signals upon target binding. The agonistic mAbs are characterized by the ability to activate cells, mobilize Ca^{2+} from internal stores and

induce cytokine synthesis and release (Malavasi and Ferrero, 1997). Results in the present study show that the expression of CD38 on hepatocytes thus might be involved in cytokine production, which could be one of the sources that stimulates the synthesis and deposition of collagen. Experiments that have been done to date suggest that antibodies to CD38 do not suppress or activate the enzyme activity of CD38 (Howard *et al.*, 1993; Lund *et al.*, 1999), and that anti-CD38-induced signaling can proceed even when enzyme activity has been blocked (Lund *et al.*, 1999). Thus, it is likely that anti-CD38-mediated signaling in at least some cell types occurs independently of cADPR, ADPR and NAADP production.

The immunohistochemical results (section 3.3) show that CD38 is localized to the plasma membrane. Khoo and Chang (2000) reported that the localization of CD38 on the plasma membrane is domain specific manner in rat hepatocytes, in which it contradicts to the present results. Instead, it was shown that CD38 is widely distributed on the plasma membrane without any specific domain. This could be due to the different fixation methods and different batch of antibodies that were used. The hepatocyte is a highly polarized cell with at least two major domains: the sinusoidal/lateral domain and the bile canalicular domain (Evans, 1980). The sinusoidal domain participates principally in the exchange processes with the blood including the secretion of serum proteins, uptake of various molecules and communication with the surrounding environment through its receptors that bind growth factors, hormones and other biologically important ligands (Rosario *et al.*, 1988; Arias and Forgac, 1984; LeBouton, 1993) while the bile canalicular/apical domain is specialized for the excretion of bile components (Inoue *et al.*, 1983). Various cells (e.g. endothelial cells) of the immune response are known to express

CD31, a putative ligand for CD38 (refer to review by Mehta *et al.*, 1996). It is an interesting possibility that the localization of CD38 to the plasma membrane indicates a possible interaction between the hepatocytes and cells of the immune system that may be responsible for mediating immune responses.

Humoral response is increased in liver cirrhosis and this is shown by Yuka *et al.* (1996). Early plasma cells were significantly increased in the peripheral blood from patients diagnosed with liver cirrhosis with hypergammaglobulinaemia. The increase in CD38 in the early plasma cells suggests that elevated CD38 expression augments the secretion of immunoglobulin from plasma cells (Yuka *et al.*, 1996), which states another possible role of CD38. In addition, serum hyaluronate was significantly elevated in patients with liver cirrhosis (Satoh *et al.*, 2000). Hyaluronate is a glucosaminoglycan synthesized by the mesenchymal cells and degraded by hepatic sinusoidal endothelial cells by a specific receptor-mediated process. The two hyaluronate-binding motifs present in the extracellular domain of CD38 may function in attachment to the extracellular matrix (cell-matrix interaction), hinting that hyaluronic acid can act as a CD38 ligand (Nishina *et al.*, 1994). Further, it has been shown that hepatocytes bind proteoglycans and this binding can be saturated, implying a receptor-mediated interaction (Kirch *et al.*, 1987; Laurent *et al.*, 1986). According to these findings, it is likely that some components of the extracellular matrix in the liver such as hyaluronate could interact with CD38 leading to changes in the properties of CD38 and its involvement in the cell signaling cascades.

Besides the widespread application of the molecule as an ancillary tool in the classification of hematological disorders and attribution of cell lineage, CD38 is finding a

novel role in the study of different pathologies. The present study has provided new insights in the involvement of CD38 in liver cirrhosis. CD38 could play a vital role in the pathogenesis of cirrhosis. However, many questions remain to be resolved. More studies will be necessary to clarify the speculations and whether the increase in CD38 expression is caused by inflammatory responses or profibrogenic responses. As known, hepatic stellate cells (HSC) play a major role in hepatic fibrosis and regeneration when activated as a response to liver injury (Baba *et al.*, 2004). Future work that involves the characterization of CD38 in hepatic stellate cells and studies that focus on the correlation between the altered CD38 expression and the activation of stellate cells would conclude whether CD38 plays a part of the pathogenesis of liver fibrosis. It would also be interesting to characterize CD38 at different developmental stages of liver cirrhosis (time-frame) to assess whether CD38 could act as a prognostic marker of liver cirrhosis. Since CD38 might play important roles in immune responses, apoptotic cell killing and liver regeneration, additional studies using other models of liver injury (i.e., LPS- and Fas-induced liver injuries) and liver regeneration after partial hepatectomy will also provide us better understandings.

CHAPTER 5

CONCLUSION

It is nearly twenty five years since the first papers on CD38 appeared in the scientific community (Reinherz *et al.*, 1980; Terhorst *et al.*, 1981). Through the initial pioneering work of various immunology laboratories, there are numerous evidence to conclude that CD38 is an important surface immunoregulatory molecule; its myriad of possible functions include the induction of B and T cells proliferation (Funaro *et al.*, 1990), regulation of the humoral immune response (Cockayne *et al.*, 1998), apoptosis (Zupo *et al.*, 1994), tyrosine phosphorylation of various proteins (Kirkham *et al.*, 1994), activation of certain kinases (Kitanaka *et al.*, 1996) and cytokine release (Ausiello *et al.*, 1995). In addition, CD38 also displays adhesion properties and might possibly mediate a selectin-type adhesion between different blood populations and human vascular endothelial cells via its putative ligand, CD31 (Deaglio *et al.*, 1996).

Our lab has shown that CD38 is expressed in a variety of non-hematopoietic cells including organs as diverse as the lung (Khoo and Chang, 1998), eye (Khoo and Chang, 1999), cerebellum (Yamada *et al.*, 1997) and liver (Khoo and Chang, 2000) but the precise function(s) of CD38 in these organs is still vague. Future work needs to be done to ascertain the function(s) of CD38 in these cells. Despite the multitude of studies done on CD38 and its role in cellular signaling, there is still no discovery of an encompassing "physio-functional role" correlated with CD38. This perplexing enigma has been partially solved through the work of Hiroshi Okamoto's lab where the studies were performed not on hematopoietic cells but rather on Islet cells. It was shown that CD38 mediates a cyclic

ADP-ribose dependent signaling pathway involved in insulin secretion. It is a well-known fact that glucose induces an increase in the intracellular Ca^{2+} concentration in pancreatic β-cells of the islets of Langerhans, which then results in the secretion of insulin. The accepted hypothesis is that the ATP produced in the process of glucose metabolism, inhibits the potassium channel and thus inducing membrane depolarization and the opening of the voltage-dependent Ca^{2+}-channels (Ashcroft and Ashcroft, 1992).

Nevertheless, based on the work of Okamoto and his colleagues, they proposed an alternative model of insulin secretion by glucose via cADPR-mediated Ca^{2+}-mobilization from an intracellular Ca^{2+} pool. In this particular model, ATP inhibits the cADPR hydrolase activity of CD38, which causes the accumulation of cADPR. This metabolite then acts as a second messenger for Ca^{2+}-mobilization from intracellular stores resulting in insulin secretion (Okamoto, 2002). Subsequently, they went on to show that the presence of anti-CD38 autoantibodies in non-insulin-dependent diabetes mellitus (NIDDM) patients might possibly be the one of the major causes of impaired glucose-induced insulin secretion in NIDDM (Ikehata *et al.*, 1998). Further investigative studies by Okamoto's group led to the observation that the Arg140Trp mutation on CD38 could contribute to the development of Type II diabetes mellitus via the impairment of glucose-induced insulin secretion (Yagui *et al.*, 1998).

However, despite the studies of Okamoto's group, they have failed to shed any light on how an ectoenzyme like CD38 with its catalytic site in the extracellular environment is able to transport its produced metabolite, cADPR, into the intracellular medium in order for it to play an intracellular calcium mobilizing role leading to insulin secretion. De Flora's group managed to propose a model that involves the transmembrane

juxtaposition of two or four CD38 monomers which can generate a catalytically active channel for selective formation and influx of cADPR to reach cADPR-responsive intracellular calcium stores (Franco *et al.*, 1998). On the other hand, da Silva *et al.* (1998) showed that there was no direct involvement of ectocellular synthesis of cADPR on the regulation of the cADPR-mediated intracellular calcium signaling in T-lymphocytes. In that study, they also observed that there was no increase of intracellular cADPR when the intact cells were incubated with NAD^+. Therefore, this model is still debated and further work needs to be done to clarify the paradoxical results observed thus far.

Despite the studies that were done on various diseases in search for a possible physiological relevance of CD38, the role of CD38 in liver cirrhosis has yet to be determined. The results described in the current study may provide a possible resolution of this issue. Here it was shown that there was a significant increase in CD38 mRNA level in the cirrhotic liver. Similarly, CD38 protein expression was elevated in the cirrhotic liver and it was localized at the plasma membrane of rat hepatocytes. Then, it was further demonstrated that the immunoblot analysis revealed an increase in CD38 expression in the microsomes of cirrhotic liver compared to the normal liver. The increase in CD38 expression was supported by the detection of higher level of ADP-ribosyl cyclase activity in the cirrhotic liver compared to that in the control. In addition to CD38, the cADPR level was demonstrated to be modestly but significantly augmented in cirrhotic liver and in contrast, there was a significant decrease in the endogenous NAD^+ in cirrhotic liver. Together, these results raised the possibility that altered CD38 expression and a concomitant elevation of the ADP-ribosyl cyclase activity as well as cADPR may play an important role in the pathogenesis of liver cirrhosis.

This study has provided new insights in the involvement of CD38 in liver cirrhosis. However, many questions remain to be resolved. More studies will be necessary to clarify the speculations and whether the increase in CD38 expression is a cause or consequence in liver cirrhosis. It is essential that we determine the intracellular calcium level in the control and TAA-treated rat livers. It also remains to be elucidated whether the calcium release from intracellular stores is mediated by cADPR that activates the ryanodine receptor. There is ample evidence that alteration of calcium concentrations can affect cellular events that are totally controlled endogenously, such as cell division (Poenie *et al.*, 1985; Steinhardt and Alderton, 1988; Twigg *et al.*, 1988), which is controlled by the mitotic clock and does not require an external stimulus.

It is interesting to characterize CD38 at different developmental stages of liver cirrhosis to assess whether CD38 could act as a prognostic marker of liver cirrhosis. It was reported that CD38 as a relevant marker in HIV infection (Salazar-Gonzalez *et al.*, 1985). High $CD38^+/CD8^+$ ratios were reported as closely correlating with the HIV infection, becoming a dependable marker of poor prognosis and disease progression (Giorgi *et al.*, 1993; Ho *et al.*, 1993; Liu *et al.*, 1998). Its persistence during progression of the disease suggested that CD38 expression may exert a protective function (Savarino *et al.*, 1996). It is also essential to carry out additional experiments using CD38-deficient mice to define the active role(s) of CD38 in liver cirrhosis.

Other areas of research not directly involving the calcium mobilizing properties associated with the metabolites of CD38, which should also be addressed, includes the crystallization of CD38 in order to solve its molecular structure and thus, to provide clues for identifying the correlation between the receptorial-enzymatic-regulatory properties of

this molecule. Over the years, CD38 has been labeled, among other thing, eclectic, paradoxical and an enigma to those who study this fascinating molecule. Its diverse unusual properties still leave many questions unanswered. Indeed, the very nature of its "peculiarity" in a scientific context, especially with regards to its apparent redundancy in terms of intrinsic functions dictate the need for a multidisciplinary approach to address the unresolved questions being asked of this molecule.

In conclusion, our study has provided new insights in the involvement of CD38 in liver cirrhosis. In this study, our results raised the possibility that increased CD38 expression and the ADP-ribosyl cyclase activity as well as a concomitant elevation of cADPR level may play an important role in the pathogenesis of liver cirrhosis.

REFERENCES

Aarhus R, Graeff RM, Dickey DM, Walseth TF, and Lee HC. ADP-ribosyl cyclase and CD38 catalyze the synthesis of a calcium-mobilizing metabolite from NADP. J Biol Chem 1995;270:30327-30333.

Adriouch S, Ohlrogge W, Haag F, Koch-Nolte F, and Seman M. Rapid induction of naive T cell apoptosis by ecto-nicotinamide adenine dinucleotide: requirement for mono (ADP-ribosyl) transferase 2 and a downstream effector. J Immunol 2001;167:196-203.

Aiken C, Konner J, Landau NR, Lenburg ME, and Trono D. Nef induces CD4 endocytosis: requirement for a critical dileucine motif in the membrane-proximal CD4 cytoplasmic domain. Cell 1994;76:853-864.

Al-Bader A, Mathew TC, Khoursheed M, Asfar S, Al-Sayer H, and Dashti HM. Thioactamide toxicity and the spleen: histological and biochemical analysis. Anatomia, Histologia, Embryologia 2000;29:3-8.

Anthony PP, Ishak KG, Nayak NC, Poulsen HE, Scheuer PJ, and Sobin LH. The morphology of cirrhosis: definition, nomenclature and classification. Bull WHO 1977;55:521-540.

Anthony PP, Ishak KG, Nayak NC, Poulsen HE, Scheuer PJ, and Sobin LH. The morphology of cirrhosis. J Clin Pathol 1978;31:395-414.

Arias IM and Forgac M. The sinusoidal domain of the plasma membrane of rat hepatocytes contains an amiloride-sensitive Na^+/H^+ antiport. J Biol Chem 1984;259:5406-5408.

Ausiello CM, Urbani F, la Sala A, Funaro A, and Malavasi F. CD38 ligation induces discrete cytokine mRNA expression in human cultured lymphocytes. Eur J Immunol 1995;25:1477-1480.

Baba S, Fujii H, Hirose T, Yasuchika K, Azuma H, Hoppo T, Naito M, Machimoto T, and Ikai I. Commitment of bone marrow cells to hepatic stellate cells in mouse. J Hepatol 2004;40:255-260.

Beaune P, Dansette PM, Mansuy D, Kiffel L, Finck M, Amar C, Leroux JP, and Homberg JC. Human anti-endoplasmic reticulum autoantibodies appearing in a drug-induced hepatitis are directed against a human liver cytochrome P-450 that hydroxylates the drug. Proc Natl Acad Sci USA 1987;84:551-555.

Bennett DL, Cheek TR, Berridge MJ, De Smedt H, Parys JB, Missiaen L, and Bootman MD. Expression and function of ryanodine receptors in nonexcitable cells. J Biol Chem 1996;271:6356-6362.

Berridge MJ. Calcium oscillations. J Biol Chem 1990;265:9583-9586.

Berridge MJ. Elementary and global aspects of calcium signalling. J Physiol 1997;499:291-306.

Bioulac-Sage P, Lafon ME, Saric J, and Balabaud C. Nerves and perisinusoidal cells in human liver. J Hepatol 1990;10:105-112.

Bismuth H. Surgical anatomy and anatomical surgery of the liver. World J Surg 1982;6:3-9.

Bofill M, Mocroft A, Lipman M, Medina E, Borthwick NJ, Sabin CA, Timms A, Winter M, Baptista L, Johnson MA, Lee CA, Phillips AN, and Janossy G. Increased numbers of primed activated CD8+CD38+CD45RO+ T cells predict the decline of CD4+ T cells in HIV-1-infected patients. AIDS 1996;10:827-834.

Bolen JB. Nonreceptor tyrosine protein kinases. Oncogene 1993;8:2025-2031.

Bradford MM. A rapid and sensitive method for the quantitation of microgram quantities of protein utilizing the principle of protein-dye binding. Anal Biochem 1976;72:248-254.

Bruzzone S, Guida L, Franco L, Zocchi E, Corte G, and De Flora A. Dimeric and tetrameric forms of catalytically active transmembrane CD38 in transfected HeLa cells. FEBS Lett 1998;433:275-278.

Cakir-Keifer C, Muller-Steffner H, and Schuber F. Unifying mechanism for *Aplysia* ADP-ribosyl cyclase and CD38/NAD^+ glycohydrolase. Biochem J 2000;349:203-210.

Cesano A, Visonneau S, Deaglio S, Malavasi F, and Santoli D. Role of CD38 and its ligand in the regulation of MHC-nonrestricted cytotoxic T cells. J Immunol 1998;160:1106-1115.

Chini EN and Dousa TP. Nicotinate-adenine dinucleotide phosphate-induced Ca(2+)-release does not behave as a Ca(2+)-induced Ca(2+)-release system. Biochem J 1996;316:709-711.

Clapper DL, Walseth TF, Dargie PJ, and Lee HC. Pyridine nucleotide metabolites stimulate calcium release from sea urchin egg microsomes desensitized to inositol trisphosphate. J Biol Chem 1987;262:9561-9568.

Conley ME. Molecular approaches to analysis of X-linked immunodeficiencies. Annu Rev Immunol 1992;10:215-238.

Crawford JM. Liver cirrhosis. In: MacSween RNM, Burt AD, Portmann BC, Ishak KG, Scheuer PJ, Anthony PP, eds. Pathology of the Liver. 4th ed. London: Churchill Livingstone, 2002:575-620.

Cuomo R, Dattilo M, Pumpo R, Capuano G, Boselli L, and Budillon G. Nicotinamide methylation in patients with cirrhosis. J Hepatol 1994;20:138-142.

Cuomo R, Pumpo R, Sarnelli G, Capuano G, and Budillon G. Nicotinamide methylation and hepatic energy reserve: a study by liver perfusion in vitro. J Hepatol 1995;23:465-470.

Cutrona G, Ulivi M, Fais F, Roncella S, and Ferrarini M. Transfection of the c-myc oncogene into normal Epstein-Barr virus-harboring B cells results in new phenotypic and functional features resembling those of Burkitt lymphoma cells and normal centroblasts. J Exp Med 1995;181:699-711.

da Silva CP, Potter BV, Mayr GW, and Guse AH. Quantification of intracellular levels of cyclic ADP-ribose by high-performance liquid chromatography. J Chromatography B Biomed Sci Appl 1998;707:43-50.

Dashti H, Jeppsson B, Hagersrrand I, Hultberg B, Stinivas U, Abdulla M, Joclsson B, and Bengmark S. Early biochemical and histological changes in rats exposed to a single injection of thioacetamide. Pharmacol Toxicol 1987;60:171-174.

Dashti H, Mathew TC, Jadaun MM, and Ashkanani E. Zinc and liver cirrhosis: biochemical and histopathologic assessment. Nutrition 1997;13:206-212.

Deaglio S, Dianzani U, Horenstein AL, Fernandez JE, van Kooten C, Bragardo M, Funaro A, Garbarino G, Di Virgilio F, Banchereau J, and Malavasi F. Human CD38 ligand. A 120-KDA protein predominantly expressed on endothelial cells. J Immunol 1996;156:727-734.

Deaglio S, Morra M, Mallone R, Ausiello CM, Prager E, Garbarino G, Dianzani U, Stockinger H, and Malavasi F. Human CD38 (ADP-ribosyl cyclase) is a counter-receptor of CD31, an Ig superfamily member. J Immunol 1998;160:395-402.

De Flora A, Guida L, Franco L, and Zocchi E. The CD38/cyclic ADP-ribose system: a topological paradox. Int J Biochem Cell Biol 1997;29:1149-1166.

Di Luzio NR. Prevention of the acute ethanol induced fatty liver by antioxidants. Physiologist 1963;6:169.

Dianzani U, Funaro A, DiFranco D, Garbarino G, Bragardo M, Redoglia V, Buonfiglio D, De Monte LB, Pileri A, and Malavasi F. Interaction between endothelium and CD4+CD45RA+ lymphocytes. Role of the human CD38 molecule. J Immunol 1994;153:952-959.

Diez-Fernandez C, Sanz N, and Cascales M. Intracellular calcium concentration impairment in hepatocytes from thioacetamide-treated rats. Implications for the activity of Ca^{2+}-dependent enzymes. J Hepatol 1996;24:460-467.

DiMonte D, Bellomo G, Thor H, Nicotera P, and Orrenius S. Menadione-induced cytotoxicity is associated with protein thiol oxidation and alteration in intracellular Ca^{2+} homeostasis. Arch Biochem Biophys 1984;235:2390-2392.

Drach J, McQueen T, Engel H, Andreeff M, Robertson KA, Collins SJ, Malavasi F, and Mehta K. Retinoic acid-induced expression of CD38 antigen in myeloid cells is mediated through retinoic acid receptor-alpha. Cancer Res 1994;54:1746-1752.

Dufour JF, Luthi M, Forestier M, and Magnino F. Expression of inositol 1,4,5-trisphophate receptor isoforms in rat cirrhosis. Hepatology 1999;30:1018-1026.

Ellis JH, Barber KA, Tutt A, Hale C, Lewis AP, Glennie MJ, Stevenson GT, and Crowe JS. Engineered anti-CD38 monoclonal antibodies for immunotherapy of multiple myeloma. J Immunol 1995;155:925-937.

Evans WH. A biochemical dissection of the functional polarity of the plasma membrane of the hepatocyte. Biochim Biophys Acta 1980;604:27-64.

Fedele G, Frasca L, Palazzo R, Ferrero E, Malavasi F, and Ausiello CM. CD38 is expressed on human mature monocyte-derived dendritic cells and is functionally involved in CD83 expression and IL-12 induction. Eur J Immunol 2004;34:1342-1350.

Fernandez JE, Deaglio S, Donati D, Beusan IS, Corno F, Aranega A, Forni M, Falini B, and Malavasi F. Analysis of the distribution of human CD38 and of its ligand CD31 in normal tissues. J Biol Regul Homeost Agents 1998;12:81-91.

Ferrero E and Malavasi F. The metamorphosis of a molecule: from soluble enzyme to the leukocyte receptor CD38. J Leukoc Biol 1999;65:151-161.

Fitzhugh OG and Nielson AA. Liver tumors in rats fed thiourea or thioacetamide. Science 1948;108:626-628.

Flavell DJ, Cooper S, Morland B, French R, and Flavell SU. Effectiveness of combinations of bispecific antibodies for delivering saporin to human acute T-cell lymphoblastic leukaemia cell lines via CD7 and CD38 as cellular target molecules. Br J Cancer 1992;65:545-551.

Flavell DJ, Boehm DA, Emery L, Noss A, Ramsay A, and Flavell SU. Therapy of human B-cell lymphoma bearing SCID mice is more effective with anti-CD19- and anti-CD38-saporin immunotoxins used in combination than with either immunotoxin used alone. Int J Cancer 1995;62:337-344.

Franco L, Guida L, Bruzzone S, Zocchi E, Usai C, and De Flora A. The transmembrane glycoprotein CD38 is a catalytically active transporter responsible for generation and influx of the second messenger cyclic ADP-ribose across membranes. FASEB J 1998;12:1507-1520.

French RR, Penney CA, Browning AC, Stirpe F, George AJ, and Glennie MJ. Delivery of the ribosome-inactivating protein, gelonin, to lymphoma cells via CD22 and CD38 using bispecific antibodies. Br J Cancer 1995;71:986-994.

Funaro A, Spagnoli GC, Ausiello CM, Alessio M, Roggero S, Delia D, Zaccolo M, and Malavasi F. Involvement of the multilineage CD38 molecule in a unique pathway of cell activation and proliferation. J Immunol 1990;145:2390-2396.

Funaro A, Morra M, Calosso L, Zini MG, Ausiello CM, and Malavasi F. Role of the human CD38 molecule in B cell activation and proliferation. Tissue Antigens 1997;49:7-15.

Furuya Y, Takasawa S, Yonekura H, Tanaka T, Takahara J, and Okamoto H. Cloning of a cDNA encoding rat bone marrow stromal cell antigen 1 (BST-1) from the islets of Langerhans. Gene 1995;165:329-330.

Galione A, Lee HC, and Busa WB. Ca(2+)-induced Ca2+ release in sea urchin egg homogenates: modulation by cyclic ADP-ribose. Science 1991;253:1143-1146.

Gallagher CH, Gupta DN, Judah JD, and Rees KR. Biochemical changes in acute thioacetamide intoxication. J Pathol Bacteriol 1956;72:193-201.

Genazzani AA, Bak J, and Galione A. Inhibition of cADPR-Hydrolase by ADP-ribose potentiates cADPR synthesis from beta-NAD+. Biochem Biophys Res Commun 1996;223:502-507.

Germain M, Scovassi I, and Poirier GG. Role of poly(ADP-ribose) polymerase in apoptosis. In: Szabó C, ed. Cell Death – The Role of Poly(ADP-ribose) polymerase. Boca Raton, FL: CRC Press, 2000:209-225.

Giannini G, Conti A, Mammarella S, Scrobogna M, and Sorrentino V. The ryanodine receptor/calcium channel genes are widely and differentially expressed in murine brain and peripheral tissues. J Cell Biol 1995;128:893-904.

Giorgi JV, Liu Z, Hultin LE, Cumberland WG, Hennessey K, and Detels R. Elevated levels of CD38+ CD8+ T cells in HIV infection add to the prognostic value of low CD4+ T cell levels: results of 6 years of follow-up. The Los Angeles Center, Multicenter AIDS Cohort Study. J Acquir Immune Defic Syndr 1993;6:904-912.

Graeff RM, Walseth TF, Fryxell K, Branton WD, and Lee HC. Enzymatic synthesis and characterizations of cyclic GDP-ribose. A procedure for distinguishing enzymes with ADP-ribosyl cyclase activity. J Biol Chem 1994;269:30260-30267.

Graeff RM, Walseth TF, Hill HK, and Lee HC. Fluorescent analogs of cyclic ADP-ribose: synthesis, spectral characterization, and use. Biochemistry 1996;35:379-386.

Graeff RM, Walseth TF, and Lee HC. Radioimmunoassay for measuring endogenous levels of cyclic ADP-ribose in tissues. Methods Enzymol 1997;280:230-241.

Graeff R and Lee HC. A novel cyclic assay for cellular cADP-ribose with nanomolar sensitivity. Biochem J 2002;361:379-384.

Grimaldi JC, Balasubramanian S, Kabra NH, Shanafelt A, Bazan JF, Zurawski G, and Howard MC. CD38-mediated ribosylation of proteins. J Immunol 1995;155:811-817.

Guengerich FP. Common and uncommon cytochrome P450 reactions related to metabolism and chemical toxicity. Chem Res Toxicol 2001;14:611-650.

Guida L, Franco L, Zocchi E, and De Flora A. Structural role of disulfide bridges in the cyclic ADP-ribose related bifunctional ectoenzyme CD38. FEBS Lett 1995;368:481-484.

Gupta DN. Production of the cancer of the bile ducts with thioacetamide. Nature 1955;175:257.

Gupta DN. Acute changes in the liver after administration of thioacetamide. J Pathol Bacteriol 1956a;72:183-192.

Gupta DN. Nodular cirrhosis and metastasizing tumour produced in the liver of rat by prolonged feeding by TAA. J Pathol Bacteriol 1956b; 72:415.

Guse AH. Cyclic ADP-ribose: A novel Ca^{2+} mobilizing second messenger. Cell Signal 1999;11:309-316.

Guse AH, da Silva CP, Berg I, Skapenko AL, Weber K, Heyer P, Hohenegger M, Ashamu GA, Schulze-Koops H, Potter BV, and Mayr GW. Regulation of calcium signaling in T lymphocytes by the second messenger cyclic ADP-ribose. Nature 1999;398:70-73.

Han DW. Intestinal endotoxemia as a pathogenetic mechanism in liver failure. World J Gastroenterol 2002;8:961-965.

Harada N, Santos-Argumedo L, Chang R, Grimaldi JC, Lund FE, Brannan CI, Copeland NG, Jenkins NA, Heath AW, Parkhouse RM, and Howard M. Expression cloning of a cDNA encoding a novel murine B cell activation marker. Homology to human CD38. J Immunol 1993;151:3111-3118.

Hellmich MR and Strumwasser F. Purification and characterization of a molluscan egg-specific NADase, a second-messenger enzyme. Cell Regul 1991;2:193-202.

Hirata Y, Kimura N, Sato K, Ohsugi Y, Takasawa S, Okamoto H, Ishikawa J, Kaisho T, Ishihara K, and Hirano T. ADP ribosyl cyclase activity of a novel bone marrow stromal cell surface molecule, BST-1. FEBS Lett 1994;356:244-248.

Ho HN, Hultin LE, Mitsuyasu RT, Matud JL, Hausner MA, Bockstoce D, Chou CC, O'Rourke S, Taylor JM, and Giorgi JV. Circulating HIV-specific CD8+ cytotoxic T cells express CD38 and HLA-DR antigens. J Immunol 1993;150:3070-3079.

Horenstein AL, Stockinger H, Imhof BA, and Malavasi F. CD38 binding to human myeloid cells is mediated by mouse and human CD31. Biochem J 1998;330:1129-1135.

Hoshino S, Kukimoto I, Kontani K, Inoue S, Kanda Y, Malavasi F, and Katada T. Mapping of the catalytic and epitopic sites of human CD38/NAD+ glycohydrolase to a functional domain in the carboxyl terminus. J Immunol 1997;158:741-747.

Howard M, Grimaldi JC, Bazan JF, Lund FE, Santos-Argumedo L, Parkhouse RM, Walseth TF, and Lee HC. Formation and hydrolysis of cyclic ADP-ribose catalyzed by lymphocyte antigen CD38. Science 1993;262:1056-1059.

Ikehata F, Satoh J, Nata K, Tohgo A, Nakazawa T, Kato I, Kobayashi S, Akiyama T, Takasawa S, Toyota T, and Okamoto H. Autoantibodies against CD38 (ADP-ribosyl cyclase/cyclic ADP-ribose hydrolase) that impair glucose-induced insulin secretion in noninsulin- dependent diabetes patients. J Clin Invest 1998;102:395-401.

Inageda K, Takahashi K, Tokita K, Nishina H, Kanaho Y, Kukimoto I, Kontani K, Hoshino S, and Katada T. Enzyme properties of Aplysia ADP-ribosyl cyclase: comparison with NAD glycohydrolase of CD38 antigen. J Biochem 1995;117:125-131.

Inoue M, Kinne R, Tran T, Biempica L, and Arias IM. Rat liver canalicular membrane vesicles. Isolation and topological characterization. J Biol Chem 1983;258:5183-5188.

Inoue S, Kontani K, Tsujimoto N, Kanda Y, Hosoda N, Hoshino S, Hazeki O, and Katada T. Protein-tyrosine phosphorylation by IgG1 subclass CD38 monoclonal antibodies is mediated through stimulation of the FcgammaII receptors in human myeloid cell lines. J Immunol 1997;159:5226-5232.

Itoh M, Ishihara K, Tomizawa H, Tanaka H, Kobune Y, Ishikawa J, Kaisho T, and Hirano T. Molecular cloning of murine BST-1 having homology with CD38 and Aplysia ADP-ribosyl cyclase. Biochem Biophys Res Commun 1994;203:1309-1317.

Jackson DG and Bell JI. Isolation of a cDNA encoding the human CD38 (T10) molecule, a cell surface glycoprotein with an unusual discontinuous pattern of expression during lymphocyte differentiation. J Immunol 1990;144:2811-2815.

Kato I, Takasawa S, Akabane A, Tanaka O, Abe H, Takamura T, Suzuki Y, Nata K, Yonekura H, Yoshimoto T, et al. Regulatory role of CD38 (ADP-ribosyl cyclase/cyclic ADP-ribose hydrolase) in insulin secretion by glucose in pancreatic beta cells. Enhanced insulin secretion in CD38-expressing transgenic mice. J Biol Chem 1995;270:30045-30050.

Kato I, Yamamoto Y, Fujimura M, Noguchi N, Takasawa S, and Okamoto H. CD38 disruption impairs glucose-induced increases in cyclic ADP-ribose, [Ca2+]i, and insulin secretion. J Biol Chem 1999;274:1869-1872.

Katz F, Povey S, Parkar M, Schneider C, Sutherland R, Stanley K, Solomon E, and Greaves M. Chromosome assignment of monoclonal antibody-defined determinants on human leukemic cells. Eur J Immunol 1983;13:1008-1013.

Kew MC and Popper H. Relationship between hepatocellular carcinoma and cirrhosis. Semin Liver Dis 1984;4:136-146.

Khoo KM. The CD38 paradigm: A study of its distribution and role in the non-hematopoietic system. National University of Singapore. Thesis, 1999.

Khoo KM and Chang CF. Localization of plasma membrane CD38 is domain specific in rat hepatocyte. Arch Biochem Biophys 2000;373:35-43.

Khoo KM, Han MK, Park JB, Chae SW, Kim UH, Lee HC, Bay BH, and Chang CF. Localization of the cyclic ADP-ribose-dependent calcium signaling pathway in hepatocyte nucleus. J Biol Chem 2000;275:24807-24817.

Kikuchi Y, Yasue T, Miyake K, Kimoto M, and Takatsu K. CD38 ligation induces tyrosine phosphorylation of Bruton tyrosine kinase and enhanced expression of interleukin 5-receptor alpha chain: synergistic effects with interleukin 5. Proc Natl Acad Sci USA 1995;92:11814-11818.

Kim H, Jacobson EL, and Jacobson MK. Synthesis and degradation of cyclic ADP-ribose by NAD glycohydrolases. Science 1993a;261:1330-1333.

Kim UH, Kim JS, Han MK, Park BH, and Kim HR. Purification and characterization of NAD glycohydrolase from rabbit erythrocytes. Arch Biochem Biophys 1993b;305:147-152.

Kirch HC, Lammers M, and Gressner AM. Binding of chondroitin sulfate, dermatan sulfate and fat-storing cell-derived proteoglycans to rat hepatocytes. Int J Biochem 1987;19:1119-1126.

Kirkham PA, Santos-Argumedo L, Harnett MM, and Parkhouse RM. Murine B-cell activation via CD38 and protein tyrosine phosphorylation. Immunology 1994;83:513-516.

Kitanaka A, Ito C, Coustan-Smith E, and Campana D. CD38 ligation in human B cell progenitors triggers tyrosine phosphorylation of CD19 and association of CD19 with lyn and phosphatidylinositol 3-kinase. J Immunol 1997;159:184-192.

Koch-Nolte F, Petersen D, Balasubramanian S, Haag F, Kahlke D, Willer T, Kastelein R, Bazan F, and Thiele HG. Mouse T cell membrane proteins Rt6-1 and Rt6-2 are

arginine/protein mono(ADPribosyl)transferases and share secondary structure motifs with ADP-ribosylating bacterial toxins. J Biol Chem 1996;271:7686-7693.

Koguma T, Takasawa S, Tohgo A, Karasawa T, Furuya Y, Yonekura H, and Okamoto H. Cloning and characterization of cDNA encoding rat ADP-ribosyl cyclase/cyclic ADP-ribose hydrolase (homologue to human CD38) from islets of Langerhans. Biochim Biophys Acta 1994;1223:160-162.

Koradi R, Billeter M, and Wuthrich K. MOLMOL: A program for display and analysis of macromolecular structures. J Mol Graph 1996;14:51-55.

Kukimoto I, Hoshino S, Kontani K, Inageda K, Nishina H, Takahashi K, and Katada T. Stimulation of ADP-ribosyl cyclase activity of the cell surface antigen CD38 by zinc ions resulting from inhibition of its NAD+ glycohydrolase activity. Eur J Biochem 1996;239:177-182.

Kumagai M, Coustan-Smith E, Murray DJ, Silvennoinen O, Murti KG, Evans WE, Malavasi F, and Campana D. Ligation of CD38 suppresses human B lymphopoiesis. J Exp Med 1995;181:1101-1110.

Kuntz E and Kuntz HD. Hepatology: Principles and Practice. Germany: Springer-Verlag, 2002:12.

Laemmli UK. Cleavage of structural proteins during the assembly of the head of bacteriophage T4. Nature 1970;227:680-685.

Laurent TC, Fraser JR, Pertoft H, and Smedsrod B. Binding of hyaluronate and chondroitin sulphate to liver endothelial cells. Biochem J 1986;234:653-658.

Lautt W and Greenway C. Conceptual review of the hepatic vascular bed. Hepatology 1987;7:952-963.

LeBouton AV. Molecular and Cell Biology of the Liver. Boca Raton, CRC Press 1993.

Lee BS, Sessanna S, Laychock SG, and Rubin RP. Expression and cellular localization of a modified type 1 ryanodine receptor and L-type channel proteins in non-muscle cells. J Membr Biol 2002;189:181-190.

Lee HC. Potentiation of calcium- and caffeine-induced calcium release by cyclic ADP-ribose. J Biol Chem 1993;268:293-299.

Lee HC. Enzymatic functions and structures of CD38 and homologs. In: Mehta K, Malavasi F, eds. Human CD38 and Related Molecules. Chem Immunol. Volume 75. Basel: Karger, 2000:39-59.

Lee HC. Physiological functions of cyclic ADP-ribose and NAADP as calcium messengers. Annu Rev Pharmacol Toxicol 2001;41:317-345.

Lee HC, Walseth TF, Bratt GT, Hayes RN, and Clapper DL. Structural determination of a cyclic metabolite of NAD+ with intracellular Ca2+-mobilizing activity. J Biol Chem 1989;264:1608-1615.

Lee HC and Aarhus R. ADP-ribosyl cyclase: an enzyme that cyclizes NAD^+ into a calcium-mobilizing metabolite. Cell Regul 1991;2:203-209.

Lee HC and Aarhus R. Wide distribution of an enzyme that catalyzes the hydrolysis of cyclic ADP-ribose. Biochim Biophys Acta 1993;1164:68-74.

Lee HC, Zocchi E, Guida L, Franco L, Benatti U, and De Flora A. Production and hydrolysis of cyclic ADP-ribose at the outer surface of human erythrocytes. Biochem Biophys Res Commun 1993;191:639-645.

Lee HC, Aarhus R, and Levitt D. The crystal structure of cyclic ADP-ribose. Nat Struct Biol 1994a;1:143-144.

Lee HC, Galione A, and Walseth TF. Cyclic ADP-ribose: metabolism and calcium mobilizing function. Vitam Horm 1994b;48:199-257.

Lee HC and Aarhus R. A derivative of NADP mobilizes calcium stores insensitive to inositol trisphosphate and cyclic ADP-ribose. J Biol Chem 1995;270:2152-2157.

Lee HC, Aarhus R, and Graeff RM. Sensitization of calcium-induced calcium release by cyclic ADP-ribose and calmodulin. J Biol Chem 1995a;270:9060-9066.

Lee HC, Graeff R, and Walseth TF. Cyclic ADP-ribose and its metabolic enzymes. Biochimie 1995b;77:345-355.

Lee HC, Aarhus R, Gee KR, and Kestner T. Caged nicotinic acid adenine dinucleotide phosphate. Synthesis and use. J Biol Chem 1997a;272:4172-4178.

Lee HC, Graeff RM, and Walseth TF. ADP-ribosyl cyclase and CD38. Multi-functional enzymes in Ca+2 signaling. Adv Exp Med Biol 1997b;419:411-419.

Lee HC, Munshi C, and Graeff R. Structures and activities of cyclic ADP-ribose, NAADP and their metabolic enzymes. Mol Cell Biochem 1999;193:89-98.

Lee WM. Drug-induced hepatotoxicity. N Engl J Med 2003;349:474-485.

Li Q, Yamada Y, Yasuda K, Ihara Y, Okamoto Y, Kaisaki PJ, Watanabe R, Ikeda H, Tsuda K, and Seino Y. A cloned rat CD38-homologous protein and its expression in pancreatic islets. Biochem Biophys Res Commun 1994;202:629-636.

Liu Z, Cumberland WG, Hultin LE, Kaplan AH, Detels R, and Giorgi JV. CD8+ T-lymphocyte activation in HIV-1 disease reflects an aspect of pathogenesis distinct from viral burden and immunodeficiency. J Acquir Immune Defic Syndr Hum Retrovirol 1998;18:332-340.

Liu ZX, AzhipaO, Okamoto S, Govindarajan S, and Dennert G. Extracellular nicotinamide adenine dinucleotide induces T cell apoptosis in vivo and in vitro. J Immunol 2001;167:4942-4947.

Lu KP and Means AR. Regulation of the cell cycle by calcium and calmodulin. Endocr Rev 1993;14:40-58.

Lund F, Solvason N, Grimaldi JC, Parkhouse RM, and Howard M. Murine CD38: an immunoregulatory ectoenzyme. Immunol Today 1995;16:469-473.

Lund FE, Yu N, Kim KM, Reth M, and Howard MC. Signaling through CD38 augments B cell antigen receptor (BCR) responses and is dependent on BCR expression. J Immunol 1996;157:1455-1467.

Lund FE, Muller-Steffner HM, Yu N, Stout CD, Schuber F, and Howard MC. CD38 signaling in B lymphocytes is controlled by its ectodomain but occurs independently of enzymatically generated ADP-ribose or cyclic ADP-ribose. J Immunol 1999;162:2693-2702.

MacKrill JJ. Protein-protein interactions in intracellular Ca2+-release channel function. Biochem J 1999;337:345-361.

Malavasi F, Funaro A, Alessio M, DeMonte LB, Ausiello CM, Dianzani U, Lanza F, Magrini E, Momo M, and Roggero S. CD38: a multi-lineage cell activation molecule with a split personality. Int J Clin Lab Res 1992;22:73-80.

Malavasi F and Ferrero E. Human CD38, a leukocyte receptor and ectoenzyme, is a member of a novel eukaryotic gene family of nicotinamide adenine dinucleotide^{+}-converting enzymes: extensive structural homology with the genes for murine bone marrow stromal cell antigen 1 and aplysian ADP-ribosyl cyclase. J Immunol 1997;159:3858-3865.

Martinez-Merlos T, Canedo-Merino R, and Diaz-Munoz M. Ryanodine receptor binding constants in skeletal muscle, heart, brain and liver of the Mexican volcano mouse (Neotomodon alstoni alstoni; Rodentia: Cricetidae). Comparison with five other rodent species. Int J Biochem Cell Biol 1997;29:529-539.

McLean IW and Nakane PK. Periodate-lysine-paraformaldehyde fixative. A new fixation for immunoelectron microscopy. J Histochem Cytochem 1974;22:1077-1083.

Mehta K, Shahid U, and Malavasi F. Human CD38, a cell-surface protein with multiple functions. FASEB J 1996;10:1408-1417.

Meszaros V, Socci R, and Meszaros LG. The kinetics of cyclic ADP-ribose formation in heart muscle. Biochem Biophys Res Commun 1995;210:452-456.

Millward-Sadler GH. Liver cirrhosis. In: MacSween NMR, Anthony PP, Scheuer JP, Burt DA, Portmann CB, eds. Pathology of the Liver. 3rd ed. London: Churchill Livingstone, 1994:397-424.

Miyai K. Structural organization of the liver. In: Meeks RG, Harrison SD, Bull RJ, eds. Hepatotoxicology. Florida: CRC Press, 1991:1-65.

Mizuguchi M, Otsuka N, Sato M, Ishii Y, Kon S, Yamada M, Nishina H, Katada T, and Ikeda K. Neuronal localization of CD38 antigen in the human brain. Brain Res 1995;697:235-240.

Moore M, Thor H, Moore G, Nelson S, Moldeus P, and Orrenius S. The toxicity of acetaminophen and N-acetyl-p-benzoquinoneimide in isolated hepatocytes is associated with thiol depletion and increased cytosolic Ca^{2+}. J Biol Chem 1985;260:13035-13040.

Morra M, Zubiaur M, Terhorst C, Sancho J, and Malavasi F. CD38 is functionally dependent on the TCR/CD3 complex in human T cells. FASEB J 1998;12:581-592.

Nakagawara K, Mori M, Takasawa S, Nata K, Takamura T, Berlova A, Tohgo A, Karasawa T, Yonekura H, Takeuchi T, et al. Assignment of CD38, the gene encoding human leukocyte antigen CD38 (ADP-ribosyl cyclase/cyclic ADP-ribose hydrolase), to chromosome 4p15. Cytogenet Cell Genet 1995;69:38-39.

Nishina H, Inageda K, Takahashi K, Hoshino S, Ikeda K, and Katada T. Cell surface antigen CD38 identified as ecto-enzyme of NAD glycohydrolase has hyaluronate-binding activity. Biochem Biophys Res Commun 1994;203:1318-1323.

Okamoto H, Takasawa S, and Tohgo A. New aspects of the physiological significance of NAD^+, poly ADP-ribose and cyclic ADP-ribose. Biochimie 1995;77:356-363.

Okamoto H and Takasawa S. Recent advances in the Okamoto model: The CD38-cyclic ADP-ribose signal system and the regenerating gene protein (Reg)-Reg receptor system in β-cells. Diabetes 2002;51:S462-473.

Okazaki IJ and Moss J. Structure and function of eukaryotic mono-ADP-ribosyltransferases. Rev Physiol Biochem Pharmacol 1996;129:51-104.

Osada S, Okano Y, Saji S, and Nozawa Y. Spontaneous Ca2+ release from a caffeine and ryanodine-sensitive intracellular Ca2+ store in freshly prepared hepatocytes. Hepatology 1994;19:514-517.

Pessayre D, Berson A, Fromenty B, and Mansouri A. Mitochondria in steatohepatitis. Semin Liver Dis 2001;21:57-69.

Poenie M, Alderton J, Tsien RY, and Steinhardt RA. Changes of free calcium levels with stages of the cell division cycle. Nature 1985;315:147-149.

Prasad GS, McRee DE, Stura EA, Levitt DG, Lee HC, and Stout CD. Crystal structure of Aplysia ADP ribosyl cyclase, a homologue of the bifunctional ectoenzyme CD38. Nat Struct Biol 1996;3:957-964.

Ramaschi G, Torti M, Festetics ET, Sinigaglia F, Malavasi F, and Balduini C. Expression of cyclic ADP-ribose-synthetizing CD38 molecule on human platelet membrane. Blood 1996;87:2308-2313.

Reed JC. Apoptosis-regulating proteins as targets for drug discovery. Trends Mol Med 2001;7:314-319.

Reinherz EL, Kung PC, Goldstein G, Levey RH, and Schlossman SF. Discrete stages of human intrathymic differentiation: analysis of normal thymocytes and leukemic lymphoblasts of T-cell lineage. Proc Natl Acad Sci USA 1980;77:1588-1592.

Richardson P and Withrington P. Liver Blood Flow. I. Intrinsic and nervous control of liver blood flow. Gastroenterology 1981;81:159-173.

Robin M-A, Le Roy M, Descatoire V, and Pessayre D. Plasma membrane cytochromes P450 as neoantigens and autoimmune targets in drug-induced hepatitis. J Hepatol 1997;26:Suppl 1:23-30.

Rosario J, Sutherland E, Zaccaro L, and Simon FR. Ethinylestradiol administration selectively alters liver sinusoidal membrane lipid fluidity and protein composition. Biochemistry 1988;27:3939-3946.

Salazar-Gonzalez JF, Moody DJ, Giorgi JV, Martinez-Maza O, Mitsuyasu RT, and Fahey JL. Reduced ecto-5'-nucleotidase activity and enhanced OKT10 and HLA-DR expression on CD8 (T suppressor/cytotoxic) lymphocytes in the acquired immune deficiency syndrome: evidence of CD8 cell immaturity. J Immunol 1985;135:1778-1785.

Santos-Argumedo L, Lund FE, Heath AW, Solvason N, Wu WW, Grimaldi JC, Parkhouse RM, and Howard M. CD38 unresponsiveness of xid B cells implicates Bruton's tyrosine kinase (btk) as a regular of CD38 induced signal transduction. Int Immunol 1995;7:163-170.

Satoh T, Ichida T, Matsuda Y, Sugiyama M, Yonekura K, Ishikawa T, and Asakura H. Interaction between hyaluronan and CD44 in the development of dimethylnitrosamine-induced liver cirrhosis. J Gastroenterol Hepatol 2000;15:402-411.

Savarino A, Pugliese A, Martini C, Pich PG, Pescarmona GP, and Malavasi F. Investigation of the potential role of membrane CD38 in protection against cell death induced by HIV-1. J Biol Regul Homeost Agents 1996;10:13-18.

Sayle R. RasMol v2.5. Greenford, Glaxo Research and Development 1996.

Shapiro AL, Vinuela E, and Maizel JV Jr. Molecular weight estimation of polypeptide chains by electrophoresis in SDS-polyacrylamide gels. Biochem Biophys Res Commun 1967;28:815-820.

Shubinsky G and Schlesinger M. The CD38 lymphocyte differentiation marker: new insight into its ectoenzymatic activity and its role as a signal transducer. Immunity 1997;7:315-324.

Silvennoinen O, Nishigaki H, Kitanaka A, Kumagai M, Ito C, Malavasi F, Lin Q, Conley ME, and Campana D. CD38 signal transduction in human B cell precursors. Rapid induction of tyrosine phosphorylation, activation of syk tyrosine kinase, and phosphorylation of phospholipase C-gamma and phosphatidylinositol 3-kinase. J Immunol 1996;156:100-107.

States DJ, Walseth TF, and Lee HC. Similarities in amino acid sequences of *Aplysia* ADP-ribosyl cyclase and human lymphocyte antigen CD38. Trends Biochem Sci 1992;17:495.

Steinhardt RA and Alderton J. Intracellular free calcium rise triggers nuclear envelope breakdown in the sea urchin embryo. Nature 1988;332:364-366.

Stevenson FK, Bell AJ, Cusack R, Hamblin TJ, Slade CJ, Spellerberg MB, and Stevenson GT. Preliminary studies for an immunotherapeutic approach to the treatment of human myeloma using chimeric anti-CD38 antibody. Blood 1991;77:1071-1079.

Takahashi K, Kukimoto I, Tokita K, Inageda K, Inoue S, Kontani K, Hoshino S, Nishina H, Kanaho Y, and Katada T. Accumulation of cyclic ADP-ribose measured by a specific radioimmunoassay in differentiated human leukemic HL-60 cells with all-trans-retinoic acid. FEBS Lett 1995;371:204-208.

Takasawa S, Nata K, Yonekura H, and Okamoto H. Cyclic ADP-ribose in insulin secretion from pancreatic beta cells. Science 1993a;259:370-373.

Takasawa S, Tohgo A, Noguchi N, Koguma T, Nata K, Sugimoto T, Yonekura H, and Okamoto H. Synthesis and hydrolysis of cyclic ADP-ribose by human leukocyte antigen CD38 and inhibition of the hydrolysis by ATP. J Biol Chem 1993b;268:26052-26054.

Takasawa S and Okamoto H. Pancreatic β-cell death, regeneration and insulin secretion: roles of poly(ADP-ribose) polymerase and cyclic ADP-ribose. Int J Exp Diabetes Res 2002;3:79-96.

Tanaka Y and Tashjian AH Jr. Calmodulin is a selective mediator of Ca(2+)-induced Ca2+ release via the ryanodine receptor-like Ca2+ channel triggered by cyclic ADP-ribose. Proc Natl Acad Sci U S A 1995;92:3244-3248.

Terstappen LW, Huang S, Safford M, Lansdorp PM, and Loken MR. Sequential generations of hematopoietic colonies derived from single nonlineage-committed CD34+CD38- progenitor cells. Blood 1991;77:1218-1227.

Tohgo A, Takasawa S, Noguchi N, Koguma T, Nata K, Sugimoto T, Furuya Y, Yonekura H, and Okamoto H. Essential cysteine residues for cyclic ADP-ribose synthesis and hydrolysis by CD38. J Biol Chem 1994;269:28555-28557.

Tohgo A, Munakata H, Takasawa S, Nata K, Akiyama T, Hayashi N, and Okamoto H. Lysine 129 of CD38 (ADP-ribosyl cyclase/cyclic ADP-ribose hydrolase) participates in the binding of ATP to inhibit the cyclic ADP-ribose hydrolase. J Biol Chem 1997;272:3879-3882.

Towbin H, Staehelin T, and Gordon J. Electrophoretic transfer of proteins from polyacrylamide gels to nitrocellulose sheets: procedure and some applications. Proc Natl Acad Sci USA 1979;76:4350-4354.

Trauner M, Meier PJ, and Boyer J. Molecular pathogenesis of cholestasis. N Engl J Med 1998;339:1217-1227.

Tsujimoto N, Kontani K, Inoue S, Hoshino S, Hazeki O, Malavasi F, and Katada T. Potentiation of chemotactic peptide-induced superoxide generation by CD38 ligation in human myeloid cell lines. J Biochem (Tokyo) 1997;121:949-956.

Twigg J, Patel R, and Whitaker M. Translational control of InsP3-induced chromatin condensation during the early cell cycles of sea urchin embryos. Nature 1988;332:366-369.

Umar S, Malavasi F, and Mehta K. Post-translational modification of CD38 protein into a high molecular weight form alters its catalytic properties. J Biol Chem 1996;271:15922-15927.

Weber K and Osborn M. The reliability of molecular weight determinations by dodecyl sulfate-polyacrylamide gel electrophoresis. J Biol Chem 1969;244:4406-4412.

Weinshilboum R. Inheritance and drug response. N Engl J Med 2003;348:529-537.

Yagui K, Shimada F, Mimura M, Hashimoto N, Suzuki Y, Tokuyama Y, Nata K, Tohgo A, Ikehata F, Takasawa S, Okamoto H, Makino H, Saito Y, and Kanatsuka A. A missense mutation in the CD38 gene, a novel factor for insulin secretion: association with Type II diabetes mellitus in Japanese subjects and evidence of abnormal function when expressed in vitro. Diabetologia 1998;41:1024-1028.

Yang JM, Han DW, Xie CM, Liang QC, Zhao YC, and Ma XH. Endotoxins enhance hepatocarcinogenesis induced by oral intake of thioacetamide in rats. World J Gastroenterol 1998;4:128-132.

Harada Y, Kawano MM, Huang N, Mahmoud MS, Lisukov IA, Mihara K, Tsujimoto T, and Kuramoto A. Identification of early plasma cells in peripheral blood and their clinical significance. Br J Haematol 1996;92:184-191.

Yun CH, Okerholm RA, and Guengerich FP. Oxidation of the antihistamine drug terfenadine in human liver microsomes: role of cytochrome P-450 3A(4) in N-dealkylation and C-hydroxylation. Drug Metab Dispos 1993;21:403-409.

Zimmermann T, Muller A, Machnic G, Frank H, Schubert H, and Dargel R. Biochemical and morphological studies on production and regression of experimental liver cirrhosis induced by thioacetamide in Uje: WIST rats. Z Versuchstierkd 1987;30:165-180.

Zocchi E, Franco L, Guida L, Benatti U, Bargellesi A, Malavasi F, Lee HC, and De Flora A. A single protein immunologically identified as CD38 displays NAD+ glycohydrolase, ADP-ribosyl cyclase and cyclic ADP-ribose hydrolase activities at the outer surface of human erythrocytes. Biochem Biophys Res Commun 1993;196:1459-1465.

Zocchi E, Franco L, Guida L, Calder L, and De Flora A. Self-aggregation of purified and membrane-bound erythrocyte CD38 induces extensive decrease of its ADP-ribosyl cyclase activity. FEBS Lett 1995;359:35-40.

Zocchi E, Franco L, Guida L, Piccini D, Tacchetti C, and De Flora A. NAD^+-dependent internalization of the transmembrane glycoprotein CD38 in human Namalwa B cells. FEBS Lett 1996;396:327-332.

Zubiaur M, Izquierdo M, Terhorst C, Malavasi F, and Sancho J. CD38 ligation results in activation of the Raf-1/mitogen-activated protein kinase and the CD3-zeta/zeta-associated protein-70 signaling pathways in Jurkat T lymphocytes. J Immunol 1997;159:193-205.

Zupo S, Rugari E, Dono M, Taborelli G, Malavasi F, and Ferrarini M. CD38 signaling by agonistic monoclonal antibody prevents apoptosis of human germinal center B cells. Eur J Immunol 1994;24:1218-1222.

Zupo S, Isnardi L, Megna M, Massara R, Malavasi F, Dono M, Cosulich E, and Ferrarini M. CD38 expression distinguishes two groups of B-cell chronic lymphocytic leukemias with different responses to anti-IgM antibodies and propensity to apoptosis. Blood 1996;88:1365-1374.